USGS
science for a changing world

Prepared in cooperation with the Bureau of Reclamation

Revision and Proposed Modification of a Total Maximum Daily Load Model for Upper Klamath Lake, Oregon

Scientific Investigations Report 2015–5041

U.S. Department of the Interior
U.S. Geological Survey

Revision and Proposed Modification of a Total Maximum Daily Load Model for Upper Klamath Lake, Oregon

By Susan A. Wherry, Tamara M. Wood, and Chauncey W. Anderson

Prepared in cooperation with the Bureau of Reclamation

Scientific Investigations Report 2015–5041

U.S. Department of the Interior
U.S. Geological Survey

U.S. Department of the Interior
SALLY JEWELL, Secretary

U.S. Geological Survey
Suzette M. Kimball, Acting Director

U.S. Geological Survey, Reston, Virginia: 2015

Suggested citation:
Wherry, S.A., Wood, T.M., and Anderson, C.W., 2015, Revision and proposed modification of a total maximum daily load model for Upper Klamath Lake, Oregon: U.S. Geological Survey Scientific Investigations Report 2015–5041, 55 p., http://dx.doi.org/10.3133/sir20155041.

ISSN 2328-0328 (online)

Contents

Figures

Tables

Conversion Factors

Inch/pound to International System of Units

Multiply	By	To obtain
	Concentration	
parts per billion (ppb)	1.0	micrograms per liter (µg/L)

International System of Units to inch/pound

Multiply	By	To obtain
	Length	
meter (m)	3.281	foot (ft)
kilometer (km)	0.6214	mile (mi)
	Area	
square meter (m^2)	0.0002471	acre
square meter (m^2)	10.76	square foot (ft^2)
	Volume	
liter (L)	33.82	ounce, fluid (fl. oz)
	Flow rate	
meter per second (m/s)	3.281	foot per second (ft/s)
meter per day (m/d)	3.281	foot per day (ft/d)
square meter per day (m^2/d)	10.764	square foot per day (ft^2/d)
	Mass	
milligram (mg)	0.0000353	ounce, avoirdupois (oz)
gram (g)	0.03527	ounce, avoirdupois (oz)
kilogram (kg)	2.205	pound avoirdupois (lb)

Temperature in degrees Celsius (°C) may be converted to degrees Fahrenheit (°F) as $F = (1.8 \times °C) + 32$.

Datums

Vertical coordinate information is referenced to the Bureau of Reclamation datum, which is 1.78 feet above National Geodetic Vertical Datum of 1929 (NGVD 29).

Horizontal coordinate information is referenced to the North American Datum of 1927 (NAD 27).

Elevation, as used in this report, refers to distance above the vertical datum.

Supplemental Information

Concentrations of chemical constituents in water are given in either milligrams per liter (mg/L) or micrograms per liter (µg/L).

Abbreviations

AIC	Akaike's Information Criterion
AFA	*Aphanizomenon flos-aquae*
CR	community respiration
CSTR	continuously stirred tank reactor
DO	dissolved oxygen
GPP	gross primary production
MET	meteorological
NPP	net primary production
NS	Nash-Sutcliffe statistic
R	correlation coefficient
R^2	coefficient of determination
RMSE	root mean square error
SOD	sediment-oxygen demand
TMDL	total maximum daily load
TP	total phosphorus
UKL	Upper Klamath Lake
USGS	U.S. Geological Survey
WQ	water quality

Revision and Proposed Modification of a Total Maximum Daily Load Model for Upper Klamath Lake, Oregon

By Susan A. Wherry, Tamara M. Wood, and Chauncey W. Anderson

Executive Summary

This report presents Phase 2 of the review and development of the mass balance water-quality model, originally developed in 2001, that guided establishment of the phosphorus (P) total maximum daily load (TMDL) for Upper Klamath and Agency Lakes, Oregon. The purpose of Phase 2 was to incorporate a longer (19-year) set of external phosphorus loading data into the lake TMDL model than had originally been available, and to develop a proof-of-concept method for modeling algal mortality and the consequent decrease in chlorophyll *a* that had not been possible with the 2001 TMDL model formulation.

Using the extended 1991–2010 external phosphorus loading dataset, the lake TMDL model was recalibrated following the same procedures outlined in the Phase 1 review. The version of the model selected for further development incorporated an updated sediment initial condition, a numerical solution method for the chlorophyll *a* model, changes to light and phosphorus factors limiting algal growth, and a new pH-model regression, which removed Julian day dependence in order to avoid discontinuities in pH at year boundaries. This updated lake TMDL model was recalibrated using the extended dataset in order to compare calibration parameters to those obtained from a calibration with the original 7.5-year dataset. The resulting algal settling velocity calibrated from the extended dataset was more than twice the value calibrated with the original dataset, and, because the calibrated values of algal settling velocity and recycle rate are related (more rapid settling required more rapid recycling), the recycling rate also was larger than that determined with the original dataset. These changes in calibration parameters highlight the uncertainty in critical rates in the Upper Klamath Lake TMDL model and argue for their direct measurement in future data collection to increase confidence in the model predictions.

Comparison of Model Results

We compared model predictions of steady-state water-column conditions in response to the 40-percent reduction in external phosphorus loads stipulated in the 2001 TMDL, using the original model and the recalibrated version with revisions as described in this report. The qualitative prediction of reduced concentrations in response to external load reductions, occurring over a period on the order of decades, is consistent across model versions and is a reliable feature of the equations that describe a coupled sediment and water-column system. The quantitative predictions of the original and revised models differ in time required to achieve steady state (50 years and 19 years, respectively) and the associated steady-state concentration of water column total P (40 and 74 parts per billion, or ppb, respectively), with chlorophyll *a* concentrations being similar (25 and 27 ppb, respectively). The quantitative predictions, however, have a high degree of uncertainty because they depend on calibration parameters that vary greatly with changes in assumptions or the calibration dataset, and neither set of calibration parameters resulted in a model with good fit statistics outside of the calibration period. If a model that can predict water column concentrations in response to TMDL implementation with less uncertainty is required, several improvements to the current model can be pursued and are briefly explained.

Improvements to Modeling Cyanobacterial Dynamics

After comparing recalibrated parameters and results, we incorporated algal mortality (bloom decline) into the algal submodel. The original lake TMDL algal submodel relied on a mass balance that included terms for growth and respiration, the latter a combined term that was intended to include mortality. Both terms were modified throughout the season by the product of limitation factors that were determined by input data averaged over the lake area and biweekly time step. This common modeling approach is relatively simple and can be run with low-resolution data (biweekly); however, it introduces error when used to describe a highly variable system such as Upper Klamath Lake instead of a small, homogeneous parcel of water, and does not capture the cumulative effects of short-term variability. Our proof-of-concept alternative makes use of high-resolution data to better capture spatial and temporal dynamics of algal growth and mortality by substituting the original model terms with metabolic terms, gross primary production (GPP) and community respiration (CR), as calculated from continuously monitored dissolved oxygen (DO) data.

We calculated GPP and CR during 3 years from an hourly mass balance of dissolved oxygen that included reaeration and sediment oxygen demand (SOD), and assumed that GPP ceased during times of darkness. To minimize effects of vertical transport of DO, we evaluated only the nine shallow sites in operation during 2006–08. Hourly data were accumulated each day and stoichiometric ratios relating oxygen to carbon, and carbon to chlorophyll *a*, were used to convert daily estimates of production and consumption of DO to changes in chlorophyll *a* concentration. Lake-averaged GPP and CR were substituted for algal growth and respiration terms, respectively, in the model, and the model was recalibrated. The initial runs were promising in that the mid-season bloom declines were captured and statistics describing simulated chlorophyll *a* concentration (coefficient of determination [R^2] = 0.19–0.43) were comparable to those found over the same period for the revised and recalibrated model as previously described (R^2 = 0.25–0.27). Because this metabolism-based approach was able to capture bloom declines and performed as well as the TMDL model over 3 years of data, we developed a statistical model for predicting GPP and CR based on independent variables for which long-term records existed.

Regression analysis was used to relate GPP and CR to meteorological (wind and solar radiation) variables and water temperature. The goal was to derive relations that could be incorporated in the TMDL model equations to improve accuracy in the prediction of the state variables in response to implementation of TMDL constraints on external phosphorus loading. Wind, solar radiation, and water temperature were used as explanatory variables for model predictions of the response to changes in external loads because they are not expected to change due to changing phosphorus conditions.

As a result of an initial, exploratory analysis, GPP and CR were determined to correlate to explanatory variables differently depending on season; therefore, season-specific regression models were developed. Each model comprised a seasonal component determined from biweekly data and a weekly component determined from daily values that were calculated from hourly measurements. Potentially explanatory variables tested in the seasonal model included 14-day lakewide average chlorophyll *a*, solar radiation, and temperature. Potentially explanatory variables tested in the weekly model included wind speed, measures of water temperature deviation from a seasonal fit and rate of change, water-column stratification, and solar radiation deviation from a seasonal fit. The results of the combined models generally were good, with R^2 greater than or equal to 0.53 for CR and R^2 greater than or equal to 0.62 for GPP. The next step in this analysis would be incorporation of the regression model of metabolism in the lake TMDL model in place of algal growth and respiration; however, that step would require additional data extraction and model calibration that was beyond the scope of this project.

Based on the results of the recalibration of the lake TMDL model with the updated, extended dataset and explorations of alternative methods for modeling chlorophyll *a*, we propose five steps that could be explored to improve the lake TMDL model in the future:

1. Use a daily time step for modeling. A daily time step is straightforward to implement and is reasonable in the context of the following steps that make use of continuously (hourly) collected data.

2. Use a spatially explicit model to interpolate between sampling sites and to accurately calculate (1) the lakewide average of variables as a function of the measured values at sampling sites, and (2) the concentrations in the lake outflow, so as to improve the accuracy of estimated downstream P and chlorophyll *a* loads.

3. Substitute GPP and CR for algal growth and respiration terms in the model. We have shown the proof-of-concept for using continuously measured DO to calculate the lake metabolism terms. Further work needs to be done to improve the empirical models that enable the prediction of GPP and CR from allowable explanatory variables before GPP and CR are formally substituted for the algal growth and respiration terms of the model.

4. Expand equations used to model internal phosphorus loading. Specifically, create explicit, separate terms for benthic invertebrate excretion, groundwater flux, diffusive flux, desorption at high pH, and rapid bacterial recycling.

5. Improve the model treatment of net settling velocity. The treatment of net settling velocity as a single calibration parameter is not satisfactory for reasons related to the scaling-up process in general (appendix A), but particularly because the net settling velocity varies across time with the proportion of buoyant and non-buoyant colonies in the water column.

   Two complementary approaches are proposed to improve net settling velocity. The first approach relies on using continuous monitor data to estimate daily depth-integrated algal biomass values at a monitor site. Estimates at individual continuous monitoring sites would be combined to create a lakewide average. Daily estimates of lakewide biomass storage in combination with daily values of net primary production (NPP) allow the daily settling flux to be calculated by difference. This approach can be pursued only in combination with the calculation of GPP and CR (step 3). The second approach relies on field work to measure rising and falling velocities and to estimate the fraction of rising and falling colonies as a function

of environmental variables. After measurements are obtained, one-dimensional water-column models that investigate only the interaction between buoyancy and stratification, and three-dimensional models that add horizontal transport, would be used to assist the scaling-up process.

The combination of the suggested improvements is expected to result in a modeling framework that can better account for spatial and temporal variations in water quality in the lake, while using independent variables to predict future algal-mortality events. Ultimately, this would provide better tools to represent the time frames needed to achieve desired outcomes based on prescribed reductions in external loading.

Introduction

Upper Klamath Lake (UKL) in south-central Oregon (fig. 1) has a long history of harmful cyanobacterial blooms, with biomass dominated by the cyanobacterium *Aphanizomenon flos-aquae* (AFA), and associated poor water quality, dating from at least the early 1990s (Wood and others, 1996; Eilers and others, 2004; Wood and others, 2006). Among the problems associated with these blooms are (1) episodically low concentrations of dissolved oxygen (DO), high pH, and high ammonia concentrations that negatively affect endangered fish in the lake (Burdick and others, 2009); (2) the production of cyanobacterial toxins that could have negative health effects on wildlife and humans (VanderKooi and others, 2010; Eldridge and others, 2012); and (3) the export of nutrients, cyanobacteria, and associated toxins, and organic carbon to downstream reaches (Sullivan and others, 2011). In 2002, Oregon Department of Environmental Quality promulgated a Total Maximum Daily Load (TMDL) (Oregon Department of Environmental Quality, 2002) that set allowable limits on the amount of phosphorus entering the lake from external sources as a means to reduce the frequency, magnitude, and extent of algal blooms and thereby improve water quality.

The TMDL was based on a lake nutrient budget developed by Kann and Walker (1999), and used a spreadsheet-based model that approximated lake average concentrations of total phosphorus (TP) for the combined Upper Klamath and Agency Lakes, assuming that the lake behaved as a continuously stirred tank reactor (CSTR) (Walker, 2001). The model boundary conditions were derived from external loads estimated from bi-weekly samples, and the model was calibrated using biweekly in-lake monitoring data and internal recycling data derived from mass-balance calculations (Walker and others, 2012). Model outputs included TP concentration (water-column and sediment-bound), chlorophyll *a* concentration, and pH.

In 2011, the U.S. Geological Survey (USGS) began a multi-phase technical review of the UKL TMDL model in order to evaluate the strengths and limitations of the model and to determine whether improvements could be made using information and data derived from studies completed since the development of the model. Phase 1 (Wood and others, 2013) included a literature review of major hydrological and biogeochemical processes relevant to UKL, incorporation of recent field and laboratory studies, and a technical review and evaluation of the spreadsheet-based CSTR model. Strengths and weaknesses of the existing CSTR approach were described. One of the primary advantages of the existing model is its applicability to long-term simulations that are computationally achievable and that can give insights into large-scale lake responses to different management approaches. A limitation is its coarse representation of the lake's water quality, both spatially and temporally, compared to scales that likely operate in the lake during peak growing season. Temporal wavelet analysis of hourly water quality and meteorological data in the summer of 2006 indicated variability at time scales as low as 5.8–7.6 days, and spatial wavelet analysis of phycocyanin fluorescence data (an indicator of cyanobacteria) collected along two lake transects during bloom events in 2012 showed variability at distances as small as 0.25 km (Eldridge and others, 2014). Because a whole-lake average is not necessarily the same as the concentration in the outflow, the model may not accurately predict water quality exported from the lake. Downstream reaches also have significant water quality concerns—specifically, elevated ammonia concentrations and anoxic conditions owing to decomposing AFA exported from UKL (Sullivan and others, 2011). A model that provides more accurate (throughout the year) and higher resolution boundary conditions to downstream reaches would be useful for water management in the Klamath River and Klamath Irrigation Project.

In Phase 1, improvements were made to the growth limitation factors used in the original spreadsheet model, and the model then was re-scripted in R (R Core Team, 2014) with a Runge-Kutta solution method and re-calibrated. The lake sediment initial conditions were updated with the most recent information (Simon and others, 2009; Simon and Ingle, 2011). Modifications to the R-script model were used to explore the long-term behavior of model simulations. Further improvements were identified but could not be incorporated into the Phase 1 report. These improvements included (1) updating the model's 7.5-year input dataset of external nutrient loading and lake monitoring data (Kann and Walker, 1999) with a 19-year dataset (Walker and others, 2012), and (2) researching and developing algorithms to predict mid-season bloom declines caused by a transition from a primary-production-dominated to a community-respiration-dominated (where community respiration includes cyanobacterial respiration and mortality) system. The inability to simulate mid-season bloom declines was a large source of error in the original model formulation (Wood and others, 2013). It also was suggested in the Phase 1 report that settling velocities could be measured rather than calibrated.

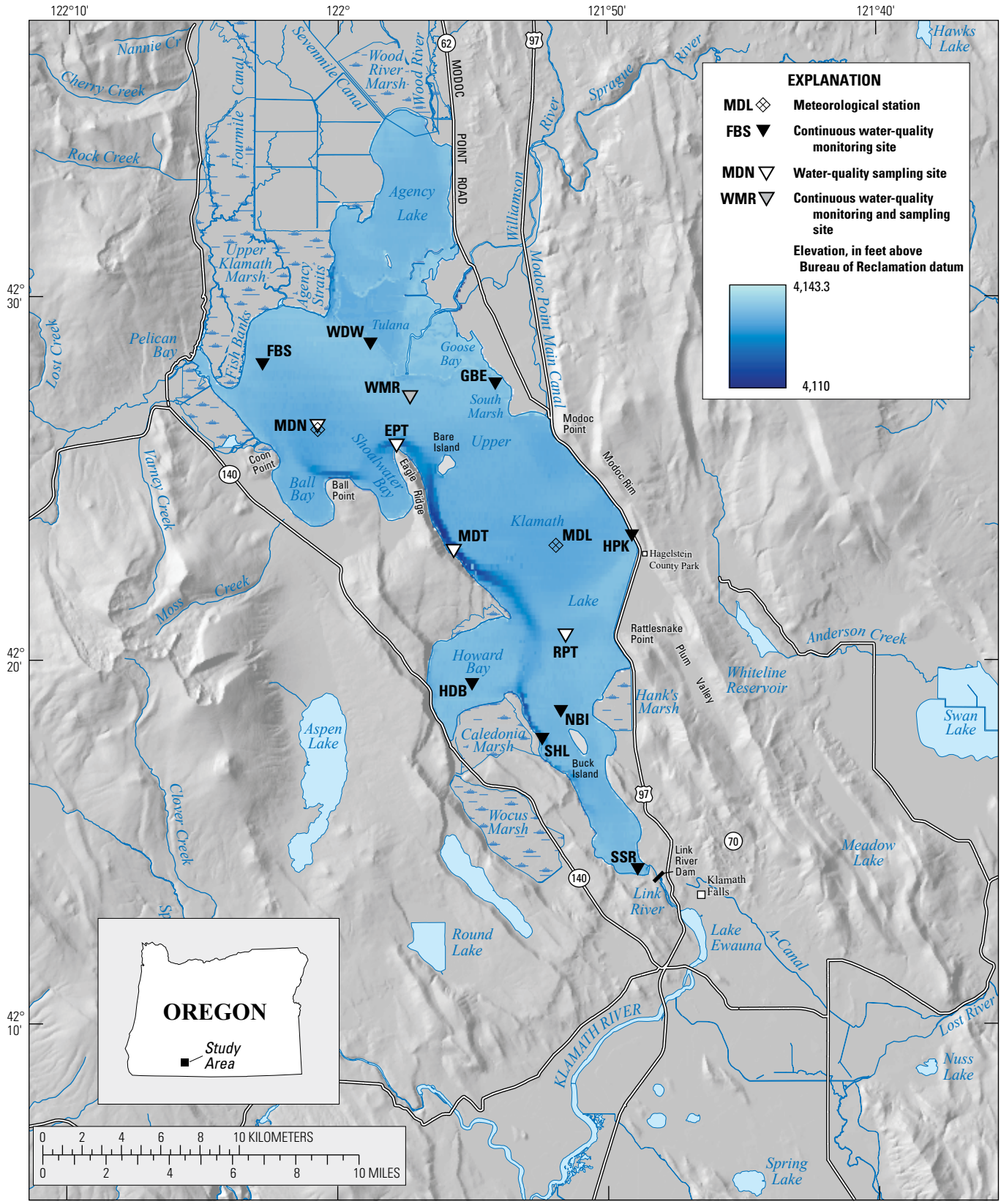

Base modified from USGS and other digital sources, various scales.
Coordinate system is UTM, Zone 10N; North American Datum of 1927.

Figure 1. Location of meteorological stations and continuous water-quality monitoring and sampling sites, Upper Klamath Lake, Oregon.

This report further discusses the meaning of the net settling velocity in a system dominated by buoyant cyanobacteria, as well as the implications of calibration. With the availability of the updated monitoring data from Walker and others (2012) and new research on lake metabolism, the CSTR model calibration could be updated and new model algorithms could be pursued.

Although the biomass in UKL is dominated by cyanobacteria, the original TMDL model and its appropriate parameters and variables were described by the term "algal" instead of "cyanobacterial." The following terms from the model are used in the remainder of this report: algal submodel, algal growth, algal settling velocity, algal phosphorus, and nonalgal phosphorus.

Purpose and Scope

This report presents the results of Phase 2 of the review of the 2001 TMDL model (Oregon Department of Environmental Quality, 2002) with the objective of evaluating modifications to the CSTR that include updated calibration data and alternate algorithms for important processes affecting water quality in the lake. The revised model is intended to help resource managers better (1) assess the efficacy of management strategies and restoration activities, and (2) understand topical areas needing additional data or research to reduce uncertainty in decision making.

Specifically, the report describes additional development of the R-script model from Phase 1 (Wood and others, 2013) and updated calibrations using newly available monitoring data (Walker and others, 2012), and derives a new, alternative algorithm to better account for removal of algal phosphorus from the system as the AFA bloom transitions from a growth-dominated to respiration-dominated regime. We describe the revised model calibration and verification, and we suggest five steps toward a new modeling framework that would preserve the computational speed and straightforward approach of the CSTR model. We anticipate that a model that incorporated these steps would prove to be an improved model, based on statistics describing its ability to simulate the calibration dataset. If so, such a model would provide more accurate predictions of water-column concentrations far into the future, while simulation of long-term response to management scenarios, such as TMDL implementation, would be improved.

This report builds on Phase 1, and provides basic background on that effort as it pertains to specific modifications for the purposes of Phase 2; however, the reader is encouraged to consult the Phase 1 report together with this report in order to fully explain the history and rationale for the initial review, and for specific information about certain model parameter values or outcomes from the review.

Review of Phase 1 Results

In Phase 1, the verified R-script was used to make three changes that would improve representation of lake processes in the model as understood by established lake modeling techniques (Bowie and others, 1985; Chapra, 1997):

1. Improve the light limitation factor by integrating the limitation function over the lake depth as opposed to calculating limitation from depth-integrated light;
2. Use Michaelis-Menten kinetics to describe phosphorus limitation and calibrate the half-saturation constant in tandem with other model parameters; and
3. Remove the assumption that chlorophyll *a* reaches equilibrium with light and nutrients over the time step.

Following these changes, we incorporated new data collected in UKL since the TMDL model was originally developed, notably sediment phosphorus concentrations from multiple locations and sediment depths around the lake (Simon and others, 2009; Simon and Ingle, 2011), and recalibrated the model parameters. Once the model was recalibrated, we ran long-term simulations and conducted sensitivity analyses. These simulations allowed us to evaluate the lake's predicted responses to changes in external phosphorus loading and to identify model parameters or areas of uncertainty that would benefit from additional study. Results of these analyses were detailed by Wood and others (2013), with additional suggestions for future improvement. Here, we summarize several of the notable Phase 1 model changes and results, which form the basis for additional proposed modifications in Phase 2.

An important aspect of the TMDL model is that it fundamentally relies on a coupled system whereby compartments representing the water column and lake sediments are interdependent. As stated by Wood and others (2013, p. 2):

> … as long as external inputs to the system continue, the sediment compartment will not trend independently toward depletion until it is gone. Rather, phosphorus concentrations in the water column will reach a steady state in equilibrium with the sediment reservoir over time and the calibration parameters (not the magnitude of the sediment phosphorus reservoir) will determine the steady-state conditions.

A ramification of this model structure is that changes in one compartment are reflected in the other compartment at each biweekly time step. Thus, as calibration parameters change in Phases 1 and 2 resulting from incorporation of new datasets, there are implications for internal phosphorus loading, algal growth and maximum biomass, and pH.

These implications are described for Phase 1 by Wood and others (2013) and for Phase 2 in section, "Phase 2 Model Updates" of this report, as appropriate. Nonetheless, the Phase 2 approach does not change the basic assumption of a coupled system between nutrients in the water column and bed sediments.

Changes to Algal Submodel

In the TMDL model, an algal submodel uses a mass balance to determine biomass, with calculated lake-averaged terms for growth (*GROWTH*), respiration (*RESP*), and settling (*SETTLE*), as well as outflow concentrations from the lake (see equations 11–13 in Wood and others, 2013). *GROWTH* is a function of several factors, including a temperature factor, a phosphorus limiting factor (F_P), and a light limiting factor (F_L). In Phase 1, we modified the algorithms for F_P and F_L prior to recalibrating the model. The original formulation of F_L represented light limitation over a 24-hour period by using depth-averaged light intensity in the Steele formulation and multiplying by photoperiod. We revised the model's calculation of F_L by integrating the Steele formulation over depth and time to better approximate average light attenuation in the water column for the entire lake (see equation 26 in Wood and others, 2013). F_P originally was calculated as the percentage of nonalgal phosphorus (the difference between TP and calculated algal phosphorus) in the water column, which had the effect of underpredicting phosphorus limitation when nonalgal phosphorus was a large fraction of the TP, even if overall concentrations were low, and overpredicting phosphorus limitation when nonalgal phosphorus was a small fraction of the TP, even if large concentrations of phosphorus were available. We reformulated F_P with the Michaelis-Menten kinetics approach for phosphorus limitation, which allows the algal growth rate to approach zero as the concentration of available (nonalgal) phosphorus approaches zero, and to approach a maximum value asymptotically as the concentration of the available phosphorus becomes large.

After the light and phosphorus limitation factors were changed, the algal settling velocity, u_{alg}, was recalibrated and a new parameter necessary for Michaelis-Menten kinetics, the half-saturation constant k_{half}, was introduced and calibrated in tandem with the recycling parameters (Wood and others, 2013). The resulting calibrated algal setting velocity was 41 percent lower, and the calibrated recycling rate was 32 percent lower. The combined effect of the modifications to the phosphorus and light limitation factors and subsequent recalibration was to decrease the annual peak in predicted TP concentration relative to the original model by an average of 12 ppb. This was largely due to the lower recalibrated recycling rate; even so, the combination of lower algal settling velocity and modification to growth limitation factors resulted in higher peaks in chlorophyll *a* and pH.

In addition to modifying the calculation of the limitation factors, the structure of the algal submodel was revised so that the assumption of maximum possible algal growth during each time step was removed. This resulted in chlorophyll *a* being represented as a first-order differential equation and modeled using the Runge-Kutta 4th-order method, as was used for the sediment and water-column compartment models with model terms and parameters defined in tables 1 and 2, respectively:

$$\frac{dB}{dt} = \left(GROWTH - RESP - SETTLE - \frac{Q_{out}}{V} \right) \times B \quad (1)$$

The algal settling velocity was not recalibrated for this model, but recycling parameters were recalibrated. This change to the algal submodel structure resulted in a better model performance for the three measured variables (TP, chlorophyll *a*, pH) during the limited validation period of May–July and during the full validation period.

The changes in calibration parameters among all versions of the model were substantial, but the performance of the model based on statistics calculated over the full verification dataset was not much changed, and was uniformly poor (Wood and others, 2013, tables 9–14). Furthermore, no model version consistently produced the best or worst results among the three steady-state variables—TP, chlorophyll *a*, and pH. When only May–July was considered in calculating statistics, performance was better. Generally, the differences among the various model versions were small, but the version of the model that did not assume maximum growth during the time step performed better overall in simulating chlorophyll *a* and pH. All versions of the model, therefore, performed better during months of rapid bloom expansion than during the other months of the year.

New Information—Internal Loading and Benthic Invertebrates

The Phase 1 review benefited from new data and insights into nutrient processes in the lake that were not available until after the implementation of the original TMDL in 2002. These data included revised estimates of sediment phosphorus concentrations, and field and laboratory measurements of the large densities of benthic invertebrates (worms and leeches) in the sediments, which previously had been unaccounted for and which appear to have important effects on internal nutrient recycling (Gardner and others, 1981; Hansen and others, 1998).

Table 1. Descriptions of model terms used in this report.

Model term	Units	Description
A	square meters	Lake area
B	parts per billion	Chlorophyll *a* concentration
B_{NPP}	parts per billion	Calculated net chlorophyll *a* concentration
C	milligram per liter	Dissolved oxygen concentration
C_{sat}	milligram per liter	Saturation dissolved oxygen concentration
CR	grams of oxygen per square meter per day	Simulated community respiration
CR_S	grams of oxygen per square meter per day	Seasonal component of community respiration model
CR_W	grams of oxygen per square meter per day	Weekly component of community respiration model
D	meter	Lake depth
F_T	–	Temperature adjustment factor
F_P	–	Phosphorus limitation factor
F_L	–	Light limitation factor
I_o	microeinsteins per square meter per second	Light intensity at lake surface
I	microeinsteins per square meter per second	Site specific light intensity
Φ_{photo}	grams of oxygen per square meter per hour	Photosynthetic flux
Φ_{resp}	grams of oxygen per square meter per hour	Community respiration flux
$\Phi_{resp,20}$	grams of oxygen per square meter per hour	Community respiration flux at 20 degrees Celsius
Φ_{SOD}	grams of oxygen per square meter per hour	Sediment oxygen demand
Φ_{reaer}	grams of oxygen per square meter per hour	Reaeration
$K_{L,20}$	meter per day	Film transfer coefficient at 20 degrees Celsius
K_R	per day	Maximum phosphorus recycle rate, pH-dependent
K_G	per day	Maximum algal growth rate
K_T	per day	Maximum phosphorus recycle rate, temperature-dependent
P_{na}	parts per billion	Nonalgal phosphorus concentration
P	parts per billion	Site specific total phosphorus concentration
GPP	grams of oxygen per square meter per day	Simulated photosynthetic production
GPP_S	grams of oxygen per square meter per day	Seasonal component of photosynthetic production model
GPP_W	grams of oxygen per square meter per day	Weekly component of photosynthetic production model
$GROWTH$	per day	The algal growth component of the chlorophyll *a* submodel
$RESP$	per day	The respiration component of the chlorophyll *a* submodel
$SETTLE$	per day	The settling component of the chlorophyll *a* submodel
SET	meters per day	Space and time-dependent algal settling velocity
Q_{out}	cubic meters per day	Lake outflow rate
s	square meters	2-dimensional geographic location
T_{lake}	degrees Celsius	Average lake temperature
T	degrees Celsius	Site specific water temperature
T_{min}	degrees Celsius	Minimum temperature for algal growth to occur
$T_{(min,rec)}$	degrees Celsius	Minimum temperature at which temperature-dependent recycling begins
t	day	Time
V	cubic meters	Mean volume of the lake over the time step
z	meter	Average lake depth over the time step
z_{full}	meter	Site specific full pool depth
Δt	day	Time step
$WSPD_{10}$	meter per second	Wind speed 10 meters above the water surface
$WTDEV$	–	Daily deviation in water temperature from the seasonal trend
$SSDEV$	–	Daily deviation in shortwave solar radiation from clear sky solar radiation
$WTROC$	degrees Celsius per day	Daily rate of change in air temperature
$STRAT$	degrees Celsius per day	Degree of stratification
	Appendix variables	
u_r	meter per day	Cyanobacterial rising velocity
u_f	meter per day	Cyanobacterial falling velocity
r_{rise}	–	Proportion of cyanobacterial colony rising
r_{fall}	–	Proportion of cyanobacterial colony falling

Table 2. Descriptions, values, and sources of parameters used in the phosphorus total maximum daily load (TMDL) model, Upper Klamath Lake, Oregon.

[**Abbreviation**: NA, not applicable]

Parameter symbol	Parameter description	Value	Units	Sources of parameters
Revised chlorophyll *a* model recalibration				
u_{alg}	Net settling velocity for algal phosphorus	0.031	meter per day	Calibrated using measured total phosphorus and chlorophyll *a* data
*pH**	pH at which the total phosphorus recycle rate is one half the maximum	8.1	NA	Calibrated using measured total phosphorus, chlorophyll *a* and pH data
K_R	Maximum total phosphorus recycle rate	1.31	per year	Calibrated using measured total phosphorus, chlorophyll *a* and pH data
k_{half}	Half-saturation constant for phosphorus limitation of algal growth	0.06	parts per million	Calibrated within range provided by Bowie and others, 1985
Extended dataset recalibration				
K_{na}	Gross removal rate for nonalgal phosphorus	0.016	per day	Calibrated using measured mass balance and total phosphorus data
u_{alg}	Net settling velocity for algal phosphorus	0.07–0.087	meter per day	Calibrated using measured total phosphorus and chlorophyll *a* data
*pH**	pH at which the total phosphorus recycle rate is one half the maximum	8.2–8.3	NA	Calibrated using measured total phosphorus, chlorophyll *a* and pH data
K_R	Maximum total phosphorus recycle rate	1.61–2.09	per year	Calibrated using measured total phosphorus, chlorophyll *a* and pH data
k_{half}	Half-saturation constant for phosphorus limitation of algal growth	0.05–0.06	parts per million	Calibrated within range provided by Bowie and others, 1985
Calculated NPP model input recalibration				
u_{alg}	Net settling velocity for algal phosphorus	0.463	meter per day	Calibrated using measured total phosphorus and chlorophyll *a* data
*pH**	pH at which the total phosphorus recycle rate is one half the maximum	8.9–9	NA	Calibrated using measured total phosphorus, chlorophyll *a* and pH data
K_R	Maximum total phosphorus recycle rate	6.77–7.63	per year	Calibrated using measured total phosphorus, chlorophyll *a* and pH data

Initial development of the TMDL model prior to 2002 relied on limited data (Eilers and others, 2001) for phosphorus concentrations in lake sediment; however, 26 sediment cores subsequently were collected and analyzed during 2005–06 at discrete sediment depths (Simon and others, 2009; Simon and Ingle, 2011). The average sediment phosphorus concentration calculated from the 26 newer cores was about one-third of the concentration used in the initial model calibration; therefore, we performed a sensitivity analysis to determine the significance of the updated sediment data on model output and calibration parameters. The overall effect of the revised sediment phosphorus concentration was to increase the pH-dependent phosphorus recycling rate (K_R) of the model. Given the coupled water-column–lake sediment compartments in the model, the reduced sediment phosphorus concentration caused an increase in K_R, resulting in an overall increase in phosphorus recycling in the lake, regardless of pH.

In Phase 1, the potential contribution of benthic invertebrates to the lake's nutrient cycling was investigated (Wood and others, 2013). Based on sampling in 2009 and 2010, average invertebrate densities in the lake's sediments were high, on the order of 20,000 individuals/m^2 (standard deviation = 11,671). Invertebrate taxa primarily were Oligochaeta (worms, 65 percent), Hirudinea (leeches, 17 percent), and Chironomidae (midges, 12 percent). Invertebrate bioturbation can significantly increase the diffusion and advection of solutes, including nutrients (Michaud and others, 2005, 2006; Mermillod-Blondin and Rosenberg, 2006; Mermillod-Blondin, 2011), and invertebrate metabolic excretion can be a significant flux from the sediments into the water column (Fukuhara and Yasuda, 1985; Fukuhara and Sakamoto, 1987; Devine and Vanni, 2002). In the Phase 1 report, experiments with two types of invertebrate common in UKL produced estimates of metabolic flux of 3.8 [(mg P/m^2)/d]. There is considerable spatial and temporal variation in the actual excretion rates, according to differences in biotic and abiotic factors around the lake, such as sediment characteristics, invertebrate taxa and densities, and water temperatures (which affect growth rates). Such variability cannot be resolved with a CSTR model.

Incorporation of invertebrates into the CSTR TMDL model requires an intermediate step designed to properly "scale up" from individual locations, and is not likely to be as simple as taking a straightforward average of the quantities involved. Scaling up from small scales to the bulk system is discussed further in section, "Lake Metabolism as a Substitute for Algal Growth and Respiration."

Nutrient sources attributable to benthic invertebrates were not differentiated in the original model, but instead were incorporated into a lumped, residual-derived internal loading term. During Phase 1, the implications of bioturbation and excretion in the model were investigated by substituting the original, pH-dependent recycling mechanism with a temperature-dependent recycling mechanism that might apply to invertebrate-caused mechanisms and performing a sensitivity analysis. This did not significantly improve model performance, which indicates that neither the pH-dependent nor the temperature-dependent mechanism is uniquely suited for describing the measurements; rather, any rate-dependent first-order term that generally increased through the spring and summer (such as pH and temperature) would perform approximately equally well with the current CSTR model structure, and any such term probably would have poor performance statistics, particularly over the full validation period.

Research is still needed to refine lake-average benthic invertebrate excretion rates for future use in the model; to resolve interactions between sediment characteristics, invertebrate ecology, and water-column nutrient dynamics; and to support a more spatially explicit lake water-quality model if one is developed in the future. However, the model is not currently configured to use both the temperature-dependent and pH-dependent internal loading mechanisms. Such work would require separate calibrations to establish recycle rates that are independent from each other, which is currently not possible with the available data. Future laboratory work could provide the data necessary to include both of these terms if deemed useful. Incorporating benthic invertebrate recycling as a separate process in the model would provide opportunities to explore management options that could affect invertebrate ecology and to differentiate those effects from other physicochemical effects, such as high-pH induced phosphorus release.

203-Year Simulation and Sensitivity Analysis

Using the revised CSTR model, with variations corresponding to 0- and 40-percent reductions in external loading according to the TMDL (Oregon Department of Environmental Quality, 2002), Wood and others (2013) performed a 203-year simulation, chaining together the original 7-year, April 1991 to April 1998, nutrient budget for the lake (Kann and Walker, 1999) as input data. Model versions that were simulated included the original model and versions with and without the modifications for light and phosphorus limitation, temperature-dependent phosphorus recycling (for benthic invertebrates), and the revised solution (Runga-Kutta) for chlorophyll *a* whereby equilibrium between cyanobacterial biomass and light and nutrients is not necessarily achieved within a given 2-week time step.

All versions of the model, when used to simulate water-column concentrations characterizing a steady state 203 years into the future, produced lower TP concentrations over time, even when no reductions in the external load boundary condition were applied. When 40-percent reductions in the external load boundary condition were applied, the steady-state concentrations were always lower than when no reduction was applied. Within that broadly consistent result, however, there were large variations in the steady-state concentration that could be related to the ratio of the recycling term to the sedimentation term in the mass balance, with higher recycling rates relative to sedimentation resulting in higher concentrations. The values of the recycling and sedimentation terms are directly dependent on the value of the calibration parameters—in particular, the algal settling velocity and the recycling rate.

The phosphorus stored in the sediment reservoir generally—although not always (Wood and others, 2013, versions *O* and *B′*)—decreased over time, and as with the water-column concentrations, there was a wide range in the steady-state value achieved. These ultimate values were related to the ratios of recycled phosphorus mass to sedimented phosphorus mass (Wood and others, 2013, fig. 13) and were therefore related to the values of the calibration parameters. The higher the ratio, indicating that there is more recycling relative to sedimentation, the lower the steady-state phosphorus reservoir. It follows that the steady-state water-column phosphorus concentration was negatively correlated with the steady-state sediment reservoir—a lower steady-state sediment reservoir was associated with higher steady-state water-column phosphorus concentration.

The long-term simulations indicate that the sediment reservoir influences the long-term behavior of the modeled water-column concentrations in an important and possibly counter-intuitive way. The model results indicate that sediment phosphorus does not act as a supply that moves uniformly toward depletion over time. Rather, the model algorithms require the lake water column to reach a steady state in equilibrium with the sediments, and the steady-state conditions in the water column and sediments are determined by the calibration parameters. In some simulations, the size of the sediment phosphorus reservoir remained mostly steady or increased slightly over time as that equilibrium state was approached. A corollary is that the initial size of the sediment reservoir is not as important in determining steady-state conditions as the rate of the lake processes that add phosphorus to the sediment through settling and recycle phosphorus from sediments to the water column (Wood and others, 2013).

Finally, the importance of uncertainty in the values of the algal settling and phosphorus recycling calibration parameters was most apparent for long-term model simulations. Although short-term simulations (up to several years) using the different model versions produced similar results even though the values of these calibration parameters varied by as much as 40 percent, using different calibrated algal settling and phosphorus recycling rates resulted in relatively large differences in water-column concentrations when simulations exceeded several decades. The same was true for simulated sediment phosphorus concentrations. These findings indicate that:

1. The initial size of the sediment reservoir is not as important in determining steady-state conditions as the rates of algal and nonalgal settling and sediment phosphorus recycling;
2. These calibration parameters have a lag effect on nutrient accumulation and dynamics in the lake, where algal and nonalgal settling and sediment recycling in one year affects the water quality in the following year; and
3. The efficacy of external loading reductions is highly dependent on these calibration parameters, which are poorly understood (Wood and others, 2013).

It follows that efforts to bound the rate estimates of algal and nonalgal settling velocities and sediment phosphorus recycling with targeted field-data collection would be a high priority for reducing uncertainty in future lake management decisions.

Phase 2 Model Updates

Wood and others (2013) made several suggestions for updating the model. In particular, reducing uncertainty in the recycling and sedimentation terms is an important future research need. This can be achieved through (1) field measurement of specific parameters needed for the relevant algorithms in the model, or (2) development of new algorithms that would predict these terms from independent environmental data. The calibrated settling velocity in particular remains a challenge to interpret; measuring this parameter directly rather than determining it by calibration of the model (and the difficulty of doing so in a lake ecosystem dominated by buoyant cyanobacteria) is discussed further in section, "Future Model Needs." Field work related to recycling by benthic invertebrates is ongoing and is expected to inform future modeling efforts.

Wood and others (2013) also noted that model performance was limited by the inability of the model to simulate mid-season bloom declines, and suggested that the addition of a "mortality" term for the cyanobacteria would help capture the dynamics of bloom declines. In subsequent sections, we report on new equations to calculate cyanobacterial metabolism in the surface waters, using hourly measurements of DO available from the USGS lake monitoring program from 2006 through 2008 (Lindenberg and others, 2009; Kannarr and others, 2010). These estimates rely on independent data (water temperature, DO, and nutrient concentrations) to predict net primary production (NPP) in the lake, including cyanobacterial biomass and, importantly, the transition in NPP from dominance by primary production (autotrophy) to dominance by community respiration (heterotrophy), which includes aquatic respiration and mortality. This proof-of-concept approach is based on limited available data; additional data collection requirements to more completely develop this modeling framework are discussed in section, "Future Model Needs."

Updated CSTR Model Calibration

One of the important purposes for performing the Phase 2 evaluation of the CSTR model was inclusion of a longer dataset for model calibration because the original model was calibrated over the 1991–98 period. Since that time, data have been collected regularly and a 19-year set (1991–2010) is available for model evaluation (Walker and others, 2012). Model terms and symbols are defined in table 1 and recalibrated parameters, determined through methods outlined below, are presented in table 2.

Reevaluate Phase 1 Test Statistics Using Updated Algal Settling Velocity Calibration, 1991–98

In Phase 1, the final modification to the model structure was developed for the algal submodel. The original TMDL model included the assumption that equilibrium between growth and respiration was achieved during each time step such that net chlorophyll *a* concentration equaled zero. The updated model (versions *D* and *D′*) did not include this assumption and solved the first-order differential equation for chlorophyll *a* using the fourth-order Runge-Kutta numerical solution technique. In Phase 1, the recycling parameters were recalibrated for this model (version *D*), but algal settling velocity was not, and its value was assumed to be equal to that of the chlorophyll *a* equilibrium model (version *B*). In this review, we evaluated the sensitivity of algal settling velocity for a non-equilibrium chlorophyll *a* model, herein referred to as model version *E′*, and the parameter calibration steps follow.

Step 1—Algal Settling Velocity and Half-Saturation Constant

Algal settling velocity and the half-saturation constant (used in the Michaelis-Menten phosphorus limitation algorithm) were reevaluated in tandem over the original 7.5-year dataset following the approach outlined by Kann and

Walker (1999) and used by Wood and others (2013). Algal settling velocity values were assumed to be between 0.001 and 0.2 m/d, and half-saturation constant values were assumed to be between 0.01 and 0.06 ppm (Bowie and others, 1985); the best combination of parameter values was determined by correlating chlorophyll *a* as calculated by equation 1 (using measured phosphorus concentrations) with measured chlorophyll *a* concentrations in June–July for the 1994–98 subset of values. The calibration process minimized the sum of squared errors with the combination of u_{alg}=0.031 m/d and k_{half}=0.06 ppm. These parameter values were similar to values previously determined in Phase 1 of the evaluation.

In the process of recalibrating algal settling velocity, we also evaluated the differences in parameters when other subsets of values were used for calibration besides the previously used 1994–98 subset (Walker, 2001; Wood and others, 2013). We evaluated the subset from June to July over 1991–93 and determined that the sum of squared errors was minimized with the combination of u_{alg}=0.2 m/d and k_{half}=0.02 ppm, which is different than the previously determined set and which indicates an algal settling velocity more than six times greater than the 1994–98 subset and a half saturation constant one-third the value of the original subset. Further inspection of these results showed that 1 year of data, 1992, was primarily responsible for the large changes in calibration parameters, probably due to its higher than average TP and chlorophyll *a* concentrations. When the settling parameters were recalibrated for June–July in all years excluding 1992, the sum of squared errors was minimized with the combination of u_{alg}=0.048 m/d and k_{half}=0.06 ppm. This process highlights the potential sensitivity of the settling velocity to anomalous years and indicates the need for a longer calibration set or, preferably, actual measurement of the parameters.

Step 2—Internal Recycling Parameters

The recycling parameters, pH^* and K_R, also were recalibrated. This calibration step evaluated the recycling equation in the CSTR model by running the model and minimizing the objective function, the product of the mean squared error of the three state variables (Wood and others, 2013, equation 24), for May–July data in 1994–98. The resulting recalibrated parameters were pH^*=8.1 and K_R=1.31/yr, which are similar to those parameters used previously for model version *D′*.

Reevaluation of Phase I Test Statistics Using Extended Data, 1991–2010

The 1991–2010 model input dataset was developed using daily nutrient and hydrologic loading data (Walker and others, 2012), Tule Lake average daily air temperature and solar radiation data from California Irrigation Management Information System site TULELK2.A (University of California, 2014) and Klamath Tribes biweekly/monthly (depending on season) water temperature data (Kann, 2011) from the nine long-term sites. Following Kann and Walker (1999), a multiple regression equation relating average water temperature to the air temperature and solar radiation collected 25 mi away at Tule Lake in northern California was used to determine a biweekly average water temperature value for UKL. The biweekly nutrient and hydrologic loading set was developed by accumulating the daily masses, or volumes, across the biweekly intervals used in the model.

A biweekly dataset of water quality in UKL for the longer calibration period was developed using Klamath Tribes measured biweekly/monthly (depending on season) TP, chlorophyll *a*, and pH data. The data were averaged across space and time to represent the lakewide values for the appropriate biweekly intervals, following the procedure outlined in Kann and Walker (1999). Model parameters were calibrated with the 1991–2010 dataset following the steps outlined by Kann and Walker (1999) for the version herein referred to as *F′*, which used the updated sediment reservoir and growth limitation factors, and the Runge-Kutta algal submodel, corresponding to characteristics of model version *E′*. Recalibrated parameter values are presented in table 2.

Step 1—pH Regression Model Parameters

As reported previously (Wood and others, 2013, equation 20), we performed the initial multiple regression relating pH to the natural logarithm of chlorophyll *a* and Julian day (with a minimum value of 200) in Microsoft Excel® using biweekly, lakewide average chlorophyll *a* concentrations and pH, calculated from biweekly measurements. The regression was evaluated during June–August 1991–2010 and included 123 data points. The model coefficients and performance statistics (coefficient of determination, R^2, and standard error) compared well to those coefficients and statistics originally determined over the 1991–98 period, with R^2 slightly decreased (from 0.80 to 0.74) and standard error slightly increased (from 0.24 to 0.28). We developed a revised pH submodel regression that removed Julian day as an independent variable. This was done to prevent discontinuities in pH when Julian day changed from 365 to 1, an occurrence that was noted in the Phase 1 report (Wood and others, 2013). This new regression model was evaluated for measurements from all months in 1991–2010, as opposed to the shorter, July–August period, which included 242 data points. Again, the model coefficients and performance statistics compared well to the coefficients and statistics used in the previous approach, with R^2 slightly decreased from the original model (from 0.80 to 0.70) and standard error increased (from 0.24 to 0.37), with the reduction in model performance due partly to the change in evaluation dataset. The pH model regression coefficients and statistics are presented in table 3.

Table 3. pH model coefficients and statistics between the original total maximum daily load (TMDL) model for Upper Klamath Lake, Oregon, and the recalibration considering models with and without a Julian day component.

[**Abbreviations**: NA, not applicable; <, less than]

Quantity	Original TMDL value	Recalibration value, calibration months July–August				Recalibration value no Julian, calibration months January–December			
		1991–1998	p–value	1991–2010	p–value	1991–1998	p–value	1991–2010	p–value
pH model: intercept	7.931	7.829	<2e-16	7.729	<2e-16	7.025	<2e–16	7.161	<2e–16
pH model: chlorophyll *a* coefficient	0.5338	0.5514	<2e-16	0.5271	<2e-16	0.430	<2e–16	0.4211	<2e–16
pH model: Julian day coefficient	–0.006	–0.006	0.0169586	–0.005	0.0110999	NA	NA	NA	NA
Julian threshold	200	200	–	200	–	NA	–	NA	–
Coefficient of determination, R^2	0.80	0.78	–	0.74	–	0.73	–	0.71	–
Standard error	0.24	0.25	–	0.28	–	0.37	–	0.37	–
Sample size, N	–	52	–	123	–	113	–	242	–

Step 2—Algal Settling Velocity and Half-Saturation Constant

Algal settling velocity and the half-saturation constant were evaluated in tandem over the extended dataset following the approach by Kann and Walker (1999) and Wood and others (2013). Algal settling velocity values were assumed to be between 0.001 and 0.2 m/d and half-saturation constant values were assumed to be between 0.01 and 0.06 ppm (Bowie and others, 1985); the best value was determined by correlating chlorophyll *a* as calculated by equation 1 (using measured phosphorus concentrations) with measured chlorophyll *a* concentrations in June–July over a dataset consisting of only even years, and a second dataset consisting of only odd years, referred to as model versions F'_E and F'_O, respectively. For calibration performed using odd years, the sum of squared errors was minimized by the combination of u_{alg}=0.070 m/d and k_{half}=0.06 ppm, while the calibration performed over even years minimized the sum of squared errors with the combination of u_{alg}=0.087 m/d and k_{half}=0.05 ppm, indicating similar parameter results between calibration sets.

Step 3—Nonalgal Phosphorus Loss Rate

The nonalgal phosphorus loss rate was evaluated by applying the method outlined by Wood and others (2013) to the longer 1991–2010 dataset. The March–May datasets were isolated, and negligible recycling and predominantly nonalgal phosphorus were assumed. A trial-by-error and least-squares fit process was used for calibration, with K_{na}=0.016/d determined to minimize the sum of squared errors. This value was only slightly larger than the value of 0.015/d determined in the Phase I report and the value of 0.012/d presented in Kann and Walker (1999). The correlation coefficient (R), calculated when comparing "measured" sedimented mass (as determined from a whole-lake mass balance calculation) to the simulated mass, was still low (R=0.28), but had increased from the correlation coefficient calculated for the shorter 1991–98 time period (R=0.19). The regression coefficient was not highly significant (p=0.06). The calibrated value of K_{na} resulted in a lower average value and lower standard deviation as compared to the "measured" set, which was consistent with the results from Phase 1. The comparisons between measured and calculated nonalgal sedimentation are presented in table 4.

Step 4—Internal Recycling Parameters

The final calibration step was to evaluate the recycling equation in the CSTR model, which depended on two parameters, pH^* and K_R, by running the model and minimizing the objective function (Wood and others, 2013, equation 24). For this analysis, summation is over all May–July data in both odd and even years, versions F'_O and F'_E, respectively, and two sets of recycling parameters were compared. For calibration performed using odd years, the objective function was minimized with the combination of pH^*=8.2 and K_R=1.61/year and for calibration performed using even years, the objective function was minimized with the combination of pH^*=8.3 and K_R=2.09/year.

Two observations help with the interpretation of the calibration results of the various model versions. First, when the assumption of equilibrium was made in the algal submodel (versions O', A', B' and C'), the resulting pH^* values were greater than 8.6; however, when a Runge-Kutta technique was used to estimate for chlorophyll *a* (versions D', E' and F'), the pH^* values always were less than or equal to 8.3. This has important implications for the steady-state response of

Table 4. Descriptive statistics between measured and calculated nonalgal phosphorus mass lost to sedimentation during March–May, Upper Klamath Lake, Oregon, 1991–2010.

[Description of model parameters are shown in table 2. **Abbreviations**: kg, kilogram; NA, not applicable]

Mass lost to sedimentation	1991–1998		1991–2010	
	Average (kg)	Standard deviation (kg)	Average (kg)	Standard deviation (kg)
Calculated from measured (mass balance)	9,008	6,608	9,415	6,001
Calculated with K_{na} = 0.012 d^{-1} (original model value)	6,781	1,813	6,800	1,567
Calculated with K_{na} = 0.015 d^{-1} (recalibrated model value)	8,476	2,267	8,499	1,959
Calculated with K_{na} = 0.016 d^{-1} (recalibrated model value)	NA	NA	9,066	2,089

the model (discussed in section, "Model Performance"), as the lower *pH** threshold results in a more even distribution of bloom magnitude over many years, whereas the higher *pH** threshold results in a more bimodal response, in which blooms are large in some years and nearly nonexistent in others. Second, for a given initial sediment reservoir and recycling mechanism (but regardless of modifications to the limitation factors or algal submodel assumptions), a positive correlation was made between u_{alg} and K_R ($\rho = 0.71$, $p = 0.14$); for example, compare versions O', A', B', E', F'_O and F'_E. Therefore, any modification that increases the recycle rate also increases the algal settling velocity, and vice versa.

Model Performance

Recalibrating the model parameters for the updated chlorophyll *a* solution method (version E') resulted in little change or improvement in model performance statistics, partly because the parameters changed little. When the full validation period was considered (tables 5–7), the statistics were similar, although generally lower in the newly recalibrated model version E', for all variables. When the May–July months were isolated and evaluated for performance, model version E' performed similarly to model version D', but had slightly lower correlation coefficient, coefficient of determination, and Nash-Sutcliffe (NS) values and slightly greater root mean square error (RMSE) (tables 8–10). Overall, the model performance was not substantially changed by the parameter recalibration over the 1991–98 period even though the parameters changed.

Recalibrating the model parameters with the extended dataset (versions F'_O and F'_E) resulted in little change or improvement in model performance statistics when compared to model version E'. The performance statistics were similar for all variables when respective full validation periods were considered (tables 5–7), although model version E' tended to have slightly better performance for all variables. The performance statistics for the recalibrated models were best for pH, with correlation coefficients greater than 0.60 and NS values greater than 0.34; however, statistics for TP and chlorophyll *a* did not necessarily indicate good model performance, with correlation coefficients less than 0.45 and NS values less than 0.05. When May–July months were isolated for validation (tables 8–10), the statistics indicated better performance for all variables than when the full years were considered. However, the May–July statistics for the model calibrated and validated over the extended period (versions F'_O and F'_E) were not very different than statistics for the model calibrated and validated over the original 7.5-year period (version E'). The performance statistics were best in both model versions for TP and pH and worst for chlorophyll *a*. For TP, R^2 values were 0.61–0.64, and NS values were 0.53–0.59; for pH, R^2 values were 0.60–0.66, and NS values were 0.48–0.59; and for chlorophyll *a*, R^2 values were 0.39–0.45, and NS values were 0.27–0.32.

In figure 2, the simulated TP, chlorophyll *a*, and pH values were compared to measured values for 1991–2010 for model versions E', F'_O, and F'_E. The differences in the results of the three models appear small relative to the differences between measured and simulated values. All simulations represent a smoothed fit of the measurements, and all do a generally poor job of capturing the extremes in the data. In the graphs of TP and chlorophyll *a*, the downward trend is apparent in the simulated values that approach steady state (<200 ppb for TP and <150 ppb for chlorophyll *a*) within the 19-year data period. This downward trend was due to the combination of smaller sediment reservoir, increased recycling rates, and decreased *pH** values that allow sediment recycling to begin at lower lake-average pH values and last for a longer time period. These three components cause the recalibrated model to approach steady state relatively quickly.

Table 5. Performance statistics for total phosphorus obtained over the indicated validation periods for model versions discussed in the report.

[**Model characteristics:** EQ, Chlorophyll *a* concentration evaluated by setting dB/dt to 0; RK, Chlorophyll *a* concentration evaluated using Runge-Kutta approach; JULIAN, pH model with Julian day dependence; NO_JULIAN, pH model without Julian day dependence; INIT, Initial size of sediment reservoir calculated with original starting concentration 1,000 milligrams of phosphorus per kilogram of sediment; INIT_NEW, Initial size of sediment reservoir recalculated with starting concentration 335 milligrams of phosphorus per kilogram of sediment; REC_pH, Model relies on pH-dependent recycle mechanism; REC_T, model relies on temperature-dependent recycle mechanism; P_00, Phosphorus limitation factor calculated as the percent of non-algal phosphorus; P_MM, Phosphorus limitation factor calculated by Michaelis-Menten kinetics; L_AVG, Light limitation factor calculated using the average light intensity; L_DI, Average light limitation factor calculated by depth-integrating the light limitation equation. **Model calibration parameters:** Model characteristics and parameters are defined in the text and tables 1 and 2. **Performance statistics**: R, correlation coefficient; R^2, coefficient of determination; N, sample size; RMSE, root mean square error; NS, Nash-Sutcliffe statistic. **Abbreviations:** m d^{-1}, meter per day; yr^{-1}, year; °C, degrees Celsius; ppm, parts per million]

Model version	Compare to version	Model characteristics						Validation period
		Chlorophyll *a* model	pH model	Initial sediment reservoir	Recycle mechanism	Phosphorus limitation	Light limitation	
The rows below are repeated from Phase 1 (Wood and others, 2013, table 9)								
Original model with original calibration								
O		EQ	JULIAN	INIT	REC_pH	P_00	L_AVG	All months 1991–1993 and August–April 1994–1998
O′	*O*	EQ	JULIAN	INIT_NEW	REC_pH	P_00	L_AVG	All months 1991–1993 and August–April 1994–1998
Recalibration of original model								
A	*O*	EQ	JULIAN	INIT	REC_pH	P_00	L_AVG	All months 1991–1993 and August–April 1994–1998
A′	*A*	EQ	JULIAN	INIT_NEW	REC_pH	P_00	L_AVG	All months 1991–1993 and August–April 1994–1998
Modifications to light and phosphorus limitation								
B	*A*	EQ	JULIAN	INIT	REC_pH	P_MM	L_DI	All months 1991–1993 and August–April 1994–1998
B′	*B*	EQ	JULIAN	INIT_NEW	REC_pH	P_MM	L_DI	All months 1991–1993 and August–April 1994–1998
Temperature-dependent recycling								
C	*B*	EQ	JULIAN	INIT	REC_T	P_MM	L_DI	All months 1991–1993 and August–April 1994–1998
C′	*C*	EQ	JULIAN	INIT_NEW	REC_T	P_MM	L_DI	All months 1991–1993 and August–April 1994–1998
Runge-Kutta solution of chlorophyll *a*								
D	*B*	RK	JULIAN	INIT	REC_pH	P_MM	L_DI	All months 1991–1993 and August–April 1994–1998
D′	*D*	RK	JULIAN	INIT_NEW	REC_pH	P_MM	L_DI	All months 1991–1993 and August–April 1994–1998

Model version	Compare to version	Model calibration parameters						Performance statistics					
		u_{alg} (m d^{-1})	K_R (yr^{-1})	*pH**	K_T (yr^{-1})	$T_{(min,rec)}$ (°C)	k_{half} (ppm)	R	R^2	N	Bias (ppb)	RMSE (ppb)	NS
The rows below are repeated from Phase I (Wood and others, 2013, table 9)—Continued													
Original model with original calibration													
O		0.05	0.53	9.1	NA	NA	NA	0.56	0.32	83	-48.6	109.6	-0.58
O′	*O*	0.05	1.33	9.0	NA	NA	NA	0.60	0.36	83	-23.3	83.7	0.08
Recalibration of original model													
A	*O*	0.059	0.47	9.0	NA	NA	NA	0.59	0.35	83	-24.7	86.9	0.01
A′	*A*	0.059	1.24	8.9	NA	NA	NA	0.61	0.38	83	-10.4	75.1	0.26
Modifications to light and phosphorus limitation													
B	*A*	0.035	0.32	8.6	NA	NA	0.06	0.58	0.34	83	-23.3	82.8	0.10
B′	*B*	0.035	1.05	8.7	NA	NA	0.06	0.60	0.35	83	-23.4	83.1	0.10
Temperature-dependent recycling													
C	*B*	0.035	NA	NA	0.54	12.8	0.06	0.59	0.35	83	-31.8	90.7	-0.08
C′	*C*	0.035	NA	NA	1.62	12.8	0.06	0.60	0.36	83	-25.1	84.8	0.06
Runge-Kutta solution of chlorophyll *a*													
D	*B*	0.035	0.34	8.1	NA	NA	0.06	0.38	0.15	83	-60.0	114.9	-0.73
D′	*D*	0.035	1.18	8.1	NA	NA	0.06	0.39	0.15	83	-52.6	109.9	-0.59

Table 5. Performance statistics for total phosphorus obtained over the indicated validation periods for model versions discussed in the report.—Continued

[**Model characteristics:** EQ, Chlorophyll *a* concentration evaluated by setting dB/dt to 0; RK, Chlorophyll *a* concentration evaluated using Runge-Kutta approach; JULIAN, pH model with Julian day dependence; NO_JULIAN, pH model without Julian day dependence; INIT, Initial size of sediment reservoir calculated with original starting concentration 1,000 milligrams of phosphorus per kilogram of sediment; INIT_NEW, Initial size of sediment reservoir recalculated with starting concentration 335 milligrams of phosphorus per kilogram of sediment; REC_pH, Model relies on pH-dependent recycle mechanism; REC_T, model relies on temperature-dependent recycle mechanism; P_00, Phosphorus limitation factor calculated as the percent of non-algal phosphorus; P_MM, Phosphorus limitation factor calculated by Michaelis-Menten kinetics; L_AVG, Light limitation factor calculated using the average light intensity; L_DI, Average light limitation factor calculated by depth-integrating the light limitation equation. **Model calibration parameters:** Model characteristics and parameters are defined in the text and tables 1 and 2. **Performance statistics**: R, correlation coefficient; R^2, coefficient of determination; N, sample size; RMSE, root mean square error; NS, Nash-Sutcliffe statistic. **Abbreviations:** m d^{-1}, meter per day; yr^{-1}, year; °C, degrees Celsius; ppm, parts per million]

Model version	Compare to version	Model characteristics						Validation period
		Chlorophyll *a* model	pH model	Initial sediment reservoir	Recycle mechanism	Phosphorus limitation	Light limitation	
The rows below were generated for Phase 2								
Runge-Kutta solution of chlorophyll *a* with updated settling velocity and model structure, 7.5-year calibration set								
E'	D'	RK	NO_JULIAN	INIT_NEW	REC_pH	P_MM	L_DI	All months 1991–1993 and August–April 1994–1998
Runge-Kutta solution of chlorophyll *a* with updated settling velocity and model structure, 19-year calibration set								
F'_O	E'	RK	NO_JULIAN	INIT_NEW	REC_pH	P_MM	L_DI	All months even years and August–April odd years
F'_O	G'	RK	NO_JULIAN	INIT_NEW	REC_pH	P_MM	L_DI	All months 2006–2008
F'_E	E'	RK	NO_JULIAN	INIT_NEW	REC_pH	P_MM	L_DI	All months odd years and August–April even years
F'_E	G'	RK	NO_JULIAN	INIT_NEW	REC_pH	P_MM	L_DI	All months 2006–2008
Runge-Kutta solution of chlorophyll *a* with calculated metabolism 2006–2008								
G'_1	F'	RK	NO_JULIAN	INIT_NEW	REC_pH	NA	NA	All months 2006
G'_2	F'	RK	NO_JULIAN	INIT_NEW	REC_pH	NA	NA	All months 2007
G'_3	F'	RK	NO_JULIAN	INIT_NEW	REC_pH	NA	NA	All months 2008

Model version	Compare to version	Model calibration parameters						Performance statistics					
		u_{alg} (m d^{-1})	K_R (yr^{-1})	*pH**	K_T (yr^{-1})	$T_{(min,rec)}$ (°C)	k_{half} (ppm)	R	R^2	N	Bias (ppb)	RMSE (ppb)	NS
The rows below were generated for Phase 2—Continued													
Runge-Kutta solution of chlorophyll *a* with updated settling velocity and model structure, 7.5-year calibration set													
E'	D'	0.031	1.31	8.1	NA	NA	0.06	0.34	0.11	83	-59.7	119.6	-0.88
Runge-Kutta solution of chlorophyll *a* with updated settling velocity and model structure, 19-year calibration set													
F'_O	E'	0.070	1.61	8.2	NA	NA	0.06	0.38	0.15	183	7.9	90.2	0.05
F'_O	G'	0.070	1.61	8.2	NA	NA	0.06	0.69	0.48	33	61.7	102.7	0.04
F'_E	E'	0.087	2.09	8.3	NA	NA	0.05	0.39	0.16	181	2.2	92.1	-0.03
F'_E	G'	0.087	2.09	8.3	NA	NA	0.05	0.72	0.52	33	54.9	93.9	0.20
Runge-Kutta solution of chlorophyll *a* with calculated metabolism 2006–2008													
G'_1	F'	0.463	6.77	8.9	NA	NA	NA	0.91	0.82	9	2.3	37.9	0.82
G'_2	F'	0.463	7.63	9	NA	NA	NA	0.44	0.19	9	40.5	109.5	0.04
G'_3	F'	0.463	6.76	8.9	NA	NA	NA	0.84	0.71	9	1.8	43.2	0.71

Table 6. Performance statistics for chlorophyll *a* obtained over the indicated validation periods for model versions discussed in the report.

[**Model characteristics:** EQ, Chlorophyll *a* concentration evaluated by setting dB/dt to 0; RK, Chlorophyll *a* concentration evaluated using Runge-Kutta approach; JULIAN, pH model with Julian day dependence; NO_JULIAN, pH model without Julian day dependence; INIT, Initial size of sediment reservoir calculated with original starting concentration 1,000 milligrams of phosphorus per kilogram of sediment; INIT_NEW, Initial size of sediment reservoir recalculated with starting concentration 335 milligrams of phosphorus per kilogram of sediment; REC_pH, Model relies on pH-dependent recycle mechanism; REC_T, model relies on temperature-dependent recycle mechanism; P_00, Phosphorus limitation factor calculated as the percent of non-algal phosphorus; P_MM, Phosphorus limitation factor calculated by Michaelis-Menten kinetics; L_AVG, Light limitation factor calculated using the average light intensity; L_DI, Average light limitation factor calculated by depth-integrating the light limitation equation. **Model calibration parameters:** Model characteristics and parameters are defined in the text and tables 1 and 2. **Performance statistics**: R, correlation coefficient; R^2, coefficient of determination; N, sample size; RMSE, root mean square error; NS, Nash-Sutcliffe statistic. **Abbreviations:** m d^{-1}, meter per day; yr^{-1}, year; °C, degrees Celsius; ppm, parts per million]

Model version	Compare to version	Model characteristics						Validation period
		Chlorophyll *a* model	pH model	Initial sediment reservoir	Recycle mechanism	Phosphorus limitation	Light limitation	
The rows below are repeated from Phase I (Wood and others, 2013, table 10)								
Original model with original calibration								
O		EQ	JULIAN	INIT	REC_pH	P_00	L_AVG	All months 1991–1993 and August–April 1994–1998
O′	*O*	EQ	JULIAN	INIT_NEW	REC_pH	P_00	L_AVG	All months 1991–1993 and August–April 1994–1998
Recalibration of original model								
A	*O*	EQ	JULIAN	INIT	REC_pH	P_00	L_AVG	All months 1991–1993 and August–April 1994–1998
A′	*A*	EQ	JULIAN	INIT_NEW	REC_pH	P_00	L_AVG	All months 1991–1993 and August–April 1994–1998
Modifications to light and phosphorus limitation								
B	*A*	EQ	JULIAN	INIT	REC_pH	P_MM	L_DI	All months 1991–1993 and August–April 1994–1998
B′	*B*	EQ	JULIAN	INIT_NEW	REC_pH	P_MM	L_DI	All months 1991–1993 and August–April 1994–1998
Temperature-dependent recycling								
C	*B*	EQ	JULIAN	INIT	REC_T	P_MM	L_DI	All months 1991–1993 and August–April 1994–1998
C′	*C*	EQ	JULIAN	INIT_NEW	REC_T	P_MM	L_DI	All months 1991–1993 and August–April 1994–1998
Runge-Kutta solution of chlorophyll *a*								
D	*B*	RK	JULIAN	INIT	REC_pH	P_MM	L_DI	All months 1991–1993 and August–April 1994–1998
D′	*D*	RK	JULIAN	INIT_NEW	REC_pH	P_MM	L_DI	All months 1991–1993 and August–April 1994–1998

Model version	Compare to version	Model calibration parameters						Performance statistics					
		u_{alg} (m d^{-1})	K_R (yr^{-1})	*pH**	K_T (yr^{-1})	$T_{(min,rec)}$ (°C)	k_{half} (ppm)	R	R^2	N	Bias (ppb)	RMSE (ppb)	NS
The rows below are repeated from Phase I (Wood and others, 2013, table 10)—Continued													
Original model with original calibration													
O		0.05	0.53	9.1	NA	NA	NA	0.42	0.17	83	-56.5	129.6	-1.77
O′	*O*	0.05	1.33	9.0	NA	NA	NA	0.43	0.18	83	-45.7	115.0	-1.18
Recalibration of original model													
A	*O*	0.059	0.47	9.0	NA	NA	NA	0.42	0.18	83	-41.1	112.3	-1.08
A′	*A*	0.059	1.24	8.9	NA	NA	NA	0.43	0.18	83	-34.7	103.9	-0.78
Modifications to light and phosphorus limitation													
B	*A*	0.035	0.32	8.6	NA	NA	0.06	0.40	0.16	83	-51.1	127.5	-1.68
B′	*B*	0.035	1.05	8.7	NA	NA	0.06	0.40	0.16	83	-52.0	129.6	-1.77
Temperature-dependent recycling													
C	*B*	0.035	NA	NA	0.54	12.8	0.06	0.36	0.13	83	-59.2	143.3	-2.39
C′	*C*	0.035	NA	NA	1.62	12.8	0.06	0.37	0.14	83	-55.7	138.4	-2.16
Runge-Kutta solution of chlorophyll *a*													
D	*B*	0.035	0.34	8.1	NA	NA	0.06	0.48	0.23	83	-61.0	114.4	-1.16
D′	*D*	0.035	1.18	8.1	NA	NA	0.06	0.48	0.23	83	-57.2	112.3	-1.08

Table 6. Performance statistics for chlorophyll *a* obtained over the indicated validation periods for model versions discussed in the report.—Continued

[**Model characteristics:** EQ, Chlorophyll *a* concentration evaluated by setting dB/dt to 0; RK, Chlorophyll *a* concentration evaluated using Runge-Kutta approach; JULIAN, pH model with Julian day dependence; NO_JULIAN, pH model without Julian day dependence; INIT, Initial size of sediment reservoir calculated with original starting concentration 1,000 milligrams of phosphorus per kilogram of sediment; INIT_NEW, Initial size of sediment reservoir recalculated with starting concentration 335 milligrams of phosphorus per kilogram of sediment; REC_pH, Model relies on pH-dependent recycle mechanism; REC_T, model relies on temperature-dependent recycle mechanism; P_00, Phosphorus limitation factor calculated as the percent of non-algal phosphorus; P_MM, Phosphorus limitation factor calculated by Michaelis-Menten kinetics; L_AVG, Light limitation factor calculated using the average light intensity; L_DI, Average light limitation factor calculated by depth-integrating the light limitation equation. **Model calibration parameters:** Model characteristics and parameters are defined in the text and tables 1 and 2. **Performance statistics**: R, correlation coefficient; R^2, coefficient of determination; N, sample size; RMSE, root mean square error; NS, Nash-Sutcliffe statistic. **Abbreviations:** m d^{-1}, meter per day; yr^{-1}, year; °C, degrees Celsius; ppm, parts per million]

Model version	Compare to version	Model characteristics						Validation period
		Chlorophyll *a* model	pH model	Initial sediment reservoir	Recycle mechanism	Phosphorus limitation	Light limitation	
The rows below were generated for Phase 2								
Runge-Kutta solution of chlorophyll *a* with updated settling velocity and model structure, 7.5-year calibration set								
E'	D'	RK	NO_JULIAN	INIT_NEW	REC_pH	P_MM	L_DI	All months 1991–1993 and August–April 1994–1998
Runge-Kutta solution of chlorophyll *a* with updated settling velocity and model structure, 19-year calibration set								
F'_O	E'	RK	NO_JULIAN	INIT_NEW	REC_pH	P_MM	L_DI	All months even years and August–April odd years
F'_O	G'	RK	NO_JULIAN	INIT_NEW	REC_pH	P_MM	L_DI	All months 2006–2008
F'_E	E'	RK	NO_JULIAN	INIT_NEW	REC_pH	P_MM	L_DI	All months odd years and August–April even years
F'_E	G'	RK	NO_JULIAN	INIT_NEW	REC_pH	P_MM	L_DI	All months 2006–2008
Runge-Kutta solution of chlorophyll *a* with calculated metabolism 2006–2008								
G'_1	F'	RK	NO_JULIAN	INIT_NEW	REC_pH	NA	NA	All months 2006
G'_2	F'	RK	NO_JULIAN	INIT_NEW	REC_pH	NA	NA	All months 2007
G'_3	F'	RK	NO_JULIAN	INIT_NEW	REC_pH	NA	NA	All months 2008

Model version	Compare to version	Model calibration parameters						Performance statistics					
		u_{alg} (m d^{-1})	K_R (yr^{-1})	*pH**	K_T (yr^{-1})	$T_{(min,rec)}$ (°C)	k_{half} (ppm)	R	R^2	N	Bias (ppb)	RMSE (ppb)	NS
The rows below were generated for Phase 2—Continued													
Runge-Kutta solution of chlorophyll *a* with updated settling velocity and model structure, 7.5-year calibration set													
E'	D'	0.031	1.31	8.1	NA	NA	0.06	0.46	0.21	83	-63.9	121.9	-1.45
Runge-Kutta solution of chlorophyll *a* with updated settling velocity and model structure, 19-year calibration set													
F'_O	E'	0.070	1.61	8.2	NA	NA	0.06	0.45	0.20	183	0.183	79.6	-0.02
F'_O	G'	0.070	1.61	8.2	NA	NA	0.06	0.52	0.27	33	22.0	77.6	0.17
F'_E	E'	0.087	2.09	8.3	NA	NA	0.05	0.42	0.18	181	-3.1	81.9	-0.16
F'_E	G'	0.087	2.09	8.3	NA	NA	0.05	0.50	0.25	33	17.0	79.2	0.14
Runge-Kutta solution of chlorophyll *a* with calculated metabolism 2006–2008													
G'_1	F'	0.463	6.77	8.9	NA	NA	NA	0.44	0.19	9	8.2	68.0	0.13
G'_2	F'	0.463	7.63	9	NA	NA	NA	0.66	0.43	9	26.7	60.9	0.18
G'_3	F'	0.463	6.76	8.9	NA	NA	NA	0.52	0.27	9	40.1	96.6	0.08

Table 7. Performance statistics for pH obtained over the indicated validation periods for model versions discussed in the report.

[**Model characteristics:** EQ, Chlorophyll *a* concentration evaluated by setting dB/dt to 0; RK, Chlorophyll *a* concentration evaluated using Runge-Kutta approach; JULIAN, pH model with Julian day dependence; NO_JULIAN, pH model without Julian day dependence; INIT, Initial size of sediment reservoir calculated with original starting concentration 1,000 milligrams of phosphorus per kilogram of sediment; INIT_NEW, Initial size of sediment reservoir recalculated with starting concentration 335 milligrams of phosphorus per kilogram of sediment; REC_pH, Model relies on pH-dependent recycle mechanism; REC_T, model relies on temperature-dependent recycle mechanism; P_00, Phosphorus limitation factor calculated as the percent of non-algal phosphorus; P_MM, Phosphorus limitation factor calculated by Michaelis-Menten kinetics; L_AVG, Light limitation factor calculated using the average light intensity; L_DI, Average light limitation factor calculated by depth-integrating the light limitation equation. **Model calibration parameters:** Model characteristics and parameters are defined in the text and tables 1 and 2. **Performance statistics**: R, correlation coefficient; R^2, coefficient of determination; N, sample size; RMSE, root mean square error; NS, Nash-Sutcliffe statistic. **Abbreviations:** m d^{-1}, meter per day; yr^{-1}, year; °C, degrees Celsius; ppm, parts per million]

Model version	Compare to version	Model characteristics						Validation period
		Chlorophyll *a* model	pH model	Initial sediment reservoir	Recycle mechanism	Phosphorus limitation	Light limitation	
The rows below are repeated from Phase I (Wood and others, 2013, table 11)								
Original model with original calibration								
O		EQ	JULIAN	INIT	REC_pH	P_00	L_AVG	All months 1991–1993 and August–April 1994–1998
O′	*O*	EQ	JULIAN	INIT_NEW	REC_pH	P_00	L_AVG	All months 1991–1993 and August–April 1994–1998
Recalibration of original model								
A	*O*	EQ	JULIAN	INIT	REC_pH	P_00	L_AVG	All months 1991–1993 and August–April 1994–1998
A′	*A*	EQ	JULIAN	INIT_NEW	REC_pH	P_00	L_AVG	All months 1991–1993 and August–April 1994–1998
Modifications to light and phosphorus limitation								
B	*A*	EQ	JULIAN	INIT	REC_pH	P_MM	L_DI	All months 1991–1993 and August–April 1994–1998
B′	*B*	EQ	JULIAN	INIT_NEW	REC_pH	P_MM	L_DI	All months 1991–1993 and August–April 1994–1998
Temperature-dependent recycling								
C	*B*	EQ	JULIAN	INIT	REC_T	P_MM	L_DI	All months 1991–1993 and August–April 1994–1998
C′	*C*	EQ	JULIAN	INIT_NEW	REC_T	P_MM	L_DI	All months 1991–1993 and August–April 1994–1998
Runge-Kutta solution of chlorophyll *a*								
D	*B*	RK	JULIAN	INIT	REC_pH	P_MM	L_DI	All months 1991–1993 and August–April 1994–1998
D′	*D*	RK	JULIAN	INIT_NEW	REC_pH	P_MM	L_DI	All months 1991–1993 and August–April 1994–1998

Model version	Compare to version	Model calibration parameters						Performance statistics					
		u_{alg} (m d^{-1})	K_R (yr^{-1})	*pH**	K_T (yr^{-1})	$T_{(min,rec)}$ (°C)	k_{half} (ppm)	R	R^2	N	Bias	RMSE	NS
The rows below are repeated from Phase I (Wood and others, 2013, table 11)—Continued													
Original model with original calibration													
O		0.05	0.53	9.1	NA	NA	NA	0.57	0.32	83	-0.195	0.716	-0.09
O′	*O*	0.05	1.33	9.0	NA	NA	NA	0.56	0.32	83	-0.175	0.703	-0.05
Recalibration of original model													
A	*O*	0.059	0.47	9.0	NA	NA	NA	0.56	0.31	83	-0.155	0.700	-0.04
A′	*A*	0.059	1.24	8.9	NA	NA	NA	0.55	0.31	83	-0.143	0.694	-0.02
Modifications to light and phosphorus limitation													
B	*A*	0.035	0.32	8.6	NA	NA	0.06	0.57	0.33	83	-0.161	0.704	-0.05
B′	*B*	0.035	1.05	8.7	NA	NA	0.06	0.58	0.33	83	-0.157	0.699	-0.04
Temperature-dependent recycling													
C	*B*	0.035	NA	NA	0.54	12.8	0.06	0.57	0.32	83	-0.175	0.716	-0.09
C′	*C*	0.035	NA	NA	1.62	12.8	0.06	0.57	0.32	83	-0.168	0.712	-0.07
Runge-Kutta solution of chlorophyll *a*													
D	*B*	0.035	0.34	8.1	NA	NA	0.06	0.64	0.41	83	-0.247	0.622	0.18
D′	*D*	0.035	1.18	8.1	NA	NA	0.06	0.65	0.42	83	-0.235	0.612	0.21

Table 7. Performance statistics for pH obtained over the indicated validation periods for model versions discussed in the report.—Continued

[**Model characteristics:** EQ, Chlorophyll *a* concentration evaluated by setting dB/dt to 0; RK, Chlorophyll *a* concentration evaluated using Runge-Kutta approach; JULIAN, pH model with Julian day dependence; NO_JULIAN, pH model without Julian day dependence; INIT, Initial size of sediment reservoir calculated with original starting concentration 1,000 milligrams of phosphorus per kilogram of sediment; INIT_NEW, Initial size of sediment reservoir recalculated with starting concentration 335 milligrams of phosphorus per kilogram of sediment; REC_pH, Model relies on pH-dependent recycle mechanism; REC_T, model relies on temperature-dependent recycle mechanism; P_00, Phosphorus limitation factor calculated as the percent of non-algal phosphorus; P_MM, Phosphorus limitation factor calculated by Michaelis-Menten kinetics; L_AVG, Light limitation factor calculated using the average light intensity; L_DI, Average light limitation factor calculated by depth-integrating the light limitation equation. **Model calibration parameters:** Model characteristics and parameters are defined in the text and tables 1 and 2. **Performance statistics**: R, correlation coefficient; R^2, coefficient of determination; N, sample size; RMSE, root mean square error; NS, Nash-Sutcliffe statistic. **Abbreviations:** m d^{-1}, meter per day; yr^{-1}, year; °C, degrees Celsius; ppm, parts per million]

Model version	Compare to version	Model characteristics						Validation period
		Chlorophyll *a* model	pH model	Initial sediment reservoir	Recycle mechanism	Phosphorus limitation	Light limitation	
The rows below were generated for Phase 2								
Runge-Kutta solution of chlorophyll *a* with updated settling velocity and model structure, 7.5-year calibration set								
E'	D'	RK	NO_JULIAN	INIT_NEW	REC_pH	P_MM	L_DI	All months 1991–1993 and August–April 1994–1998
Runge-Kutta solution of chlorophyll *a* with updated settling velocity and model structure, 19-year calibration set								
F'_O	E'	RK	NO_JULIAN	INIT_NEW	REC_pH	P_MM	L_DI	All months even years and August–April odd years
F'_O	G'	RK	NO_JULIAN	INIT_NEW	REC_pH	P_MM	L_DI	All months 2006–2008
F'_E	E'	RK	NO_JULIAN	INIT_NEW	REC_pH	P_MM	L_DI	All months odd years and August–April even years
F'_E	G'	RK	NO_JULIAN	INIT_NEW	REC_pH	P_MM	L_DI	All months 2006–2008
Runge-Kutta solution of chlorophyll *a* with calculated metabolism 2006–2008								
G'_1	F'	RK	NO_JULIAN	INIT_NEW	REC_pH	NA	NA	All months 2006
G'_2	F'	RK	NO_JULIAN	INIT_NEW	REC_pH	NA	NA	All months 2007
G'_3	F'	RK	NO_JULIAN	INIT_NEW	REC_pH	NA	NA	All months 2008

Model version	Compare to version	Model calibration parameters						Performance statistics					
		u_{alg} (m d^{-1})	K_R (yr^{-1})	*pH**	K_T (yr^{-1})	$T_{(min,rec)}$ (°C)	k_{half} (ppm)	R	R^2	N	Bias	RMSE	NS
The rows below were generated for Phase 2—Continued													
Runge-Kutta solution of chlorophyll *a* with updated settling velocity and model structure, 7.5-year calibration set													
E'	D'	0.031	1.31	8.1	NA	NA	0.06	0.55	0.30	83	-0.327	0.694	-0.02
Runge-Kutta solution of chlorophyll *a* with updated settling velocity and model structure, 19-year calibration set													
F'_O	E'	0.070	1.61	8.2	NA	NA	0.06	0.63	0.40	183	-0.055	0.534	0.38
F'_O	G'	0.070	1.61	8.2	NA	NA	0.06	0.73	0.53	33	0.183	0.502	0.46
F'_E	E'	0.087	2.09	8.3	NA	NA	0.05	0.60	0.37	181	-0.038	0.552	0.34
F'_E	G'	0.087	2.09	8.3	NA	NA	0.05	0.72	0.53	33	0.182	0.504	0.45
Runge-Kutta solution of chlorophyll *a* with calculated metabolism 2006–2008													
G'_1	F'	0.463	6.77	8.9	NA	NA	NA	0.70	0.50	9	0.067	0.572	0.42
G'_2	F'	0.463	7.63	9	NA	NA	NA	0.76	0.58	9	0.431	0.548	-0.23
G'_3	F'	0.463	6.76	8.9	NA	NA	NA	0.77	0.59	9	0.167	0.366	0.48

Table 8. Performance statistics for total phosphorus obtained over the indicated May–July validation periods for model versions discussed in the report.

[**Model characteristics:** EQ, Chlorophyll *a* concentration evaluated by setting dB/dt to 0; RK, Chlorophyll *a* concentration evaluated using Runge-Kutta approach; JULIAN, pH model with Julian day dependence; NO_JULIAN, pH model without Julian day dependence; INIT, Initial size of sediment reservoir calculated with original starting concentration 1,000 milligrams of phosphorus per kilogram of sediment; INIT_NEW, Initial size of sediment reservoir recalculated with starting concentration 335 milligrams of phosphorus per kilogram of sediment; REC_pH, Model relies on pH-dependent recycle mechanism; REC_T, model relies on temperature-dependent recycle mechanism; P_00, Phosphorus limitation factor calculated as the percent of non-algal phosphorus; P_MM, Phosphorus limitation factor calculated by Michaelis-Menten kinetics; L_AVG, Light limitation factor calculated using the average light intensity; L_DI, Average light limitation factor calculated by depth-integrating the light limitation equation. **Model calibration parameters:** Model characteristics and parameters are defined in the text and tables 1 and 2. **Performance statistics**: R, correlation coefficient; R^2, coefficient of determination; N, sample size; RMSE, root mean square error; NS, Nash-Sutcliffe statistic. **Abbreviations:** m d^{-1}, meter per day; yr^{-1}, year; °C, degrees Celsius; ppm, parts per million]

Model version	Compare to version	Model characteristics						Validation period
		Chlorophyll *a* model	pH model	Initial sediment reservoir	Recycle mechanism	Phosphorus limitation	Light limitation	
The rows below are repeated from Phase I (Wood and others, 2013, table 12)								
Original model with original calibration								
O		EQ	JULIAN	INIT	REC_pH	P_00	L_AVG	May–July 1991–1993
O′	*O*	EQ	JULIAN	INIT_NEW	REC_pH	P_00	L_AVG	May–July 1991–1993
Recalibration of original model								
A	*O*	EQ	JULIAN	INIT	REC_pH	P_00	L_AVG	May–July 1991–1993
A′	*A*	EQ	JULIAN	INIT_NEW	REC_pH	P_00	L_AVG	May–July 1991–1993
Modifications to light and phosphorus limitation								
B	*A*	EQ	JULIAN	INIT	REC_pH	P_MM	L_DI	May–July 1991–1993
B′	*B*	EQ	JULIAN	INIT_NEW	REC_pH	P_MM	L_DI	May–July 1991–1993
Temperature-dependent recycling								
C	*B*	EQ	JULIAN	INIT	REC_T	P_MM	L_DI	May–July 1991–1993
C′	*C*	EQ	JULIAN	INIT_NEW	REC_T	P_MM	L_DI	May–July 1991–1993
Runge-Kutta solution of chlorophyll *a*								
D	*B*	RK	JULIAN	INIT	REC_pH	P_MM	L_DI	May–July 1991–1993
D′	*D*	RK	JULIAN	INIT_NEW	REC_pH	P_MM	L_DI	May–July 1991–1993

Model version	Compare to version	Model calibration parameters						Performance statistics					
		u_{alg} (m d^{-1})	K_R (yr^{-1})	*pH**	K_T (yr^{-1})	$T_{(min,rec)}$ (°C)	k_{half} (ppm)	R	R^2	N	Bias (ppb)	RMSE (ppb)	NS
The rows below are repeated from Phase I (Wood and others, 2013, table 12)—Continued													
Original model with original calibration													
O		0.05	0.53	9.1	NA	NA	NA	0.94	0.89	16	8.3	28.8	0.88
O′	*O*	0.05	1.33	9.0	NA	NA	NA	0.92	0.85	16	9.7	35.9	0.82
Recalibration of original model													
A	*O*	0.059	0.47	9.0	NA	NA	NA	0.93	0.86	16	14.9	36.5	0.81
A′	*A*	0.059	1.24	8.9	NA	NA	NA	0.90	0.81	16	13.7	43.1	0.74
Modifications to light and phosphorus limitation													
B	*A*	0.035	0.32	8.6	NA	NA	0.06	0.94	0.88	16	17.4	39.3	0.78
B′	*B*	0.035	1.05	8.7	NA	NA	0.06	0.96	0.92	16	21.6	36.6	0.81
Temperature-dependent recycling													
C	*B*	0.035	NA	NA	0.54	12.8	0.06	0.95	0.91	16	25.8	44.1	0.72
C′	*C*	0.035	NA	NA	1.62	12.8	0.06	0.95	0.90	16	26.6	45.6	0.71
Runge-Kutta solution of chlorophyll *a*													
D	*B*	0.035	0.34	8.1	NA	NA	0.06	0.94	0.88	16	-6.8	34.4	0.83
D′	*D*	0.035	1.18	8.1	NA	NA	0.06	0.94	0.88	16	-14.3	35.5	0.82

Table 8. Performance statistics for total phosphorus obtained over the indicated May–July validation periods for model versions discussed in the report.—Continued

[**Model characteristics:** EQ, Chlorophyll *a* concentration evaluated by setting dB/dt to 0; RK, Chlorophyll *a* concentration evaluated using Runge-Kutta approach; JULIAN, pH model with Julian day dependence; NO_JULIAN, pH model without Julian day dependence; INIT, Initial size of sediment reservoir calculated with original starting concentration 1,000 milligrams of phosphorus per kilogram of sediment; INIT_NEW, Initial size of sediment reservoir recalculated with starting concentration 335 milligrams of phosphorus per kilogram of sediment; REC_pH, Model relies on pH-dependent recycle mechanism; REC_T, model relies on temperature-dependent recycle mechanism; P_00, Phosphorus limitation factor calculated as the percent of non-algal phosphorus; P_MM, Phosphorus limitation factor calculated by Michaelis-Menten kinetics; L_AVG, Light limitation factor calculated using the average light intensity; L_DI, Average light limitation factor calculated by depth-integrating the light limitation equation. **Model calibration parameters:** Model characteristics and parameters are defined in the text and tables 1 and 2. **Performance statistics**: R, correlation coefficient; R^2, coefficient of determination; N, sample size; RMSE, root mean square error; NS, Nash-Sutcliffe statistic. **Abbreviations:** m d^{-1}, meter per day; yr^{-1}, year; °C, degrees Celsius; ppm, parts per million]

Model version	Compare to version	Model characteristics						Validation period
		Chlorophyll *a* model	pH model	Initial sediment reservoir	Recycle mechanism	Phosphorus limitation	Light limitation	
The rows below were generated for Phase 2								
Runge-Kutta solution of chlorophyll *a* with updated settling velocity and model structure, 7.5-year calibration set								
E'	D'	RK	NO_JULIAN	INIT_NEW	REC_pH	P_MM	L_DI	May–July 1991–1993
Runge-Kutta solution of chlorophyll *a* with updated settling velocity and model structure, 19-year calibration set								
F'_O	E'	RK	NO_JULIAN	INIT_NEW	REC_pH	P_MM	L_DI	May–July even years
F'_O	G'	RK	NO_JULIAN	INIT_NEW	REC_pH	P_MM	L_DI	May–July 2006–2008
F'_E	E'	RK	NO_JULIAN	INIT_NEW	REC_pH	P_MM	L_DI	May–July odd years
F'_E	G'	RK	NO_JULIAN	INIT_NEW	REC_pH	P_MM	L_DI	May–July 2006–2008
Runge-Kutta solution of chlorophyll *a* with calculated metabolism 2006–2008								
G'_1	F'	RK	NO_JULIAN	INIT_NEW	REC_pH	NA	NA	May–July 2006
G'_2	F'	RK	NO_JULIAN	INIT_NEW	REC_pH	NA	NA	May–July 2007
G'_3	F'	RK	NO_JULIAN	INIT_NEW	REC_pH	NA	NA	May–July 2008

Model version	Compare to version	Model calibration parameters						Performance statistics					
		u_{alg} (m d^{-1})	K_R (yr^{-1})	*pH**	K_T (yr^{-1})	$T_{(min,rec)}$ (°C)	k_{half} (ppm)	R	R^2	N	Bias (ppb)	RMSE (ppb)	NS
The rows below were generated for Phase 2 —Continued													
Runge-Kutta solution of chlorophyll *a* with updated settling velocity and model structure, 7.5-year calibration set													
E'	D'	0.031	1.31	8.1	NA	NA	0.06	0.92	0.85	16	-27.9	43.5	0.73
Runge-Kutta solution of chlorophyll *a* with updated settling velocity and model structure, 19-year calibration set													
F'_O	E'	0.070	1.61	8.2	NA	NA	0.06	0.78	0.61	60	1.2	48.6	0.59
F'_O	G'	0.070	1.61	8.2	NA	NA	0.06	0.74	0.54	19	26.4	71.1	0.29
F'_E	E'	0.087	2.09	8.3	NA	NA	0.05	0.80	0.64	58	18.4	50.7	0.53
F'_E	G'	0.087	2.09	8.3	NA	NA	0.05	0.76	0.58	19	28.5	67.0	0.37
Runge-Kutta solution of chlorophyll *a* with calculated metabolism 2006–2008													
G'_1	F'	0.463	6.77	8.9	NA	NA	NA	0.83	0.69	5	-0.3	42.5	0.69
G'_2	F'	0.463	7.63	9	NA	NA	NA	0.99	0.99	4	34.6	55.8	0.70
G'_3	F'	0.463	6.76	8.9	NA	NA	NA	0.95	0.90	5	-26.7	34.0	0.71

Table 9. Performance statistics for chlorophyll *a* obtained over the indicated May–July validation periods for model versions discussed in the report.

[**Model characteristics:** EQ, Chlorophyll *a* concentration evaluated by setting dB/dt to 0; RK, Chlorophyll *a* concentration evaluated using Runge-Kutta approach; JULIAN, pH model with Julian day dependence; NO_JULIAN, pH model without Julian day dependence; INIT, Initial size of sediment reservoir calculated with original starting concentration 1,000 milligrams of phosphorus per kilogram of sediment; INIT_NEW, Initial size of sediment reservoir recalculated with starting concentration 335 milligrams of phosphorus per kilogram of sediment; REC_pH, Model relies on pH-dependent recycle mechanism; REC_T, model relies on temperature-dependent recycle mechanism; P_00, Phosphorus limitation factor calculated as the percent of non-algal phosphorus; P_MM, Phosphorus limitation factor calculated by Michaelis-Menten kinetics; L_AVG, Light limitation factor calculated using the average light intensity; L_DI, Average light limitation factor calculated by depth-integrating the light limitation equation. **Model calibration parameters:** Model characteristics and parameters are defined in the text and tables 1 and 2. **Performance statistics**: R, correlation coefficient; R^2, coefficient of determination; N, sample size; RMSE, root mean square error; NS, Nash-Sutcliffe statistic. **Abbreviations:** m d^{-1}, meter per day; yr^{-1}, year; °C, degrees Celsius; ppm, parts per million]

Model version	Compare to version	Model characteristics						Validation period
		Chlorophyll *a* model	pH model	Initial sediment reservoir	Recycle mechanism	Phosphorus limitation	Light limitation	
The rows below are repeated from Phase I (Wood and others, 2013, table 13)								
Original model with original calibration								
O		EQ	JULIAN	INIT	REC_pH	P_00	L_AVG	May–July 1991–1993
O′	*O*	EQ	JULIAN	INIT_NEW	REC_pH	P_00	L_AVG	May–July 1991–1993
Recalibration of original model								
A	*O*	EQ	JULIAN	INIT	REC_pH	P_00	L_AVG	May–July 1991–1993
A′	*A*	EQ	JULIAN	INIT_NEW	REC_pH	P_00	L_AVG	May–July 1991–1993
Modifications to light and phosphorus limitation								
B	*A*	EQ	JULIAN	INIT	REC_pH	P_MM	L_DI	May–July 1991–1993
B′	*B*	EQ	JULIAN	INIT_NEW	REC_pH	P_MM	L_DI	May–July 1991–1993
Temperature-dependent recycling								
C	*B*	EQ	JULIAN	INIT	REC_T	P_MM	L_DI	May–July 1991–1993
C′	*C*	EQ	JULIAN	INIT_NEW	REC_T	P_MM	L_DI	May–July 1991–1993
Runge-Kutta solution of chlorophyll *a*								
D	*B*	RK	JULIAN	INIT	REC_pH	P_MM	L_DI	May–July 1991–1993
D′	*D*	RK	JULIAN	INIT_NEW	REC_pH	P_MM	L_DI	May–July 1991–1993

Model version	Compare to version	Model calibration parameters						Performance statistics					
		u_{alg} (m d^{-1})	K_R (yr^{-1})	*pH**	K_T (yr^{-1})	$T_{(min,rec)}$ (°C)	k_{half} (ppm)	R	R^2	N	Bias (ppb)	RMSE (ppb)	NS
The rows below are repeated from Phase I (Wood and others, 2013, table 13)—Continued													
Original model with original calibration													
O		0.05	0.53	9.1	NA	NA	NA	0.74	0.55	16	-48.9	85.4	0.28
O′	*O*	0.05	1.33	9.0	NA	NA	NA	0.75	0.56	16	-48	82.3	0.33
Recalibration of original model													
A	*O*	0.059	0.47	9.0	NA	NA	NA	0.75	0.56	16	-39.6	77.8	0.40
A′	*A*	0.059	1.24	8.9	NA	NA	NA	0.75	0.56	16	-40.6	78.0	0.40
Modifications to light and phosphorus limitation													
B	*A*	0.035	0.32	8.6	NA	NA	0.06	0.77	0.59	16	-37.6	77.1	0.41
B′	*B*	0.035	1.05	8.7	NA	NA	0.06	0.77	0.59	16	-33.4	76.2	0.43
Temperature-dependent recycling													
C	*B*	0.035	NA	NA	0.54	12.8	0.06	0.75	0.56	16	-27.5	74.0	0.46
C′	*C*	0.035	NA	NA	1.62	12.8	0.06	0.75	0.56	16	-26.6	73.1	0.47
Runge-Kutta solution of chlorophyll *a*													
D	*B*	0.035	0.34	8.1	NA	NA	0.06	0.81	0.65	16	11.6	61.4	0.63
D′	*D*	0.035	1.18	8.1	NA	NA	0.06	0.80	0.65	16	7.6	61.8	0.62

Table 9. Performance statistics for chlorophyll *a* obtained over the indicated May–July validation periods for model versions discussed in the report.—Continued

[**Model characteristics:** EQ, Chlorophyll *a* concentration evaluated by setting dB/dt to 0; RK, Chlorophyll *a* concentration evaluated using Runge-Kutta approach; JULIAN, pH model with Julian day dependence; NO_JULIAN, pH model without Julian day dependence; INIT, Initial size of sediment reservoir calculated with original starting concentration 1,000 milligrams of phosphorus per kilogram of sediment; INIT_NEW, Initial size of sediment reservoir recalculated with starting concentration 335 milligrams of phosphorus per kilogram of sediment; REC_pH, Model relies on pH-dependent recycle mechanism; REC_T, model relies on temperature-dependent recycle mechanism; P_00, Phosphorus limitation factor calculated as the percent of non-algal phosphorus; P_MM, Phosphorus limitation factor calculated by Michaelis-Menten kinetics; L_AVG, Light limitation factor calculated using the average light intensity; L_DI, Average light limitation factor calculated by depth-integrating the light limitation equation. **Model calibration parameters:** Model characteristics and parameters are defined in the text and tables 1 and 2. **Performance statistics**: R, correlation coefficient; R^2, coefficient of determination; N, sample size; RMSE, root mean square error; NS, Nash-Sutcliffe statistic. **Abbreviations:** m d^{-1}, meter per day; yr^{-1}, year; °C, degrees Celsius; ppm, parts per million]

Model version	Compare to version	Model characteristics						Validation period
		Chlorophyll *a* model	pH model	Initial sediment reservoir	Recycle mechanism	Phosphorus limitation	Light limitation	
The rows below were generated for Phase 2								
Runge-Kutta solution of chlorophyll *a* with updated settling velocity and model structure, 7.5-year calibration set								
E'	D'	RK	NO_JULIAN	INIT_NEW	REC_pH	P_MM	L_DI	May–July 1991–1993
Runge-Kutta solution of chlorophyll *a* with updated settling velocity and model structure, 19-year calibration set								
F'_O	E'	RK	NO_JULIAN	INIT_NEW	REC_pH	P_MM	L_DI	May–July even years
F'_O	G'	RK	NO_JULIAN	INIT_NEW	REC_pH	P_MM	L_DI	May–July 2006–2008
F'_E	E'	RK	NO_JULIAN	INIT_NEW	REC_pH	P_MM	L_DI	May–July odd years
F'_E	G'	RK	NO_JULIAN	INIT_NEW	REC_pH	P_MM	L_DI	May–July 2006–2008
Runge-Kutta solution of chlorophyll *a* with calculated metabolism 2006–2008								
G'_1	F'	RK	NO_JULIAN	INIT_NEW	REC_pH	NA	NA	May–July 2006
G'_2	F'	RK	NO_JULIAN	INIT_NEW	REC_pH	NA	NA	May–July 2007
G'_3	F'	RK	NO_JULIAN	INIT_NEW	REC_pH	NA	NA	May–July 2008

Model version	Compare to version	Model calibration parameters						Performance statistics					
		u_{alg} (m d^{-1})	K_R (yr^{-1})	*pH**	K_T (yr^{-1})	$T_{(min,rec)}$ (°C)	k_{half} (ppm)	R	R^2	N	Bias (ppb)	RMSE (ppb)	NS
The rows below were generated for Phase 2—Continued													
Runge-Kutta solution of chlorophyll *a* with updated settling velocity and model structure, 7.5-year calibration set													
E'	D'	0.031	1.31	8.1	NA	NA	0.06	0.80	0.64	16	-1.3	64.6	0.59
Runge-Kutta solution of chlorophyll *a* with updated settling velocity and model structure, 19-year calibration set													
F'_O	E'	0.070	1.61	8.2	NA	NA	0.06	0.67	0.45	60	32.2	75.1	0.32
F'_O	G'	0.070	1.61	8.2	NA	NA	0.06	0.44	0.19	19	18.1	83.2	0.14
F'_E	E'	0.087	2.09	8.3	NA	NA	0.05	0.62	0.39	58	27.6	70.3	0.27
F'_E	G'	0.087	2.09	8.3	NA	NA	0.05	0.42	0.18	19	15.9	84.5	0.11
Runge-Kutta solution of chlorophyll *a* with calculated metabolism 2006–2008													
G'_1	F'	0.463	6.77	8.9	NA	NA	NA	0.96	0.92	5	-23.7	28.2	0.64
G'_2	F'	0.463	7.63	9	NA	NA	NA	0.94	0.89	4	-30.1	35.8	0.58
G'_3	F'	0.463	6.76	8.9	NA	NA	NA	0.83	0.69	5	30.7	87.3	0.55

Table 10. Performance statistics for pH obtained over the indicated May–July validation periods for model versions discussed in the report.

[**Model characteristics:** EQ, Chlorophyll *a* concentration evaluated by setting dB/dt to 0; RK, Chlorophyll *a* concentration evaluated using Runge-Kutta approach; JULIAN, pH model with Julian day dependence; NO_JULIAN, pH model without Julian day dependence; INIT, Initial size of sediment reservoir calculated with original starting concentration 1,000 milligrams of phosphorus per kilogram of sediment; INIT_NEW, Initial size of sediment reservoir recalculated with starting concentration 335 milligrams of phosphorus per kilogram of sediment; REC_pH, Model relies on pH-dependent recycle mechanism; REC_T, model relies on temperature-dependent recycle mechanism; P_00, Phosphorus limitation factor calculated as the percent of non-algal phosphorus; P_MM, Phosphorus limitation factor calculated by Michaelis-Menten kinetics; L_AVG, Light limitation factor calculated using the average light intensity; L_DI, Average light limitation factor calculated by depth-integrating the light limitation equation. **Model calibration parameters:** Model characteristics and parameters are defined in the text and tables 1 and 2. **Performance statistics**: R, correlation coefficient; R^2, coefficient of determination; N, sample size; RMSE, root mean square error; NS, Nash-Sutcliffe statistic. **Abbreviations:** m d^{-1}, meter per day; yr^{-1}, year; °C, degrees Celsius; ppm, parts per million]

Model version	Compare to version	Model characteristics						Validation period
		Chlorophyll *a* model	pH model	Initial sediment reservoir	Recycle mechanism	Phosphorus limitation	Light limitation	
The rows below are repeated from Phase I (Wood and others, 2013, table 14)								
Original model with original calibration								
O		EQ	JULIAN	INIT	REC_pH	P_00	L_AVG	May–July 1991–1993
O′	*O*	EQ	JULIAN	INIT_NEW	REC_pH	P_00	L_AVG	May–July 1991–1993
Recalibration of original model								
A	*O*	EQ	JULIAN	INIT	REC_pH	P_00	L_AVG	May–July 1991–1993
A′	*A*	EQ	JULIAN	INIT_NEW	REC_pH	P_00	L_AVG	May–July 1991–1993
Modifications to light and phosphorus limitation								
B	*A*	EQ	JULIAN	INIT	REC_pH	P_MM	L_DI	May–July 1991–1993
B′	*B*	EQ	JULIAN	INIT_NEW	REC_pH	P_MM	L_DI	May–July 1991–1993
Temperature-dependent recycling								
C	*B*	EQ	JULIAN	INIT	REC_T	P_MM	L_DI	May–July 1991–1993
C′	*C*	EQ	JULIAN	INIT_NEW	REC_T	P_MM	L_DI	May–July 1991–1993
Runge-Kutta solution of chlorophyll *a*								
D	*B*	RK	JULIAN	INIT	REC_pH	P_MM	L_DI	May–July 1991–1993
D′	*D*	RK	JULIAN	INIT_NEW	REC_pH	P_MM	L_DI	May–July 1991–1993

Model version	Compare to version	Model calibration parameters						Performance statistics					
		u_{alg} (m d^{-1})	K_R (yr^{-1})	*pH**	K_T (yr^{-1})	$T_{(min,rec)}$ (°C)	k_{half} (ppm)	R	R^2	N	Bias	RMSE	NS
The rows below are repeated from Phase I (Wood and others, 2013, table 14)—Continued													
Original model with original calibration													
O		0.05	0.53	9.1	NA	NA	NA	0.75	0.56	16	-0.443	0.659	0.19
O′	*O*	0.05	1.33	9.0	NA	NA	NA	0.73	0.54	16	-0.456	0.677	0.14
Recalibration of original model													
A	*O*	0.059	0.47	9.0	NA	NA	NA	0.75	0.56	16	-0.417	0.644	0.22
A′	*A*	0.059	1.24	8.9	NA	NA	NA	0.73	0.53	16	-0.435	0.666	0.17
Modifications to light and phosphorus limitation													
B	*A*	0.035	0.32	8.6	NA	NA	0.06	0.74	0.55	16	-0.320	0.589	0.35
B′	*B*	0.035	1.05	8.7	NA	NA	0.06	0.78	0.60	16	-0.279	0.541	0.45
Temperature-dependent recycling													
C	*B*	0.035	NA	NA	0.54	12.8	0.06	0.77	0.60	16	-0.300	0.551	0.43
C′	*C*	0.035	NA	NA	1.62	12.8	0.06	0.78	0.60	16	-0.299	0.549	0.43
Runge-Kutta solution of chlorophyll *a*													
D	*B*	0.035	0.34	8.1	NA	NA	0.06	0.86	0.73	16	0.061	0.386	0.72
D′	*D*	0.035	1.18	8.1	NA	NA	0.06	0.86	0.74	16	0.043	0.382	0.73

Table 10. Performance statistics for pH obtained over the indicated May–July validation periods for model versions discussed in the report.—Continued

[**Model characteristics:** EQ, Chlorophyll *a* concentration evaluated by setting dB/dt to 0; RK, Chlorophyll *a* concentration evaluated using Runge-Kutta approach; JULIAN, pH model with Julian day dependence; NO_JULIAN, pH model without Julian day dependence; INIT, Initial size of sediment reservoir calculated with original starting concentration 1,000 milligrams of phosphorus per kilogram of sediment; INIT_NEW, Initial size of sediment reservoir recalculated with starting concentration 335 milligrams of phosphorus per kilogram of sediment; REC_pH, Model relies on pH-dependent recycle mechanism; REC_T, model relies on temperature-dependent recycle mechanism; P_00, Phosphorus limitation factor calculated as the percent of non-algal phosphorus; P_MM, Phosphorus limitation factor calculated by Michaelis-Menten kinetics; L_AVG, Light limitation factor calculated using the average light intensity; L_DI, Average light limitation factor calculated by depth-integrating the light limitation equation. **Model calibration parameters:** Model characteristics and parameters are defined in the text and tables 1 and 2. **Performance statistics**: R, correlation coefficient; R^2, coefficient of determination; N, sample size; RMSE, root mean square error; NS, Nash-Sutcliffe statistic. **Abbreviations:** m d^{-1}, meter per day; yr^{-1}, year; °C, degrees Celsius; ppm, parts per million]

Model version	Compare to version	Model characteristics						Validation period
		Chlorophyll *a* model	pH model	Initial sediment reservoir	Recycle mechanism	Phosphorus limitation	Light limitation	
The rows below were generated for Phase 2								
Runge-Kutta solution of chlorophyll *a* with updated settling velocity and model structure, 7.5-year calibration set								
E'	D'	RK	NO_JULIAN	INIT_NEW	REC_pH	P_MM	L_DI	May–July 1991–1993
Runge-Kutta solution of chlorophyll *a* with updated settling velocity and model structure, 19-year calibration set								
F'_O	E'	RK	NO_JULIAN	INIT_NEW	REC_pH	P_MM	L_DI	May–July even years
F'_O	G'	RK	NO_JULIAN	INIT_NEW	REC_pH	P_MM	L_DI	May–July 2006–2008
F'_E	E'	RK	NO_JULIAN	INIT_NEW	REC_pH	P_MM	L_DI	May–July odd years
F'_E	G'	RK	NO_JULIAN	INIT_NEW	REC_pH	P_MM	L_DI	May–July 2006–2008
Runge-Kutta solution of chlorophyll *a* with calculated metabolism 2006–2008								
G'_1	F'	RK	NO_JULIAN	INIT_NEW	REC_pH	NA	NA	May–July 2006
G'_2	F'	RK	NO_JULIAN	INIT_NEW	REC_pH	NA	NA	May–July 2007
G'_3	F'	RK	NO_JULIAN	INIT_NEW	REC_pH	NA	NA	May–July 2008

Model version	Compare to version	Model calibration parameters						Performance statistics					
		u_{alg} (m d^{-1})	K_R (yr^{-1})	*pH**	K_T (yr^{-1})	$T_{(min,rec)}$ (°C)	k_{half} (ppm)	R	R^2	N	Bias	RMSE	NS
The rows below were generated for Phase 2—Continued													
Runge-Kutta solution of chlorophyll *a* with updated settling velocity and model structure, 7.5-year calibration set													
E'	D'	0.031	1.31	8.1	NA	NA	0.06	0.86	0.74	16	0.114	0.395	0.71
Runge-Kutta solution of chlorophyll *a* with updated settling velocity and model structure, 19-year calibration set													
F'_O	E'	0.070	1.61	8.2	NA	NA	0.06	0.81	0.66	60	0.177	0.463	0.59
F'_O	G'	0.070	1.61	8.2	NA	NA	0.06	0.67	0.45	19	0.122	0.541	0.42
F'_E	E'	0.087	2.09	8.3	NA	NA	0.05	0.77	0.60	58	0.232	0.518	0.48
F'_E	G'	0.087	2.09	8.3	NA	NA	0.05	0.68	0.46	19	0.128	0.539	0.43
Runge-Kutta solution of chlorophyll *a* with calculated metabolism 2006–2008													
G'_1	F'	0.463	6.77	8.9	NA	NA	NA	0.88	0.77	5	-0.345	0.450	0.36
G'_2	F'	0.463	7.63	9	NA	NA	NA	0.72	0.52	4	0.232	0.455	0.35
G'_3	F'	0.463	6.76	8.9	NA	NA	NA	0.98	0.96	5	0.068	0.314	0.77

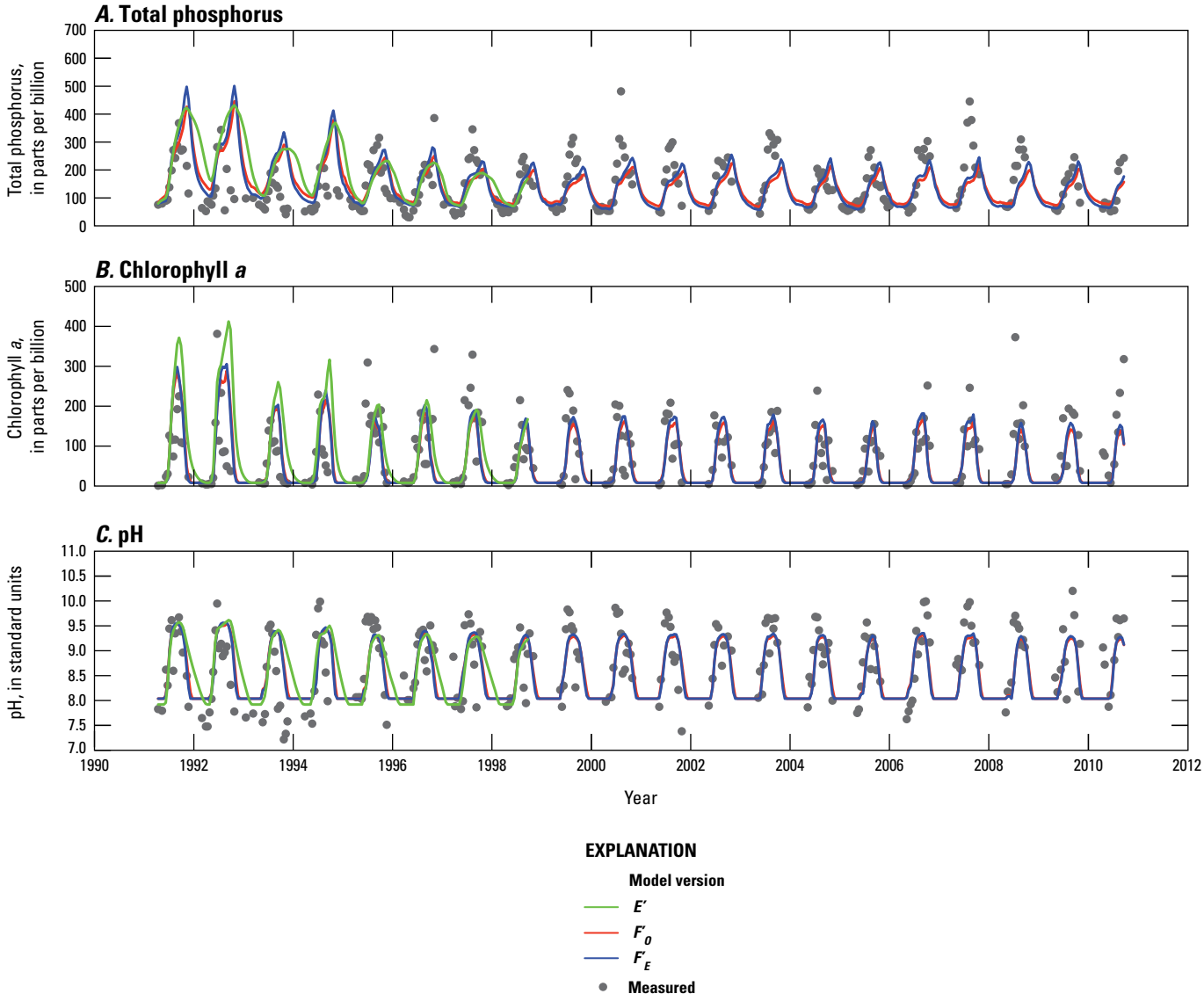

Figure 2. Simulated and measured water column (*A*) total phosphorus (as P) concentration, (*B*) chlorophyll *a* concentration, and (*C*) pH, Upper Klamath Lake, Oregon, April 1991–September 2010.

Long-Term Simulations

In order to better understand how long the system takes to achieve a steady state between the water column and sediment reservoir, long-term simulations were made with the recalibrated models (versions E', F'_O, and F'_E; table 11). The long-term simulations were achieved by chaining the 19 years of input data (mid-April 1991–mid-April 2010) to produce a continuous simulation of all variables over 209 years (eleven 19-year cycles). The recalibrated models were run with the chained input data for the base scenario of a 0-percent reduction in external phosphorus load and a TMDL scenario of a 40-percent reduction in external phosphorus load. Results as represented by 19-year averages were consistent between models (fig. 3) and previous results (Wood and others, 2013; fig. 16, represented as 7-year averages). In all model runs with the updated sediment phosphorus initial condition, the model achieved steady state in about 20 years, and the 19-year average water-column TP concentrations were about 125 ppb for the base scenario and about 75 ppb for the TMDL scenario. When the 19-year average sediment TP masses were compared (fig. 4), the trends were consistent between models and previous results (Wood and others, 2013; fig. 17, represented as 7-year averages); however, the ultimate steady-state sediment phosphorus masses varied. As for the water column, steady state was achieved in about 20 years; however, the model recalibrated with the extended dataset (versions F'_O and F'_E) had lower final sediment phosphorus mass than the model calibrated with the original 7.5-year dataset (version E'). This lower mass was related to faster sediment phosphorus depletion rates because of the combination of calibrated recycling parameters pH^* and K_R. The recalibrated extended set models (F'_O and F'_E) achieved a steady state of about 500 metric tons of sediment phosphorus with the base scenario, and a steady state of about 350 metric tons of sediment phosphorus with the TMDL scenario. By comparison, the model over the original 7.5-year time period (version E') achieved a steady state of about 400 metric tons of sediment phosphorus with the base scenario, and a steady state of about 250 metric tons of sediment phosphorus with the TMDL scenario (table 11).

In addition to considering the amount of time required to achieve steady state, we evaluated the "final" steady-state 19-year time series at the end of the 209-year model runs. Water-column TP (fig. 5) and chlorophyll *a* (fig. 6) concentrations decreased under the TMDL scenario as compared to the baseline (0-percent reduction in external loads) scenario. The decrease in water-column TP concentration was 39 percent, roughly the same as the reduction in external loads, and the decrease in chlorophyll *a* concentration was a little less but roughly similar. Across all versions of the model, the TMDL scenario resulted in a similar decrease in water-column phosphorus concentration compared to the baseline scenario (table 11). Note that, although chlorophyll *a* concentrations decreased in response to external load reductions, there were still blooms in each year (fig. 6). The blooms are smaller, and many are under the 100 ppb threshold that was applied in the Phase I review (Wood and others, 2013); however, they still occurred. Examination of the model parameters indicated that the recycling parameter pH^* plays an important role in determining whether a bloom year will be "turned on" or "turned off." When the pH^* value is low, sediment phosphorus recycling begins at a lower lake-average pH and activates the feedback loop between sediment recycling and chlorophyll *a*. Because pH is a function of chlorophyll *a*, the recycling will increase rapidly and lead to increased chlorophyll *a* as long as the chlorophyll *a* concentration at the beginning of the season is high enough given growth conditions (that is, water-column TP, light, and temperature). When the pH^* value is high, sediment recycling cannot begin until the lake-average pH also is relatively high. For example, if pH^* equals 8.1, then recycling would begin (at a low rate) when the lakewide average pH reached 7.5 and the recycle rate would reach its maximum when the lakewide average pH reached 8.8; however, if pH^* equals 9.1, then recycling would begin (at a low rate) when the lakewide average pH reached 8.5 and the maximum recycle rate would occur when lakewide average pH reached 9.8. Therefore, the models that remove the assumption of cyanobacteria achieving maximum growth during the 2-week time step and solve for chlorophyll *a* using a Runge-Kutta solution method will be less likely to have years without any bloom.

Table 11. Metrics describing the long-term simulations for various model versions discussed in the report.

[**Model characteristics:** EQ, Chlorophyll *a* concentration evaluated by setting dB/dt to 0; RK, Chlorophyll *a* concentration evaluated using Runge-Kutta approach; INIT, Initial size of sediment reservoir calculated with original starting concentration 1,000 milligrams of phosphorus per kilogram of sediment; INIT_NEW, Initial size of sediment reservoir recalculated with starting concentration 335 milligrams of phosphorus per kilogram of sediment; REC_pH, Model relies on pH-dependent recycle mechanism; P_00, Phosphorus limitation factor calculated as the percent of non-algal P; P_MM, Phosphorus limitation factor calculated by Michaelis-Menten kinetics; L_AVG, Light limitation factor calculated using the average light intensity; L_DI, Average light limitation factor calculated by depth-integrating the light limitation equation. %, percent; >, greater than; ppb, parts per billion]

Model version	Compare to version	Model characteristics						Number of "final" years
		Chlorophyll *a* model	pH model	Initial sediment reservoir	Recycle mechanism	Phosphorus limitation	Light limitation	
The rows below are repeated from Phase I (Wood and others, 2013, table 15)								
Original model with original calibration								
O′	*O*	EQ	JULIAN	INIT_NEW	REC_pH	P_00	L_AVG	7
Recalibration of original model								
A′	*A*	EQ	JULIAN	INIT_NEW	REC_pH	P_00	L_AVG	7
Modifications to light and phosphorus limitation								
B′	*B*	EQ	JULIAN	INIT_NEW	REC_pH	P_MM	L_DI	7
Runge-Kutta solution of chlorophyll *a*								
D′	*D*	RK	JULIAN	INIT_NEW	REC_pH	P_MM	L_DI	7

Model version	Compare to version	Average concentration over the final years of the long-term simulation (last 7 years of 203-year simulation or last 19 years of 209-year simulation)						Years with seasonal chlorophyll *a* peak >100 ppb over final years of the long-term simulation	
		Total P (ppb)		Sediment P (metric tons)		Chlorophyll *a* (ppb)		Number (out of number of "final" years)	
		0%	40%	0%	40%	0%	40%	0%	40%
The rows below are repeated from Phase I (Wood and others, 2013, table 15)—Continued									
Original model with original calibration									
O′	*O*	120.0	71.1	901	932	71.3	44.5	7	6
Recalibration of original model									
A′	*A*	118.4	69.4	980	897	69.1	44.0	7	6
Modifications to light and phosphorus limitation									
B′	*B*	121.5	73.0	871	1,028	72.0	39.8	7	4
Runge-Kutta solution of chlorophyll *a*									
D′	*D*	129.0	78.4	518	355	60.3	38.4	7	6

Table 11. Metrics describing the long-term simulations for various model versions discussed in the report.—Continued

[**Model characteristics:** EQ, Chlorophyll *a* concentration evaluated by setting dB/dt to 0; RK, Chlorophyll *a* concentration evaluated using Runge-Kutta approach; INIT, Initial size of sediment reservoir calculated with original starting concentration 1,000 milligrams of phosphorus per kilogram of sediment; INIT_NEW, Initial size of sediment reservoir recalculated with starting concentration 335 milligrams of phosphorus per kilogram of sediment; REC_pH, Model relies on pH-dependent recycle mechanism; P_00, Phosphorus limitation factor calculated as the percent of non-algal P; P_MM, Phosphorus limitation factor calculated by Michaelis-Menten kinetics; L_AVG, Light limitation factor calculated using the average light intensity; L_DI, Average light limitation factor calculated by depth-integrating the light limitation equation. %, percent; >, greater than; ppb, parts per billion]

Model version	Compare to version	Model characteristics						Number of "final" years
		Chlorophyll *a* model	pH model	Initial sediment reservoir	Recycle mechanism	Phosphorus limitation	Light limitation	
The rows below were generated for Phase 2								
Runge-Kutta solution of chlorophyll *a* with updated settling velocity and model structure, 7.5-year calibration set								
E'	D'	RK	NO_JULIAN	INIT_NEW	REC_pH	P_MM	L_DI	7
Runge-Kutta solution of chlorophyll *a* with updated settling velocity and model structure, 19-year calibration set								
F'_O	E'	RK	NO_JULIAN	INIT_NEW	REC_pH	P_MM	L_DI	19
F'_E	E'	RK	NO_JULIAN	INIT_NEW	REC_pH	P_MM	L_DI	19

Model version	Compare to version	Average concentration over the final years of the long-term simulation (last 7 years of 203-year simulation or last 19 years of 209-year simulation)						Years with seasonal chlorophyll *a* peak >100 ppb over final years of the long-term simulation	
		Total P (ppb)		Sediment P (metric tons)		Chlorophyll *a* (ppb)		Number (out of number of "final" years)	
		0%	40%	0%	40%	0%	40%	0%	40%
The rows below were generated for Phase 2—Continued									
Runge-Kutta solution of chlorophyll *a* with updated settling velocity and model structure, 7.5-year calibration set									
E'	D'	130.1	79.6	387	251	57.0	35.3	7	4
Runge-Kutta solution of chlorophyll *a* with updated settling velocity and model structure, 19-year calibration set									
F'_O	E'	120.3	73.5	505	334	42.4	26.5	19	3
F'_E	E'	120.5	73.9	521	357	44.2	28.1	19	13

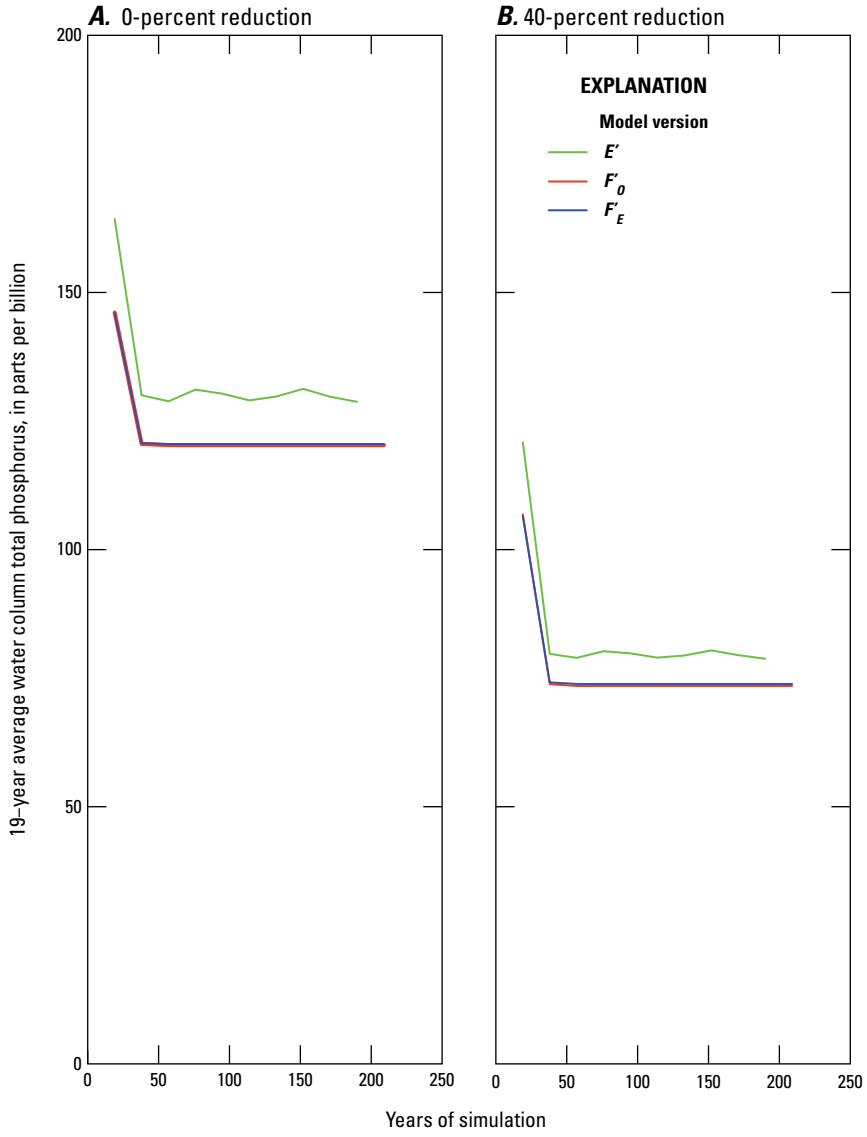

Figure 3. 19-year average water-column total phosphorus (as P) concentration under simulation conditions of (*A*) 0-percent reduction and (*B*) 40-percent reduction in external phosphorus loads to Upper Klamath Lake, Oregon.

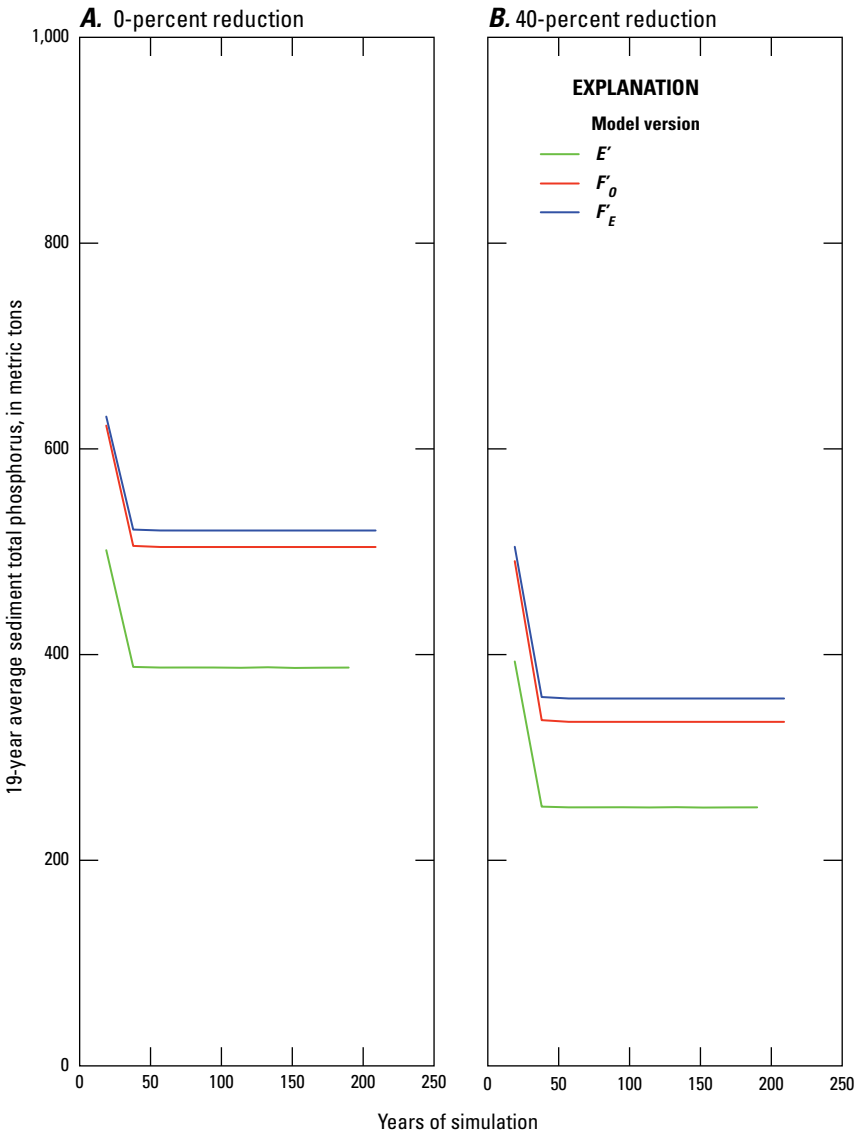

Figure 4. 19-year average sediment total phosphorus (as P) masses under simulation conditions of (*A*) 0-percent reduction and (*B*) 40-percent reduction in external phosphorus loads to Upper Klamath Lake, Oregon.

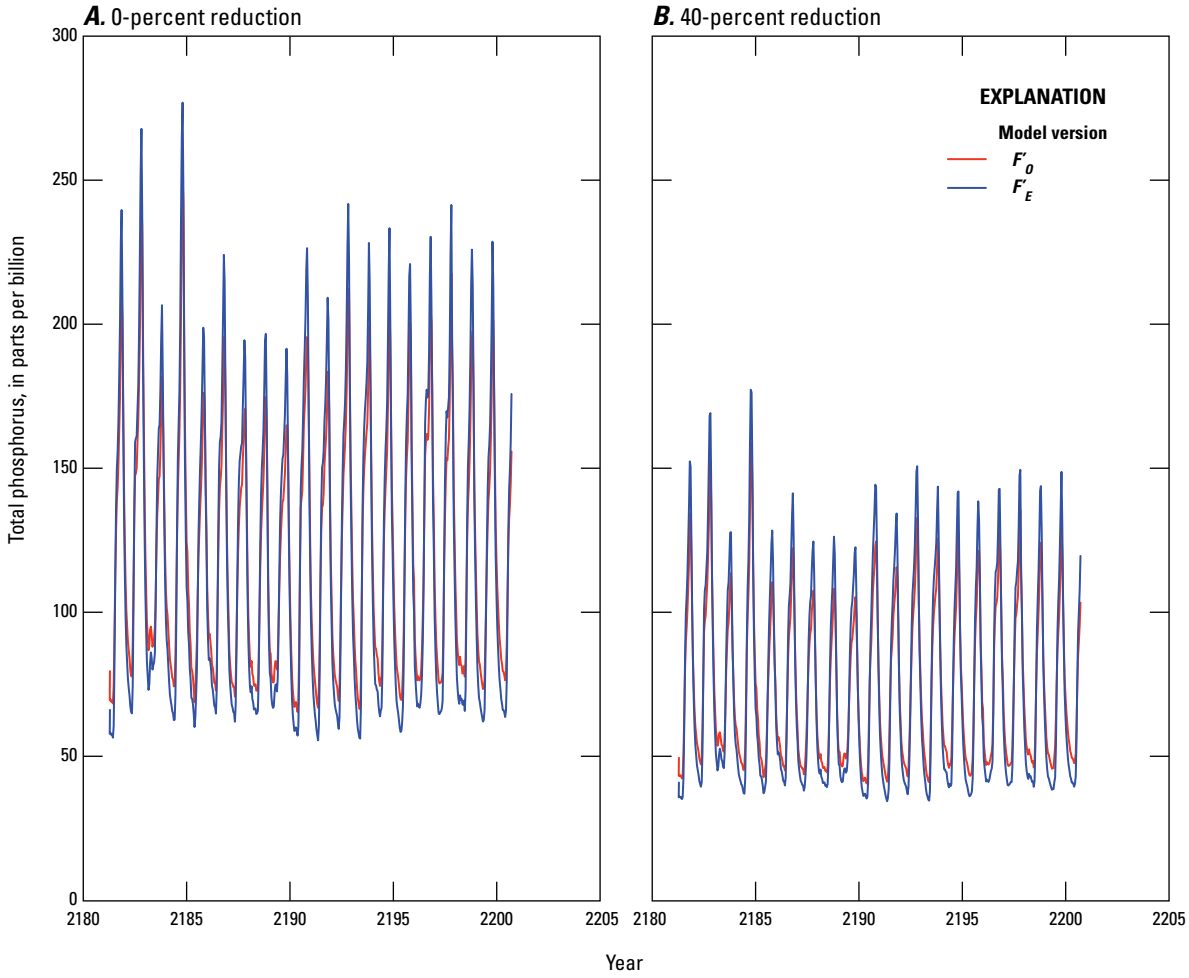

Figure 5. Water-column total phosphorus (as P) concentration during the last 19 years of a 209-year simulation (1991–2199) under conditions of (*A*) 0-percent reduction and (*B*) 40-percent reduction in external loads to Upper Klamath Lake, Oregon.

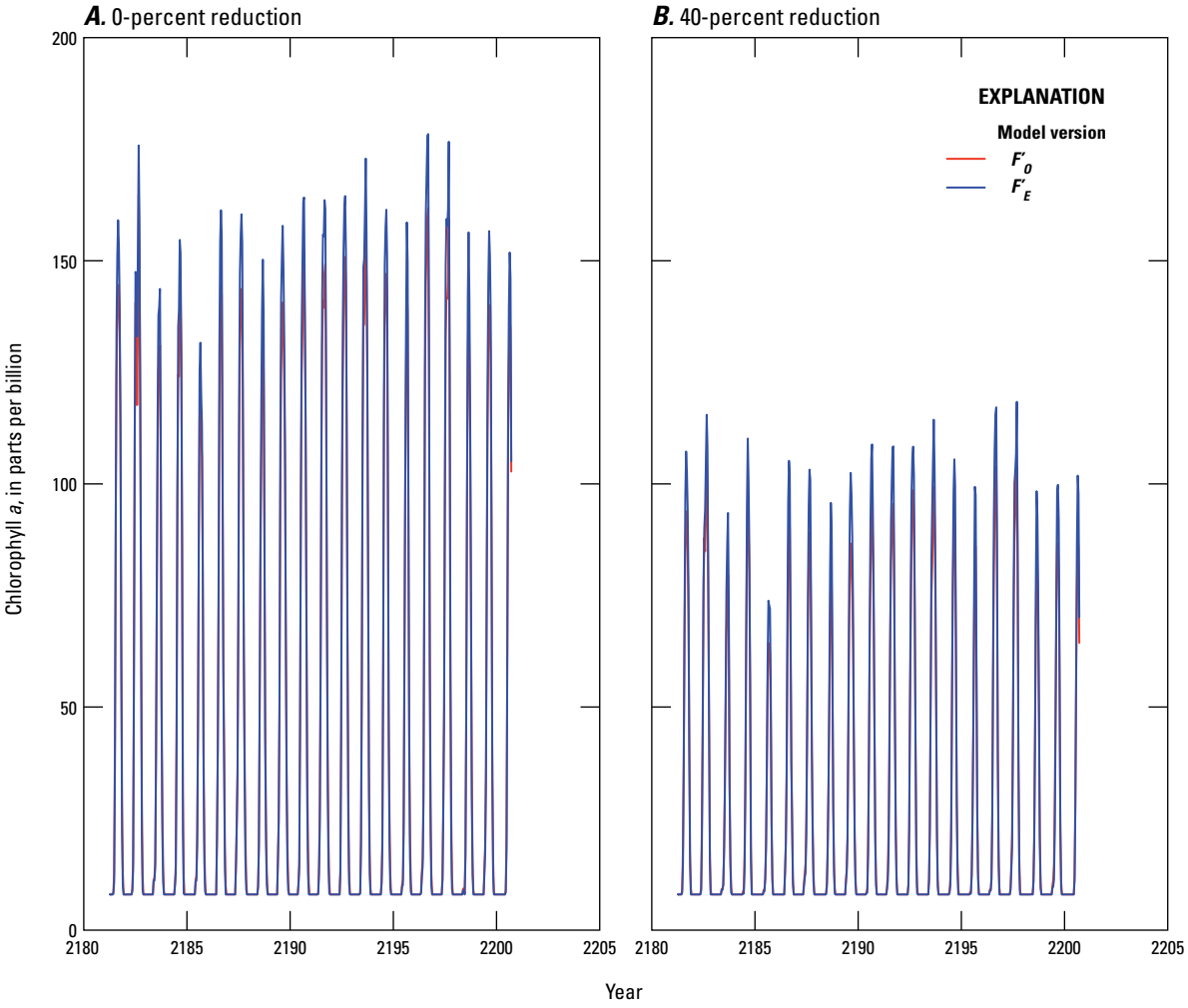

Figure 6. Water-column chlorophyll *a* concentration during the last 19 years of a 209-year simulation (1991–2199) under conditions of (*A*) 0-percent reduction and (*B*) 40-percent reduction in external loads to Upper Klamath Lake, Oregon.

Lake Metabolism as a Substitute for Algal Growth and Respiration

Perhaps the largest source of error in using the CSTR approach to model a large system that is variable in all three dimensions and time is the process by which descriptions of processes that are appropriate to small, homogeneous water parcels are "scaled up" and applied to the bulk system. This can be shown by examining the mathematical procedure for averaging terms of the three-dimensional mass balance equations to make them appropriate for a zero-dimensional CSTR model.

As an example, consider the growth and respiration terms in the mass balance equation for chlorophyll *a* (equation 1). The growth process is described as a product of a constant maximum growth rate, modified by factors that describe how the growth rate is limited by less-than-ideal amounts of light, temperature, and nutrients. This description has been shown over decades to work well, and when used in process-based models to describe growth in discrete and approximately homogeneous segments of a model domain that are selected to have the appropriate temporal and spatial scales (Bowie and others, 1985; Chapra, 1997). The application of the small-scale description of growth to the single, large, averaged volume that represents the lake in the CSTR model has been done by making the following approximations in milligrams of chlorophyll *a* per liter per day:

$$\frac{1}{DA\Delta t}\int_D\int_A\int_{\Delta t} K_G F_L\left(\hat{I}\right) F_T\left(\hat{T}\right) F_P\left(\hat{P}\right)\hat{B}\,dz\,ds\,dt \sim K_G F_T\left(T\right) F_P\left(P\right) B * \frac{1}{D\Delta t}\int_D\int_{\Delta t} F_L\left(I_0\right) dz\,dt \quad (2)$$

$$\frac{1}{DA\Delta t}\int_D\int_A\int_{\Delta t} K_R F_T\left(\hat{T}\right)\hat{B}\,dz\,ds\,dt \sim K_R F_T\left(T\right) B \quad (3)$$

where

s represents two-dimensional (latitude/longitude) geographic location,

$\frac{1}{D}\int_D dz$ represents averaging over the water-column depth,

$\frac{1}{A}\int_A ds$ represents averaging over the area of the lake,

$\frac{1}{\Delta t}\int_{\Delta t} dt$ represents averaging over the 14-day time step of the model, and

integrated functions are *GROWTH* and *RESP* as described with terms in section, "Changes to Algal Submodel." The "hat" on a variable represents values with spatial and temporal dependence (functions of depth, area, and time) and distinguishes it from the corresponding CSTR variable that has been averaged so that it has no spatial dependence and takes on values only at 14-day intervals. For example:

$$\frac{1}{DA\Delta t}\int_D\int_A\int_{\Delta t}\hat{B}\left(s,z,t\right) dz\,ds\,dt = B\left(t'\right) \quad (4)$$

where

t' is a discrete time variable that is defined at 14-day intervals.

Inaccuracy results because the spatial/temporal average of the product of multiple factors is not, in general, equal to the product of the spatial/temporal average of the individual factors. The amount of error introduced by the approximations depends on the spatial and temporal increments used for averaging—in this case, averaging is over 14 days and the entirety of UKL—and in a highly variable system, approximations (equations) 2 and 3 introduce more error than in a well-mixed system. Approaching the scaling-up problem in this way is convenient because it provides a way of parsing the growth and respiration terms into well-understood factors.

In this study, we have considered an alternative means of scaling up the description of growth and respiration. Consider that the units of equation 2 are milligrams chlorophyll *a* per liter per day. When multiplied by an appropriate stoichiometric coefficient $\delta_{Chl:C}$ that converts milligrams chlorophyll *a* to milligrams carbon, the left-hand side of equation 2 is equal to lakewide average gross primary production (GPP) expressed in milligrams of carbon per liter per day, and when $\delta_{Chl:C}$ is multiplied to the left had side of equation 3, the result is equal to the lakewide average of the autotrophic component of community respiration (CR), expressed in milligrams of carbon per liter per day.

The use of continuous (hourly to subhourly) measurements of DO to estimate aquatic ecosystem metabolism (Odum, 1956) has been increasingly refined for lotic ecosystems (Chapra and Di Toro, 1991; Bales and Nardi, 2007; Aristegi and others, 2009; Raymond and others, 2012). Similar methods for lentic environments have lagged behind, partly because of challenges in accounting for advective horizontal transport and physical reaeration contributing to spatially varying DO concentrations in lake surface waters. In a large productive lake, horizontal transport of DO was shown to lead to significant error when the estimates are made at only one sensor (Gelda and Effler, 2002). Antenucci and others (2013) used a modeling approach to determine that transport processes could lead to large errors if not accounted for, and advocated the use of non-dimensional numbers to characterize the likely importance of horizontal and vertical transport ahead of time. However, recent advances (Staehr and others, 2010) have improved the applications of these aquatic metabolic methods to lakes, offering opportunities to evaluate and model lake ecosystems as functions of physical and chemical variables that can be independently measured.

We propose the use of continuous DO measurements to scale up growth and respiration of the cyanobacterial bloom, acknowledging that the application of the technique to a very large, shallow lake, with strong wind-driven currents, substantial spatial variability, buoyant cyanobacteria, and a cycle of diurnal stratification and mixing does not completely capture the spatial variability and transport processes. As part of this study, an initial attempt was made to calculate the lakewide metabolism from continuous DO measurements taken during 2006–08. Efforts were made to mitigate the problem of vertical mixing in this initial attempt by limiting the analysis to sites shallower than the diurnally mixed layer. In doing so the estimates were weighted more heavily toward littoral zones where both GPP and CR are expected to be higher than in the pelagic zone (Van de Bogert and others, 2007), so the estimates, particularly of GPP, are likely to be biased higher than the true lakewide mean. The estimates of CR may be higher or lower than the true lakewide mean because we have not included sites where the water column extends below the diurnally mixed layer. We have attempted to limit the potential bias introduced by horizontal transport by averaging the results at several locations.

For the purpose of substituting lake metabolism for the growth and respiration terms in the CSTR model, simply calculating lake metabolism from measurements is not enough. In order to simulate the response to nutrient management scenarios, GPP and CR must be predicted (through a submodel) as an explicit function of readily observable, independent variables. In their original form, the growth and respiration terms in the model are functions of the 14-day values of lakewide averages of chlorophyll *a*, phosphorus, temperature, and incident light. In the process of substituting lake metabolism terms, the suite of possible explanatory variables can be expanded to include other variables that are known or hypothesized to influence lake metabolism—in particular, meteorological variables such as wind and air temperature, and water-column stability. This would enable the model to take advantage of the higher frequency of data collection of meteorological and water quality variables that are collected hourly or sub-hourly to improve the time integration through the 14-day time step.

The complex dependencies between bloom dynamics and meteorological variables (and water temperature, a direct consequence of meteorology) at UKL have been noted in several previous studies (for example, Wood and others, 1996, 2006; Morace, 2007). Air temperature and wind speed also determine water-column stratification, which has been related to aspects of bloom dynamics as well (Kann and Welch, 2005; Wood and Gartner, 2010). Meteorology was included in the algorithms of the original TMDL model through light limitation to growth and temperature limitation to growth and respiration, the form of which was broadly prescribed over the season. This study derived empirical functions relating (on shorter, daily time scales) algal growth and respiration to directly measured meteorological (wind and solar radiation) and water temperature variables, and measured indicators of the strength of water-column stratification based on the difference in temperature between the upper and lower water column. The goals were to derive relationships that could be incorporated into the TMDL model equations and to improve the accuracy and timing in the simulation of the state variables (chlorophyll *a* and TP concentrations, and pH) and the prediction of lake response to implementation of TMDL limits on external phosphorus loading. As noted in the TMDL model documentation (Kann and Walker, 1999) and in the Phase 1 report (Wood and others, 2013), the original and new versions (through version F'_E) of the TMDL model cannot simulate rapid declines in the bloom that typically occur after the second week in July, and, as a result, the performance of the model decreases after the early part of the growing season (May–July).

The approach used is an empirical investigation of the production and CR time series, calculated from the continuous monitors. Although production and CR will have broad seasonal dependencies on temperature, light, nutrients, and biomass that could be determined empirically from the 14-day dataset used to run the TMDL model, in this case the dependencies were not assumed to take the form prescribed in the TMDL equations. After determining the broad seasonal dependencies, the remaining variability on shorter time scales was investigated with a daily dataset as generated below.

Explanatory variables were restricted to those that were independently observable and were not expected to change with nutrient management, or those that were state variables and thus were calculated internally by the model itself. Chlorophyll *a* and phosphorus were potential explanatory variables because these were state variables in the model; incident light, wind, and air temperature were included because they were meteorological variables that were not affected by nutrient management, and water temperature was allowed as a water quality variable because it is observable but should not change with nutrient management. In contrast, DO concentration was not included because it could change with nutrient management and is not predicted internally by the model. In this study, we have explored this concept by using our calculated GPP and CR values to develop multivariate regression models that could be substituted into the CSTR mass balance equation for chlorophyll *a*.

Calculation of Upper Klamath Lake Metabolism from Continuous Dissolved Oxygen, 2006–08

Lake Metabolism Calculations

In order to evaluate the metabolism occurring in the surface waters of the lake because of cyanobacterial activity, continuous monitor data collected over 2006–08 were used to quantify GPP (photosynthesis) and CR. Hourly DO and lake temperature data collected from nine shallow water-quality (WQ) sites and hourly wind speed data collected from two meteorological (MET) sites in the lake were used for this purpose (table 12). Because continuous WQ monitors are removed during the winter, the full daily sets covered May 15–October 16, 2006, May 15–November 13, 2007, and May 5–October 13, 2008. We focused on the shallow sites (less than 3.0 m full-pool depth) so that effects of vertical transport would be minimized. WQ sites were characterized by their position in the lake as "northern" and "southern" in order to assign proximate wind speed values, necessary for reaeration calculations, and a lakewide sediment oxygen demand (SOD) areal flux rate of 1.6 grams of oxygen per square meter per day [g (O_2/m^2)/d] at 20 °C (Wood and others, 2013) was assumed for all sites. Hourly production and CR at each site then were evaluated by the following equation at each hour:

$$\frac{\Delta C}{\Delta t} z_{full} = \Phi_{photo} - \Phi_{resp} - \Phi_{SOD} + \Phi_{reaer} \quad (5)$$

To quantify reaeration, wind speed was used to calculate a film transfer coefficient and applied that transfer rate to the difference between saturation DO and measured DO. When saturation DO was less than measured DO, oxygen moved from the water to the air, and when saturation DO was greater than measured DO, oxygen moved from the air to the water. Saturation DO was calculated for each site from hourly water temperature data using the Benson and Krause equations (U.S. Geological Survey, 2011). The film transfer coefficient, in meters per day, was calculated from wind speed data using the following equation (Gelda and Effler, 2002):

$$K_{L,20} = \begin{cases} 0.2 WSPD_{10}, WSPD_{10} \le 3.5\,\text{m/s} \\ 0.057 WSPD_{10}^2, WSPD_{10} > 3.5\,\text{m/s} \end{cases} \quad (6)$$

Because USGS MET wind speed data were measured at a height of 2 m above water surface, the values were translated to 10-m values, $WSPD_{10}$, using a logarithmic approximation (Martin and McCutcheon, 1999). The film transfer rates were temperature corrected using the Van 't Hoff equation, with input parameter, θ, equal to 1.024 (Gelda and Effler, 2002), and applied to the DO deficit to calculate the areal reaeration flux for each hour:

$$\Phi_{reaer} = \frac{K_{L,20} * 1.024^{T-20} * \left(C_{sat} - C\right)}{z_{full}} \quad (7)$$

The sediment-oxygen demand (SOD) areal flux also was temperature-corrected by the Van 't Hoff equation, with θ equal to 1.065 (Chapra, 1997), to get Φ_{SOD}. At this point, the nighttime DO data (9:00 p.m.–5:00 a.m.) were extracted to calculate hourly respiration flux by setting photosynthetic flux equal to zero:

$$\Phi_{resp} = \Phi_{reaer} - \frac{\Delta C}{\Delta t} * z_{full} - \Phi_{SOD} \quad (8)$$

For each hour, respiration was reverse-temperature-corrected to find $\Phi_{resp,20}$ using equation 15 from Wood and others (2013), with T_{min} set to 4 °C instead of 14 °C. This allowed respiration to continue at lower temperatures than previously allowed in the TMDL model. $\Phi_{resp,20}$ then was averaged over each continuous nighttime segment and the average value was applied to all hours of the prior day. For example, respiration averaged from June 1, 2006, 9:00 p.m., to June 2, 2006, 5:00 a.m., was applied to all hours of June 1, 2006. With $\Phi_{resp,20}$ values now temperature-corrected for each hour, hourly photosynthetic flux was calculated:

$$\Phi_{photo} = \frac{\Delta C}{\Delta t} * z_{full} + \Phi_{resp} + \Phi_{SOD} - \Phi_{reaer} \quad (9)$$

Daily GPP and respiration were calculated for each site by accumulating the hourly values, and the lakewide totals were determined by averaging across all sites for each day. Daily totals then could be converted to chlorophyll *a* concentrations by using the average lakewide depth and published stoichiometric ratios of oxygen to carbon (2.67 gO/gC) and carbon to chlorophyll *a* (41 gC/g chlorophyll *a*) (Bowie and others, 1985). The net chlorophyll *a* concentrations (B_{NPP}) were calculated by taking the difference between these daily GPP and respiration chlorophyll *a* concentration totals.

Table 12. U.S. Geological Survey continuous monitoring sites used for metabolism analysis, Upper Klamath Lake, Oregon, 2006–08.

[Site locations are shown in figure 1. **Abbreviations:** USGS, U.S. Geological Survey; WQ, water quality; MET, meterological; NA, not applicable; m, meter]

Site name	Site name abbreviation	Type	USGS site No.	Latitude (north)	Longitude (west)	Full-pool measured depth (m)	Years	Lake orientation
Fish Banks	FBS	WQ	422808122024400	42°28'08"	122°02'44"	2.80	2006–2008	North
North Buck Island	NBI	WQ	421838121513900	42°18'38"	121°51'39"	2.80	2006–2008	South
Upper Klamath Lake at Williamson River outlet	WMR	WQ	422719121571400	42°27'19"	121°57'14"	2.50	2006–2008	North
Howard Bay	HDB	WQ	421933121550000	42°19'33"	121°55'00"	2.20	2006–2008	South
Hagelstein Park	HPK	WQ	422319121585700	42°23'19"	121°48'57"	2.60	2006	South
Skillet Handle	SHL	WQ	421746121522800	42°17'46"	121°52'28"	2.50	2006	South
South Shore	SSR	WQ	421410121492000	42°14'10"	121°49'20"	2.50	2006–2008	South
Goose Bay East	GBE	WQ	422749121540700	42°27'39"	121°54'08"	2.40	2006–2008	North
Williamson Delta West	WDW	WQ	422842121584300	42°28'48"	121°58'43"	2.20	2006–2008	North
Mid-North	MDN	MET	422622122004000	42°26'22"	122°00'40"	NA	2006–2008	North
Mid-Lake	MDL	MET	422312121515900	42°23'12"	121°51'59"	NA	2006–2008	South

Multivariate Regression Models of Lake Metabolism

The time series of daily calculated production, due to photosynthesis, and CR were modeled at two different temporal scales. We calculated the sum of a seasonal component, which represented variability at scales longer than a week, and a higher frequency (designated "weekly") component, which represented variability at scales shorter than a week: $GPP = GPP_S + GPP_W$ and $CR = CR_S + CR_W$. The seasonal component was determined by multivariate regression with the Klamath Tribes 14-day dataset, which proceeded as follows. The seasonal component was assumed to be a function of chlorophyll *a*, nonalgal phosphorus, temperature, and solar radiation, as these variables were considered to represent long-term variability at scales longer than a week.

$$GPP_S \text{ or } CR_S = f\left(\boldsymbol{B}, P_{na}, T_{lake}, I_0\right) \tag{10}$$

Each of the four variable inputs were selected from a set which included the variable itself, the natural logarithm of the variable and the square of the variable, as shown below for chlorophyll *a*, which resulted in 81 unique models tested for each of GPP_S and CR_S:

$$\boldsymbol{B} \in \left\{B, \ln\left(B\right), B^2\right\} \tag{11}$$

All 3 years of data were combined for this step and an Akaike's Information Criterion (AIC) value was computed for each tested model. The set of possible best models was the set of models with an AIC value within 2 of the minimum AIC value. A multivariate regression was run using each of these models, and the selected model was the one that resulted in the best combination of normally distributed residuals based on a comprehensive assessment of a variety of indicators including (1) visual inspection of plots of the residuals; (2) variance inflation factors indicating low collinearity of the explanatory variables; (3) a Durbin-Watson statistic close to 2, indicating low serial correlation in the residuals; (4) t-tests of the parameter estimates; and (5) parsimony when other indicators were equal.

The weekly component was determined by multivariate regression with a daily dataset of meteorological variables and water temperature as follows: A time series of daily values of the seasonal component of production and CR was calculated from daily values of the Klamath Tribes 14-day dataset, obtained with a cubic spline interpolation, and the seasonal regression parameters determined in the first step. A times series of the daily values of the weekly component of production and CR was obtained by subtracting daily values of the seasonal component from the daily values of the total production and CR, which filtered out the seasonal cycle. Five possible explanatory variables were considered (table 1):

$$GPP_W \text{ or } CR_W = f\left(WSPD_{10}, WTDEV, SSDEV, WTROC, STRAT\right) \tag{12}$$

$WSPD_{10}$ is the daily wind speed 10 m above the water surface, as determined previously. *WTDEV* is the daily deviation in water temperature from the seasonal trend, where the seasonal trend is the cubic-spline-interpolated water temperature from the 14-day dataset; it is calculated as the ratio of daily lakewide averaged water temperature divided by the interpolated daily values of the seasonal trend in lakewide averaged water temperature. *SSDEV* is the daily deviation in shortwave solar radiation from a clear sky calculation of solar radiation; it is calculated as the daily average shortwave solar radiation divided by the daily clear sky calculated values. The clear sky calculation was obtained from Environmental and Water Resources Institute (2005). *WTROC* is the daily rate of change in air temperature, defined as the difference between the water temperature of the current day and the water temperature 3 days prior, divided by 3. A window of 3 days was used to determine *WTROC* because the relation between stratification and bloom expansion has a tendency to reverse sign at 3 days (Eldridge and others, 2014). *STRAT* is a variable designed to be a surrogate for water-column stratification, and is defined as the daily cumulative sum of the difference in temperature measured by a datasonde located 1 m from the surface and a datasonde located 1 m from the bottom at the deepest site in the lake (MDT) monitored with continuous monitors. The time series in each year were divided into three segments—early, middle, and late season—as determined by a temperature rule rather than a calendar date. These segments based on temperature were based on a subjective examination of plots of chlorophyll *a* as a function of temperature. Early-season started at the beginning of the time series and ended when the daily lake-averaged water temperature exceeded 20 °C for 5 consecutive days, marking the beginning of mid-season. Mid-season transitioned to late-season when the lake-averaged water temperature was less than 20 °C for 5 consecutive days. The 5-day time window was selected subjectively by examining the variability in the time series. The multivariate modeling procedure was performed for each segment.

Calibration of the weekly component of the model, which was performed separately for the early, middle, and late seasons, considered only linear combinations of the five explanatory variables, and only data from 2007, which were selected randomly (fig. 7). The final model was determined from AIC values using multi-model inference (Burnham and Anderson, 2002). Six sets of models were created, one for each variable. Within each set an Akaike weight was calculated for each model (Burnham and Anderson, 2002). A model-averaged estimate of each model parameter was calculated as an Akaike-weighted average of the estimates from all models in a set, and the 80-percent confidence interval was calculated from a model-averaged estimate of the standard error of the parameter. Only those variables for which the 80-percent confidence interval of the model-averaged estimate of the parameter did not include zero were retained in the final model. Once the variables to be included in the final model were determined, the multivariate regression was run again with only those variables in order to determine final values of the model parameters. At this step, a variable was dropped from the model if it was found to create collinearity as determined by the variable infiltration factor.

The final model (table 13) combining the seasonal with mid- and late-season weekly components was used to re-create the daily time series of production and CR during 2006–08. The performance of the final model was assessed with a calculated bias (mean of simulated value minus measured value), a RMSE, a NS statistic, and a R^2.

Table 13. Multivariate regression equations.

[Dependent and explanatory variable definitions are provided in table 1. **Abbreviations**: R^2, coefficient of determination; RMSE, root mean square error; –, no value]

Dependent variable	Model period	Number of observations	Intercept	Coefficients of explanatory variables from 14-day dataset			Coefficients of explanatory variables from daily dataset					Regression model fit statistics	
				ln(*B*)	I_0	T_{lake}	$WSPD_{10}$	*WTDEV*	*SSDEV*	*WTROC*	*STRAT*	Adjusted R^2	RMSE
GPP_S	Entire	29	–29.56	6.11	0.034	–	–	–	–	–	–	0.63	5.56
CR_S	Entire	29	–14.21	3.71	–	0.49	–	–	–	–	–	0.55	4.45
GPP_W	Middle	65	–	–	–	–	–3.04	–	10.02	–	–	0.23	6.06
CR_W	Middle	65	–	–	–	–	–2.44	14.14	–	–	–	0.44	4.72
GPP_W	Late	71	–20.09	–	–	–	–	13.19	4.81	–	0.09	0.33	4.07
CR_W	Late	71	–13.03	–	–	–	–	12.96	–	–	0.13	0.16	4.54

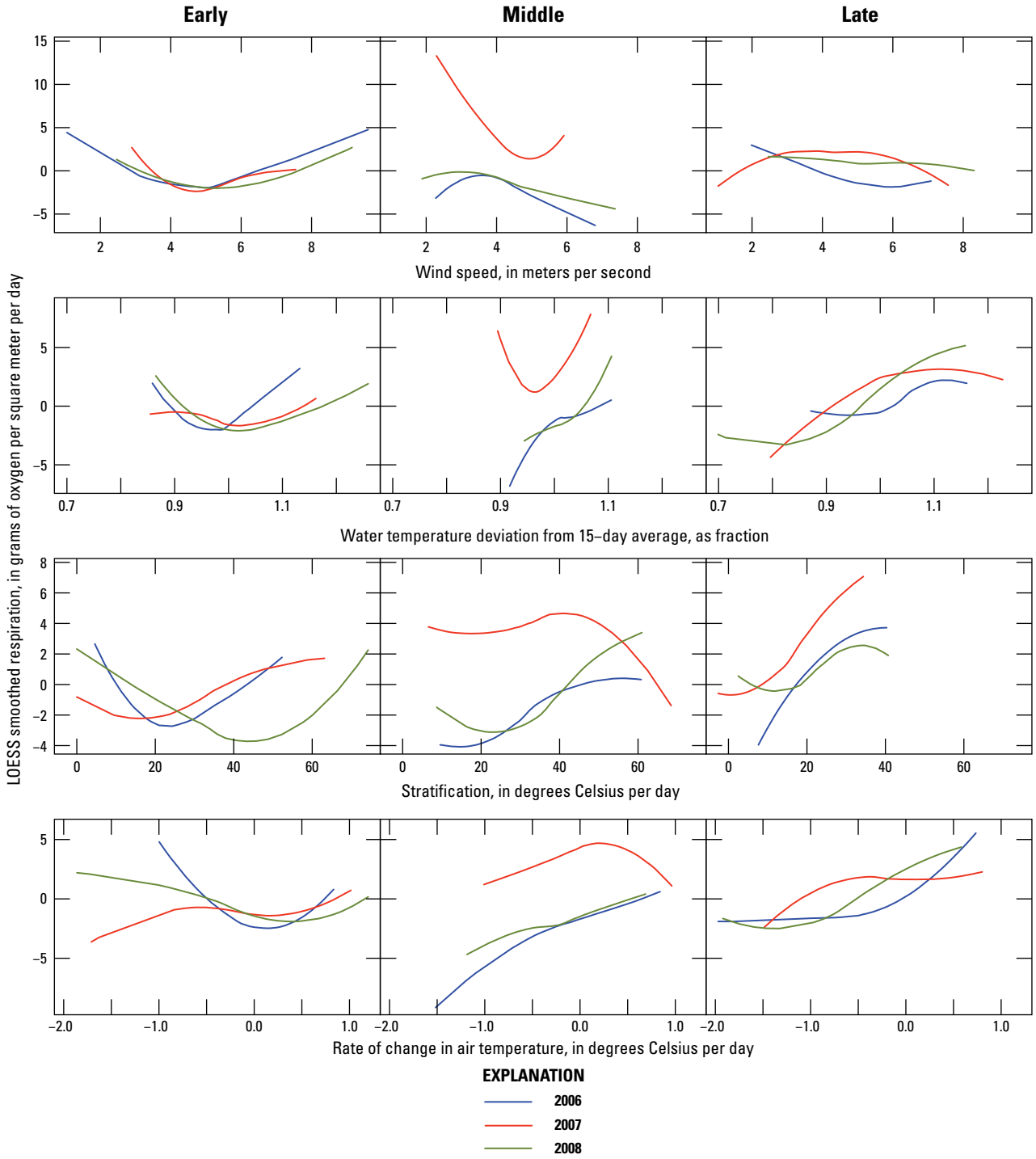

Figure 7. Local Regression (LOESS) smoothed respiration as a function of regression model of metabolism predictors, Upper Klamath Lake, Oregon, during early, middle, and late parts of summer seasons 2006–08.

Incorporation of Upper Klamath Lake Metabolism Submodel into CSTR Model

Incorporation into CSTR Model

The calculated net chlorophyll *a* concentrations, B_{NPP}, were directly incorporated in the chlorophyll *a* component of the CSTR model by accumulating the daily values over the 2-week time step and substituting as below:

$$\frac{dB}{dt} = \left(GROWTH - RESP - SETTLE - \frac{Q_{out}}{V} \right) \times B = \frac{B_{NPP}}{\Delta t} - \left(SETTLE + \frac{Q_{out}}{V} \right) \times B \qquad (13)$$

At this point, the settling velocity and recycling parameters were recalibrated over 2006–08 by following processes similar to those outlined by Kann and Walker (1999). Modified versions of calibration steps 1 and 2 (above) follow.

Step 1—Algal Settling Velocity

Algal settling velocity was evaluated by comparing calculated and measured chlorophyll *a* concentrations when the following model equation was run with measured chlorophyll *a* data from the previous biweekly interval and measured net growth data:

$$B_t = B_{t-\Delta t} + B_{NPP} - \left(\frac{u_{alg}}{z} + \frac{Q_{out}}{V} \right) \times B_{t-\Delta t} \Delta t \qquad (14)$$

Algal settling velocity values were assumed to be between 0.001 and 2.0 m/d (Bowie and others, 1985), and the best value was determined by correlating chlorophyll *a*, as calculated by equation 14, with all available measured chlorophyll *a* concentrations within the 2006–08 time period. The sum of squared errors was minimized with u_{alg}= 0.463 m/d, which is a much higher settling velocity (by an order of magnitude) than had previously been calibrated. For this model, it was unnecessary to calibrate the half-saturation constant because net growth was input as a measured variable and phosphorus limitation was not explicitly calculated.

Step 2—Internal Recycling Parameters

As before, the recycling equation for the CSTR model required two calibration parameters, *pH** and K_R, which were selected based on minimization of the objective function (Wood and others, 2013, equation 24) over a calibration set. For this analysis, calibration was performed by a cross-validation leave-one-out method, where 2 full years of the 2006–08 dataset were used for calibration, and the third year was used for validation. In this approach, the calibration/validation process was repeated three times to ensure that each year was included in the validation set at least once and included in the calibration set at least once, which resulted in three sets of calibrated recycling parameters (tables 5–10, G'_1, G'_2, G'_3) . Collectively, the calibrated *pH** value ranged from 8.9 to 9.0 and the calibrated K_R value ranged from 6.77 to 7.63/d for 2006–08,and showed little variability between results when different years were selected for calibration. Both the *pH** and K_R values were higher than those determined in the previous recalibration, with recycling rates as much as 6.5 times greater than those calculated for the CSTR model calibrated over 1991–98. The higher calibrated recycling rate is consistent with the higher calibrated settling velocity discussed above because faster settling requires faster recycling to explain the same measured dataset.

Model Performance

The performance statistics determined for the calibrated models run with calculated metabolism (tables 5–10, G'_1, G'_2, G'_3) generally indicated good model performance, although the evaluation time period was short, so statistics were calculated over small sample sets. Performance statistics were comparable to those found for model versions F'_O and F'_E subsetted over the 2006–2008 period. The whole-year validation statistics generally indicated that the metabolism models were best at simulating TP and worst at simulating chlorophyll *a*, although version G'_2 performed better for chlorophyll *a* than TP. For the whole-year validation periods, the metabolism model correlation coefficients generally were high—(0.44–0.91 for TP, 0.44–0.66 for chlorophyll *a,* and 0.70–0.77 for pH (tables 5–7). When the May–July subsets were considered, performance statistics were improved. The biweekly metabolism models were able to capture the decreases in chlorophyll *a* and pH associated with the mid-season bloom decline in 2006 and 2007, but not in 2008. This phenomenon was not achieved in any years with the previous CSTR models (fig. 8).

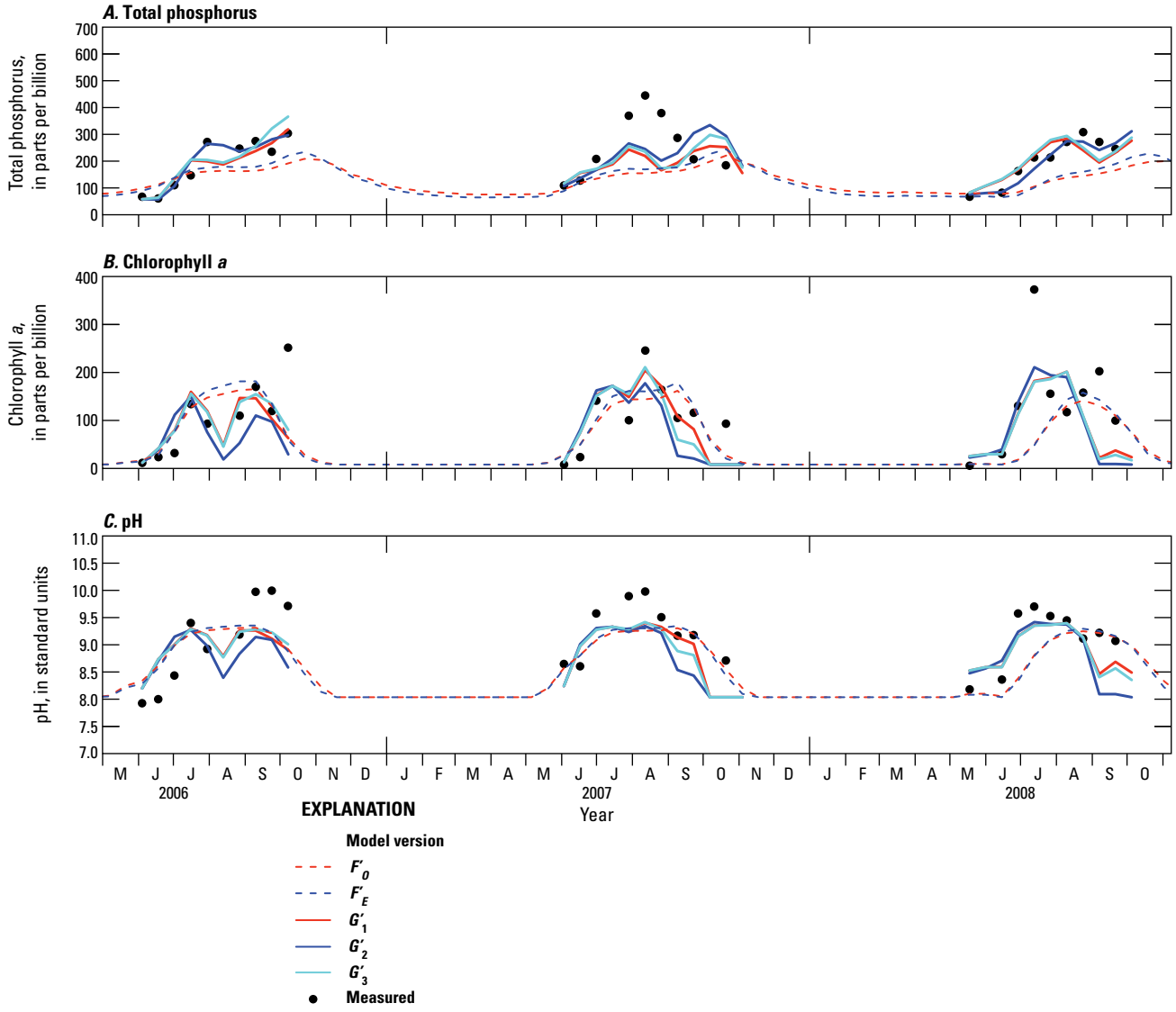

Figure 8. Biweekly simulated and measured water-column (*A*) total phosphorus (as P) concentration, (*B*) chlorophyll *a* concentration, and (*C*) pH, Upper Klamath Lake, Oregon, 2006–08.

In addition to running the CSTR biweekly model with calculated metabolism, the model also was run with a daily time step using daily boundary conditions as inputs (Walker and others, 2012) and previously calibrated parameters. Model performance statistics were not calculated separately, but plots comparing the outputs and measured data were developed. The daily time step is better at capturing the mid-season chlorophyll *a* and pH decreases than the biweekly time step (fig. 9). Daily pH as simulated by the CSTR-metabolism model was compared to daily average pH as determined from USGS continuous monitoring data (fig. 10). Although the exact values are not always the same, the shapes of the measured and metabolism-model simulated daily curves tend to match well in all 3 years; the simulated curves for the three model versions (G'_1, G'_2, G'_3) lie on top of each other when plotted. The daily metabolism models were able to capture decreases in chlorophyll *a* and pH associated with the mid-season "crash" in all years (2006–08).

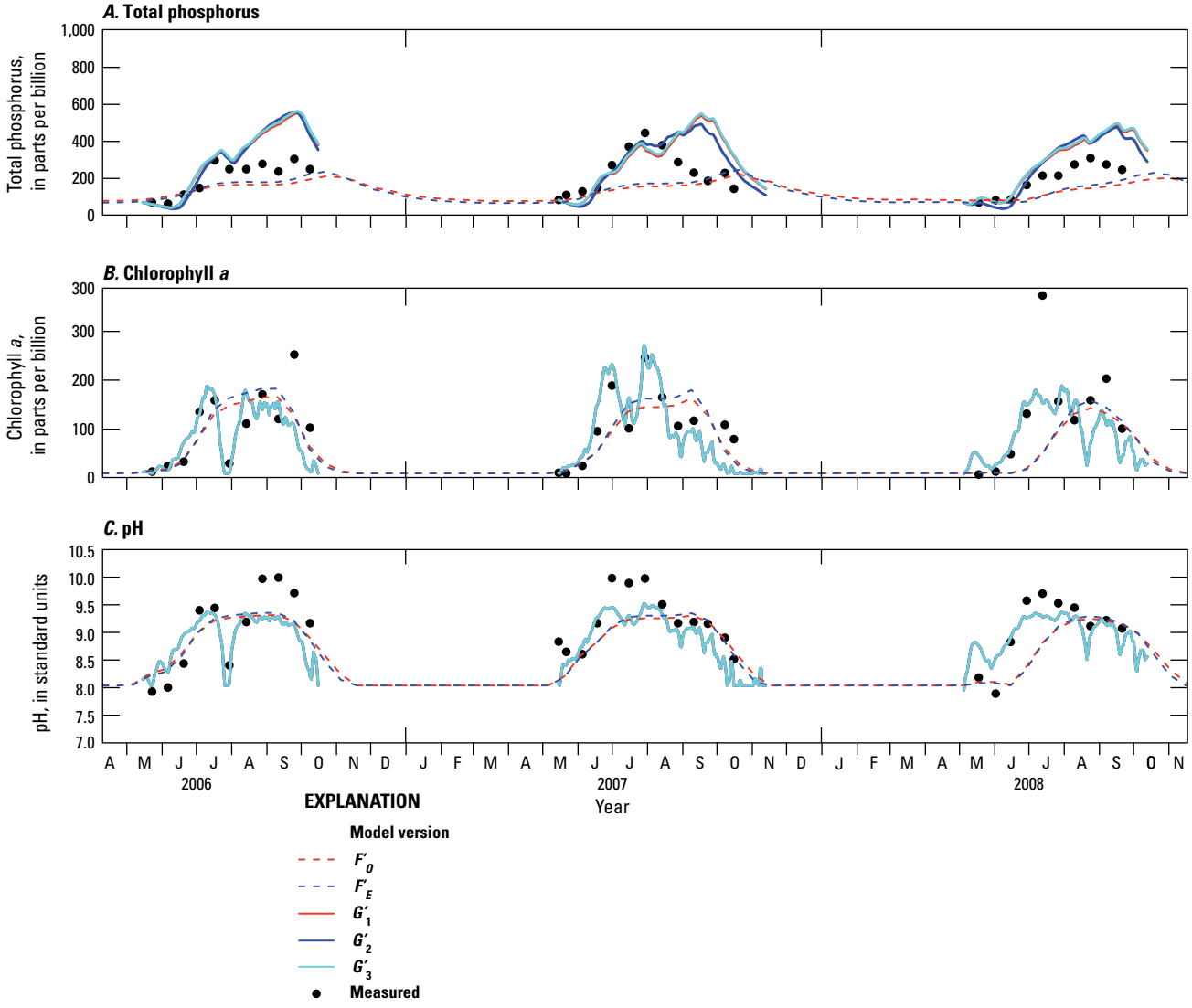

Figure 9. Simulated and measured water-column (*A*) total phosphorus (as P) concentration, (*B*) chlorophyll *a* concentration, and (*C*) pH, Upper Klamath Lake, Oregon, 2006–08.

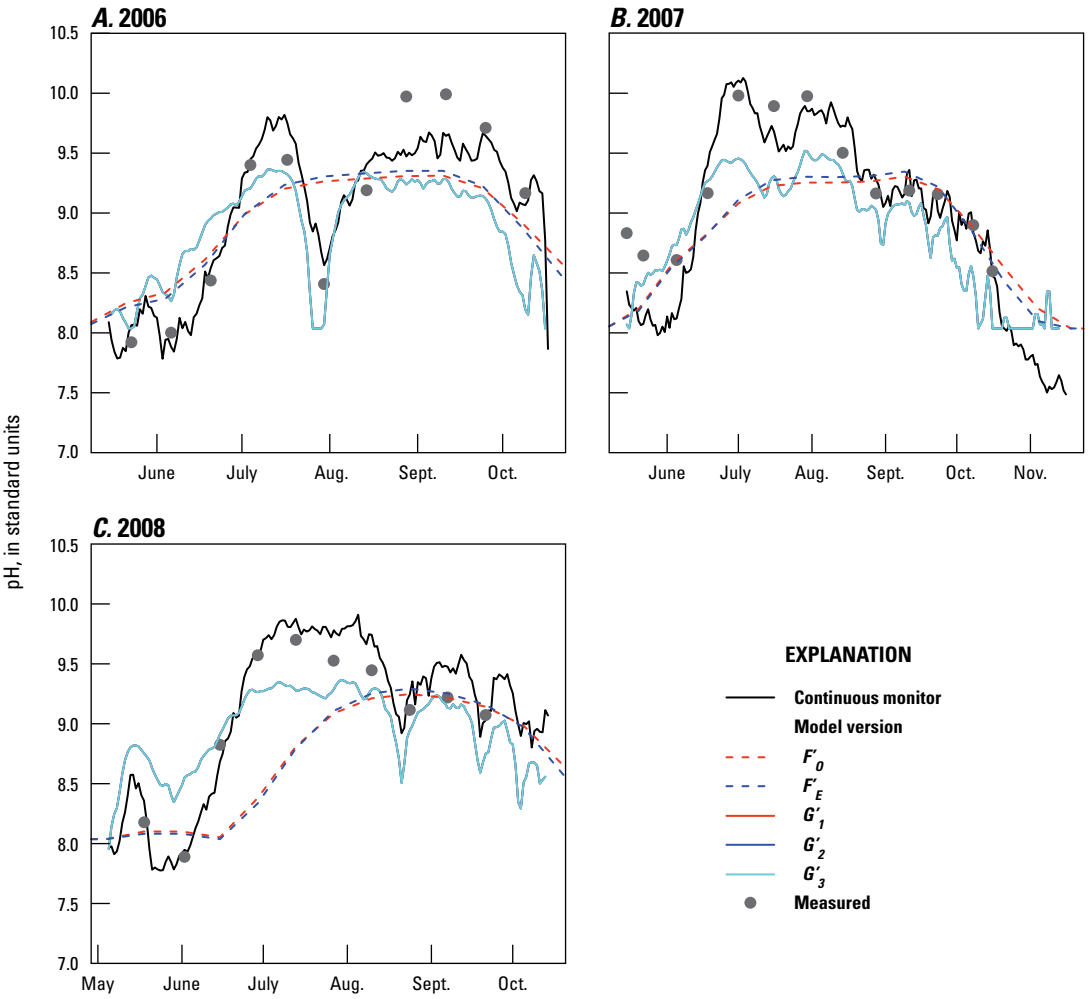

Figure 10. Simulated and measured water-column pH in (*A*) 2006, (*B*) 2007, and (*C*) 2008, Upper Klamath Lake, Oregon.

Prediction of Upper Klamath Lake Metabolism from Meteorological Variables, 2006–08

The best regression model for the seasonal component of production was determined from the 14-day dataset to include the natural logarithm of chlorophyll *a* concentration and solar radiation, and the best regression model for the seasonal component of CR included the natural logarithm of chlorophyll *a* concentration and water temperature (table 13; equations 1 and 2). The best model for production did not include water temperature or nonalgal phosphorus. This is not an indication that production does not depend on these variables; rather, there was collinearity among chlorophyll *a*, solar radiation, temperature, and nonalgal phosphorus, and not enough independent information contained in the 14-day dataset to support inclusion of more than two variables in the regression (fig. 11; time series of seasonal overlaid on time series of daily, with 14-day points as symbols).

The mid-season segment of the weekly components of CR and total production started on June 23, June 30, and June 27 in 2006, 2007, and 2008, respectively. The mid-season segment ended on August 29, September 3, and August 30 in 2006, 2007, and 2008, respectively (fig. 12; time series of weekly components with simulated values overlaid and with the boundaries between early, mid-, and late-season segments indicated). The fit of the models to the weekly component generally was poor, but best for the late-season segment. It was not possible (based on the performance statistics) to determine a minimally acceptable weekly component model

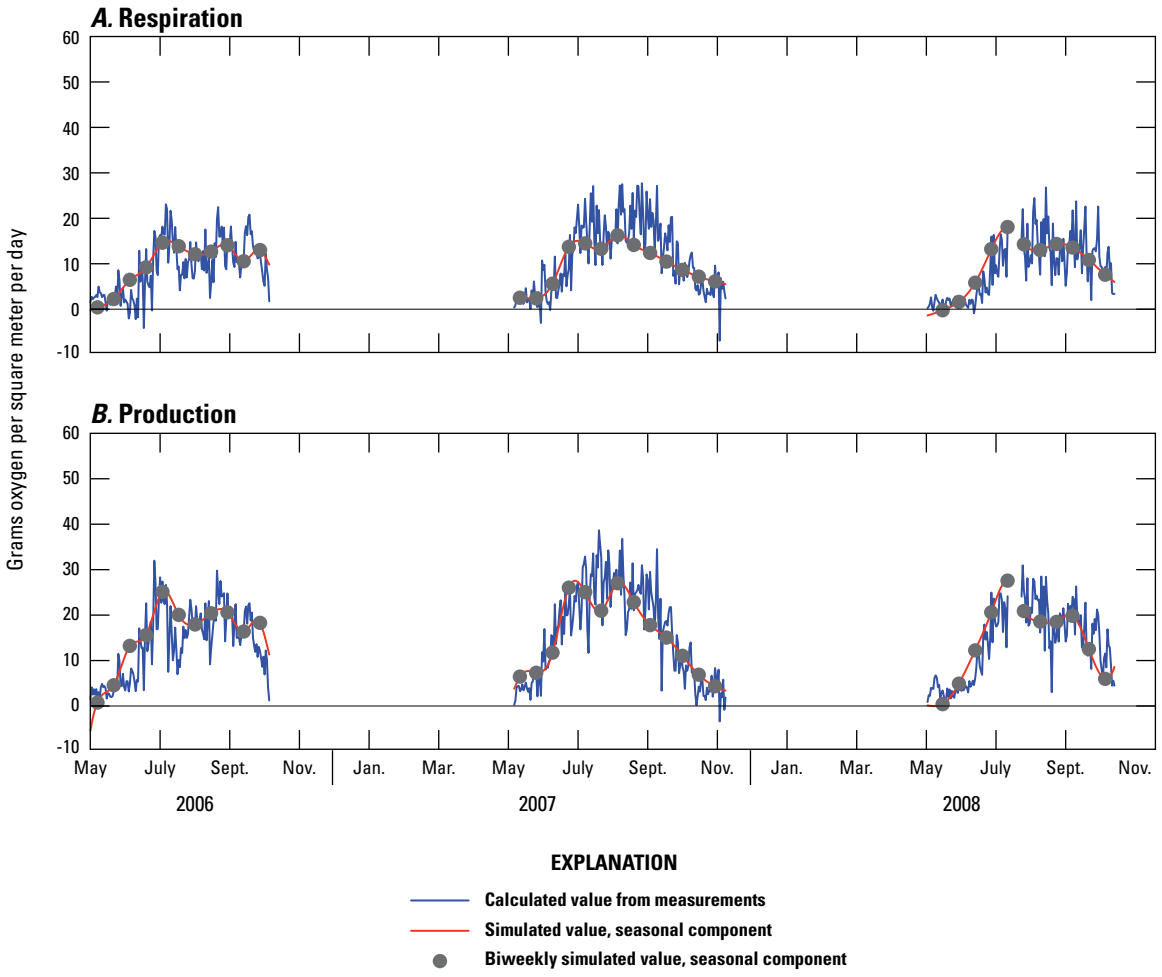

Figure 11. Measured values, calculated using dissolved oxygen data from nine, continuous, shallow-sites, U.S. Geological Survey monitors (table 12), and simulated values of the seasonal component of the regression model of metabolism, Upper Klamath Lake, Oregon, 2006–08.

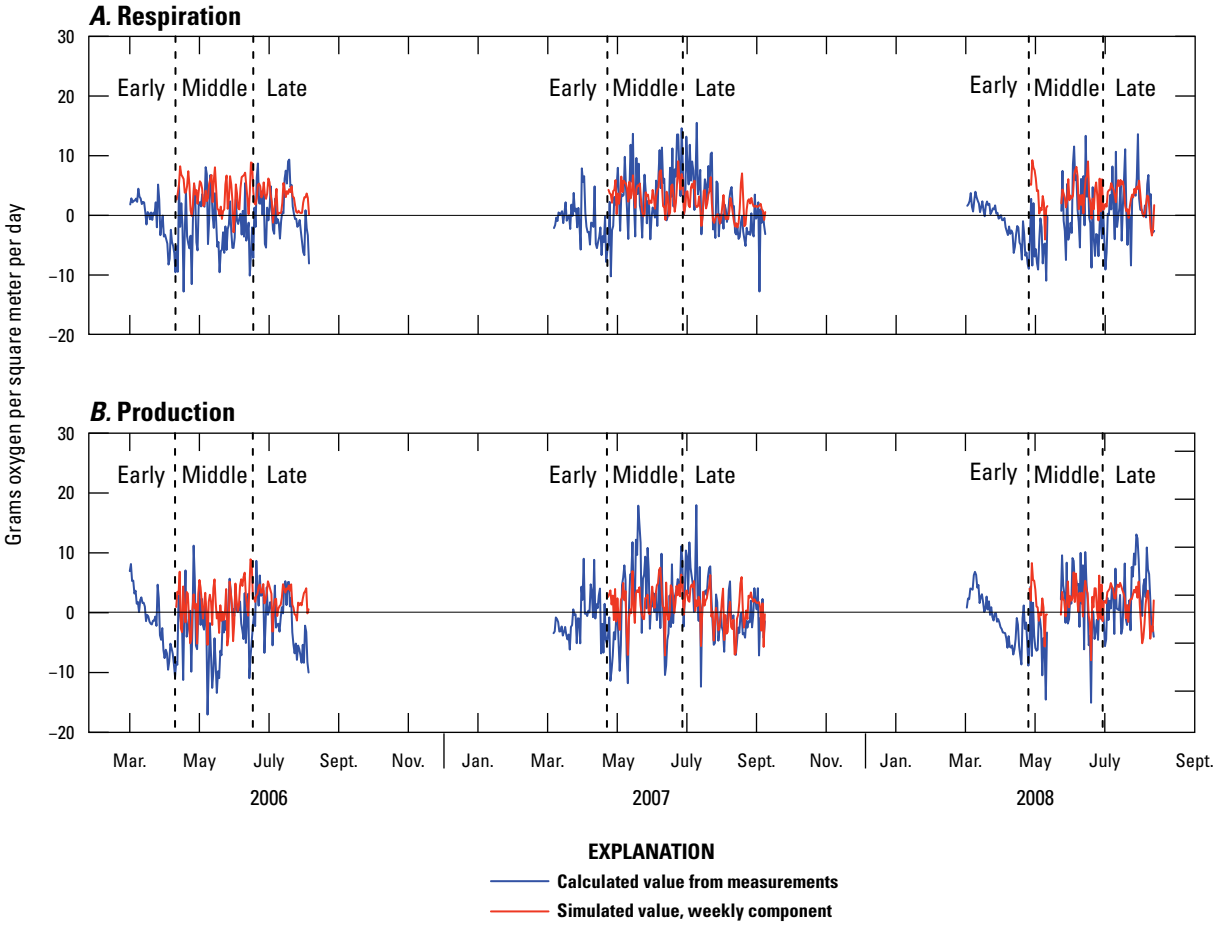

Figure 12. Respiration and production values calculated from measured data and simulated values of the weekly component of the regression model of metabolism, Upper Klamath Lake, Oregon, 2006–08.

for the early-season segment; therefore, no coefficients are reported in table 13 and only the seasonal component is shown in figure 13 (time series of CR and total production, with simulated values, and the boundaries between early, mid-, and late-season segments indicated). The coefficients in table 13 indicate that (1) mid-season GPP_W and CR_W are negatively related to wind speed, (2) CR_W is positively related to water temperature, and (3) GPP_W is positively related to shortwave solar radiation. Late-season relations show both GPP_W and CR_W positively related to water temperature and stratification, and GPP_W positively related to shortwave solar radiation.

When the seasonal and weekly models for production were combined (only the seasonal component for the early season segment), the fit statistics indicated that the combined model explained about 60–80 percent (R^2 about 0.60–0.80) of the variance over the 2006–08 period, with a minimum of 62 percent in 2006 and a maximum of 79 percent in 2007 (the year in which measurements were used for calibrating the weekly component model; table 14). When the seasonal and weekly models for CR were combined, the fit statistics indicated that the combined model explained about 50–70 percent (R^2 about 0.50–0.70) of the variance over the 2006–08 period, with a minimum of 53 percent in 2006 and a maximum of 70 percent in 2007. The combined production model was more successful than the CR model, as indicated by higher R^2 values, values of the NS statistic closer to 1, and smaller biases. Visual inspection of the time series shows that the direction of change of the simulated values often is the same as the calculated values in the mid- and late-season segments, on time scales of a few days to weeks, even though the magnitude of the variability in the simulated values is not as great as in the calculated values (fig. 13). Model performance is similar to results from Coloso and others (2011), whose study attempted multivariate regression analysis of GPP and CR. Their R^2 values for GPP and CR ranged from 0.22 to 0.43 and from 0.18 to 0.55, respectively, across 2 years and two lakes.

NPP is obtained by subtracting the CR from production (fig. 14). Negative NPP is indicative of declining bloom conditions. The daily time series of NPP calculated from continuous sonde data shows mid-season decreases in NPP, where mid-season was delineated by Julian days 174–241 in 2006, 181–246 in 2007, and 179–243 in 2008.

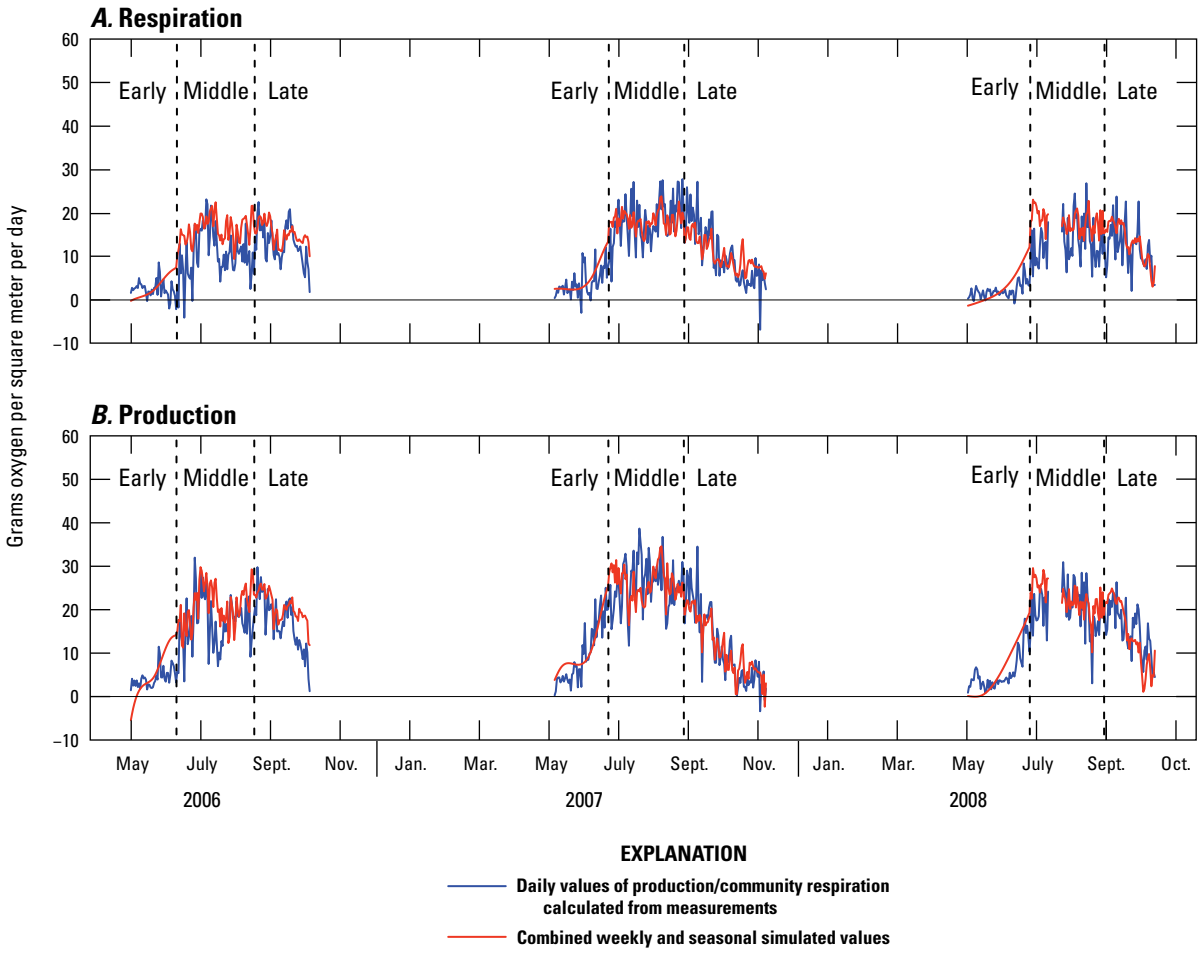

Figure 13. Respiration and production values calculated from measured data and simulated values from the combined seasonal and weekly components of the regression model of metabolism, Upper Klamath Lake, Oregon, 2006–08.

Table 14. Goodness-of-fit statistics for the combined (seasonal plus weekly component) regression models for total production and community respiration, Upper Klamath Lake, Oregon, 2006–08.

[R^2, coefficient of determination; RMSE, root mean square error; NS, Nash-Sutcliffe statistic; (g O_2/m^2)/d, grams oxygen per square meter per day]

Year	Community respiration				Production			
	Bias	NS	RMSE [(g O_2/m^2)/d]	R^2 [(g O_2/m^2)/d]	Bias	NS	RMSE [(g O_2/m^2)/d]	R^2 [(g O_2/m^2)/d]
2006	3.30	0.14	5.62	0.53	3.24	0.37	6.02	0.62
2007	0.26	0.70	4.28	0.70	0.31	0.79	4.71	0.79
2008	2.65	0.27	5.61	0.58	1.28	0.57	5.31	0.69

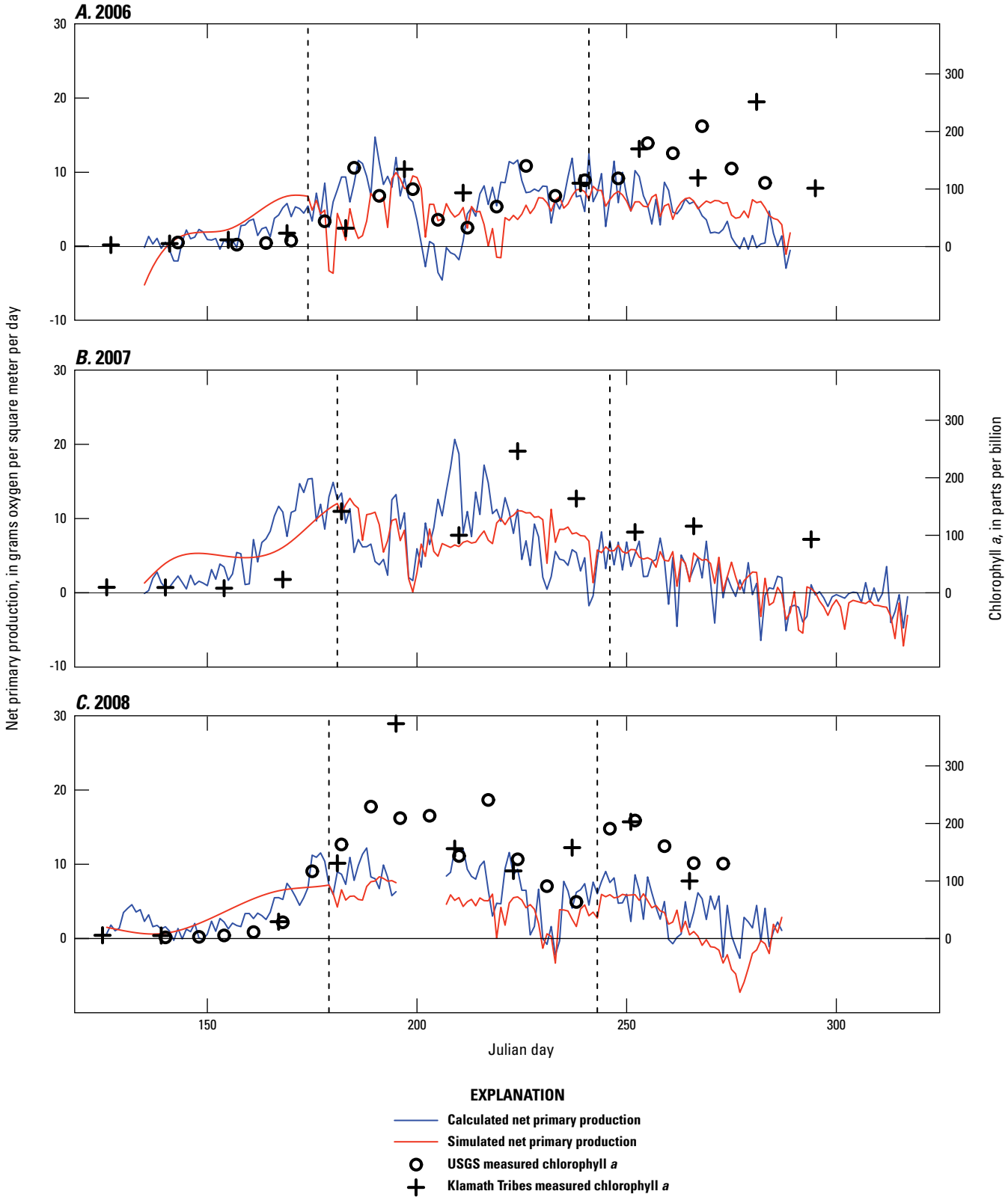

Figure 14. Comparison of the calculated and simulated net primary production to measured chlorophyll *a* values from Klamath Tribes and U.S. Geological Survey monitoring programs, Upper Klamath Lake, Oregon, 2006–08.

Negative values of NPP in late July 2006 and mid-August 2008 are consistent with low chlorophyll *a* concentrations near those dates, indicative of a severe bloom decline (Lindenberg and others 2009, Kannarr and others 2010). The mid-season decreases in 2007 occurred about 2 weeks earlier than in 2006 and did not reach negative values, consistent with an earlier and milder bloom decline in 2007 relative to 2006 and 2008, based on water-quality indicators (Kannarr and others, 2010). If the production and CR calculations are to be useful for modeling purposes, then they must be able to reproduce mid-season minima and negative values of NPP. The simulated values of NPP reproduce the timing of the mid-season minima in 2007 and 2008, but the timing in 2006 is about 2 weeks late (fig. 14). Nonetheless, because simulated NPP is the difference of two simulated quantities, the occurrence of low and negative values in the time series of simulated NPP during the mid-season is an important result.

Discussion and Suggestions for Model Improvements

Model Updates

Continuously Stirred Tank Reactor Model Calibration

The continuously stirred tank reactor (CSTR) model parameter calibrations, as performed over the original, shorter 1991–98 and longer, extended 1991–2010 datasets, provided greater insight into the sensitivity of model parameters to input data, calibration technique, and model structure. With regard to the calibration process in its current form, the steps were sequenced so that settling velocity is evaluated before recycling and the relationship between these parameters becomes apparent. For all model versions that were comparable with respect to initial sediment reservoir and recycling approach, but had varying light limitation and chlorophyll *a* model structures (versions O', A', B', E', F'_O and F'_E), there was a positive correlation between u_{alg} (net settling velocity for algal phosphorus) and K_R (maximum total phosphorus recycle rate).

The assumptions of the chlorophyll *a* model also were important for model calibration. When equilibrium was assumed for the chlorophyll *a* model, the resulting *pH** values always were greater than 8.6 (versions O', A', B' and C'); however, when a Runge-Kutta approach was used to simulate chlorophyll *a*, the *pH** values always were less than or equal to 8.3. This result is important for model simulations, because once recycling starts, the feedback in the model leads to an increase in chlorophyll *a* (a bloom event). If the model is calibrated so that recycling occurs at lower pH values, then a bloom year is more likely to occur even if the resulting maximum chlorophyll *a* of that bloom year is low. Having a low *pH** value makes "no bloom" years much less likely, regardless of recycling rate. This result is important because the algal submodel that uses the Runge-Kutta solution method is better calibrated with low *pH** values; therefore, the algal submodel using the Runge-Kutta solution method is less likely to result in "no bloom" years.

Metabolism as an Independent Predictor of Bloom Dynamics

The lake metabolism calculations provide insight into the typical seasonal bloom dynamics in Upper Klamath Lake (UKL). Net primary production (NPP) is the difference between gross primary production (GPP) and community respiration (CR), and during most of the bloom season in this lake NPP is positive, indicating the system is net autotrophic. However, NPP is the small difference of two large numbers, and provides a more comprehensive insight into the nature of what constitutes the bloom "crash," a rapid decline in chlorophyll *a* accompanied by low dissolved oxygen (DO) concentration and reduced pH that occurs in most years sometime between mid-July and mid-August. As long as GPP exceeds CR, the bloom expands, but when CR exceeds GPP, the bloom contracts. Even if the contributor(s) to bloom decline are unknown (cyanophages, bacterial infection, ultraviolet radiation damage, zooplankton grazing), the decline is manifested in the balance between GPP and CR; therefore, the decline can be described and potentially predicted as a function of external, measurable variables. Hypotheses might be that (1) there is a relation between bacterial abundance and temperature, or (2) a relation between the probability of cyanophage infection and the water-column mixing regime, or (3) a relation between ultraviolet radiation exposure and stratification. It might not be necessary to completely understand the mechanism behind the bloom decline in order to build an empirically based predictive model for it, although the results from this study were not definitive.

An assumption inherent in substituting CR for the growth term in the CSTR model is that autotrophic respiration dominates and heterotrophic respiration is a small contributor. This probably is a good assumption during peak bloom growth, but it is less clear how good an assumption it is when the bloom is in decline. The CR estimates in this study largely followed the same mid-season decline cycle as the GPP estimates (fig. 11). We hypothesize, therefore, that CR is dominated by autotrophic respiration, because if heterotrophic respiration dominated, we would expect to observe an increase in CR coincident with a decrease in GPP during bloom decline. Measurements of GPP and CR from bottles (Lindenberg and others, 2009) similarly showed that, with a few exceptions, CR and GPP tracked with one another. There was at least one indication of high heterotrophic CR during the bloom decline at a shallow site in Howard Bay, but that example also underscored the fact that such heterotrophy was not observed at other sites, at least down to the depth of the deepest light/dark bottles (1.5 meters). In this

proof-of-concept, CR also is likely underestimated because the model did not include respiration below the diurnal mixed layer. This could be one reason that our estimates of negative NPP (heterotrophy) do not coincide in time perfectly with our other measures of bloom decline.

Our regression results were moderately successful. In a previous study by Coloso and others (2011), similar attempts were made at multivariate regression analysis of estimates of GPP and CR, and the results were not better than the results of this study; the coefficient of determination (R^2) values for GPP and CR ranged from 0.22 to 0.43 and from 0.18 to 0.55, respectively, across 2 years and two lakes. Autoregressive terms were included, which is an improvement that could be made; however, no attempt was made to calibrate in 1 year and validate in another, which was an appropriate way of testing the predictive capability of our model, for the purpose of substituting it into the CSTR model. We obtained substantially better results during our calibration year than during our validation years.

Incorporation of metabolism to the CSTR model was examined as a proof-of-concept by using GPP and CR calculated from measured DO data. Model performance statistics were comparable to those found for the recalibrated CSTR model over the period of 2006–08. The proof-of-concept showed the efficacy of the metabolism approach in capturing mid-season bloom declines, particularly when running the model at the daily time step. Incorporation of metabolism in the CSTR model also produced a change in the timing of the bloom event as compared to the original recalibrated CSTR, which lagged by 2–3 weeks. This occurred because of the CSTR algal submodel reliance on a growth equation that was temperature-limited and that did not allow growth at lake temperatures of less than 14 °C. At the end of the season, when temperatures decreased to less than 14° C, chlorophyll *a* concentrations were approximately halved, due to averaging, until they decreased to less than the acceptable minimum threshold of 8 parts per billion. The models that incorporated calculated metabolism were not limited by temperature in this way. This demonstrates a need to better understand the dynamics between lake temperature and chlorophyll *a* concentrations.

Future Model Needs

After combining all the results of a technical review of the total maximum daily load (TMDL) model that was adopted in 2001, we suggest that five steps be taken toward a new model that preserves the benefits of the CSTR approach (primarily computational speed, and relative simplicity) while providing improved capability for simulating long-term response to management scenarios. Some of our findings are derived directly from the Phase 1 effort (Wood and others, 2013), and others follow from the modifications examined in this report. These steps are presented in order of least difficult to most difficult to implement, given our current understanding:

1. Use a daily time step. As currently scripted with the Runge-Kutta approach, the CSTR model runs fast enough to simulate many years with a daily time step in a reasonable amount of computation time. A daily time step is easy to implement and is reasonable in the context of the following suggestions that make use of data collected continuously (hourly).

2. Use a spatially explicit model as needed to interpolate between limited sampling sites and to accurately calculate (1) the lakewide average of variables as a function of the values at sampling sites, and (2) the concentrations in the outflow of the lake, so as to accurately calculate the load sent downstream as a function of the lakewide average.

3. Substitute GPP and CR for algal growth and respiration terms, respectively, in the model. We described the errors associated with the scaling-up process and the analytical framework for this substitution in section, "Lake Metabolism as a Substitute for Algal Growth and Respiration," and we have demonstrated the proof-of-concept for using continuously measured DO to calculate the lake metabolism terms. Improvements should be made, the most important being that our estimate of CR is low, as we limited the analysis to shallow sites within the diurnal mixed layer in order to avoid (for now) the problem of mixing from below. Much of the CR and, therefore, oxygen consumption in the lake occurs in the deepest part of the lake, in the trench along the western shoreline (Wood and others, 2006). The assumption that CR is dominated by autotrophic respiration could be investigated. Further work needs to be done to improve the empirical models that enable the prediction of GPP and CR from explanatory variables (meteorology and water quality) before these variables are substituted for the algal growth and respiration terms.

4. Expand equations used to model internal phosphorus loading. In our Phase 1 study, we determined that the value of the sediment phosphorus recycling rate, which currently is treated as a calibration parameter, exerts a strong effect on simulated long-term water-column concentrations of phosphorus, chlorophyll *a*, and pH, and on sediment phosphorus concentrations. Therefore, reducing the uncertainty of this parameter value in the model has important implications for refining long-term external nutrient loading strategies. This uncertainty can be reduced by creating explicit, separate terms for benthic invertebrate excretion, groundwater flux, diffusive flux, desorption at high pH, and rapid bacterial recycling for modeling internal phosphorus loading, and by collecting data to parameterize these terms where possible. Estimates are available for most of these terms, and work is ongoing to estimate benthic invertebrate excretion (Wood and others, 2013).

To support this comprehensive description of benthic fluxes, sediment phosphorus would be best separated into two compartments, organic and inorganic, with benthic invertebrate excretion and bacterial recycling in the organic compartment (also the compartment where direct exchange with the water column occurs) and the rest in the inorganic compartment. A slow conversion between organic and inorganic phosphorus indicating sediment diagenesis likely would be needed.

5. Improve the model treatment of net settling velocity. As explained for the sediment phosphorus recycling rate, the algal settling velocity is a critical parameter for simulated water-column and sediment concentrations over long time frames, with important implications for external loading reduction strategies. However, the treatment of net settling velocity as a single calibration parameter is not satisfactory for the purposes of modeling the dramatic cyanobacterial declines observed in the middle of the summer season because the net settling velocity varies in time with the proportion of buoyant and non-buoyant colonies in the water column. Estimates of suspended-sediment concentrations and values of rising and falling velocity of colonies based on acoustic backscatter and velocity measurements from ADCPs showed that (1) velocities, both rising and falling, are high and that colonies can traverse the water column on sub-daily time scales, and (2) the distribution between buoyant and non-buoyant colonies varies greatly spatially, vertically within the water column, and temporally, particularly in response to the amount of thermal stability (stratification) in the water column, a function of wind and air temperature (Wood and Gartner, 2010). Rapid response to wind-induced changes in water-column stratification of large, buoyant, cyanobacterial colonies has been observed elsewhere (Moreno-Ostos and others, 2009). Because stratification varies on a daily basis and with weather patterns, the treatment of net settling velocity as an invariant calibration parameter would be inadequate.

   Two complementary approaches can better estimate net settling velocity. The first approach is similar to the approach to growth and respiration in that it avoids the need to quantify individual factors and relies instead on using measurements to estimate the term as a whole. This approach relies on using continuous monitoring data to estimate daily depth-integrated mass values at a monitoring site (Eldridge and others, 2014). Estimates at individual continuous monitoring sites could be combined (perhaps with the aid of a spatially explicit model; see step 2 to create a lakewide average). Daily estimates of lakewide mass storage in combination with daily values of NPP allow the daily settling flux to be calculated by difference. This approach only can be pursued in combination with the calculation of GPP and CR (step 3).

   The second approach relies on field work to measure rising and falling velocities and to estimate the fraction of rising and falling colonies as a function of environmental variables. Some of this work has been done with acoustic instruments (Wood and Gartner, 2010), but more acoustic measurements are available and could be analyzed for information. Sampling equipment could be fabricated to capture both rising and falling colonies over short periods of time in the water column and thereby measure velocities and relative amounts of buoyant and non-buoyant colonies.

   After measurements are obtained, this approach still requires modeling (both one-dimensional water-column models that investigate only the interaction between buoyancy and stratification, and three-dimensional models that add horizontal transport to the mix) to assist the scaling-up process. A modeling effort would be greatly facilitated by a study targeted at quantifying the rates of creation and destruction of the carbohydrate ballast that the *Aphanizomenon flos-aquae* colonies use to regulate their buoyancy. Although there are a few different mechanisms that colonies use (construction of gas vesicles, turgor pressure collapse of vesicles, and ballast), it seems that the mechanism that works most effectively on the time scales of most interest (hours, because velocities indicate colonies can traverse the water column in hours over most of the lake) is the construction and destruction of carbohydrate ballast (Konopka and others, 1987; Whitton and Potts, 2000; Porat and others, 2001).

The combined results of Phases 1 and 2 of the TMDL model review have indicated strengths and limitations of the UKL TMDL model. Translating the model into the R language and adopting a numerical method for integrating the model equations has facilitated recalibration and evaluation of the effect of the different model terms on the resulting predictions of water quality. Changes were made to several model algorithms to make them consistent with current research on lake processes elsewhere. Sensitivity analysis and long-term simulations produced the calibration parameters that are both influential in determining model outcome while also having a high degree of uncertainty, suggesting areas for future research to improve understanding of the effects of changes in nutrient management strategies. Finally, we have suggested several steps to combine these findings in order to create a more robust model in the future and to better understand the likely results to changes in lake and nutrient management. Given the importance of water quality and nutrient status of Upper Klamath Lake to endangered fish and to downstream water quality in the Klamath River and the lower Klamath River Basin, finding ways to implement the suggested model refinements may help generate improvements in water quality in the Klamath River Basin.

References Cited

Antenucci, J.P., Tan, K.M., Eikaas, H.S., and Imberger, J., 2013, The importance of transport processes and spatial gradients on in situ estimates of lake metabolism: Hydrobiologia, v. 700, p. 9–12, doi:10.1007/s10750-012-1212-z.

Aristegi, L., Izagirre, O., and Elosegi, A., 2009, Comparison of several methods to calculate reaeration in streams, and their effects on estimation of metabolism: Hydrobiologia, v. 635, p. 113–124.

Bales, J.D., and Nardi, M.R., 2007, Automated routines for calculating whole-stream metabolism—Theoretical background and user's guide: U.S. Geological Survey Techniques and Methods, book 4, chap. C2, 33 p., http://pubs.usgs.gov/tm/tm4c2/.

Bowie, G.L., Mills, W.B., Porcella, D.B., Campbell, C.L., Pagenkopf, J.R., Rupp, G.L., Johnson, K.M., Chan, P.W.H., Gherini, S.A., and Chamberlin, C.E., 1985, Rates, constants, and kinetics formulations in surface water quality modeling: U.S. Environmental Protection Agency, EPA/600/3-85/040, 455 p.

Burdick, S.M., VanderKooi, S.P., and Anderson, G.O., 2009, Spring and summer spatial distribution of endangered juvenile Lost River and shortnose suckers in relation to environmental variables in Upper Klamath Lake, Oregon—2007 Annual Report: U.S. Geological Survey Open-File Report 2009-1043, 57 p., http://pubs.usgs.gov/of/2009/1043/.

Burnham, K.P., and Anderson, D.R., 2002, Model selection and multimodel inference—A practical information-theoretic approach (2d ed.): New York, Springer-Verlag.

Chapra, S.C., 1997, Surface water-quality modeling: Long Grove, Illinois, Waveland Press.

Chapra, S.C., and Di Toro, D.M., 1991, Delta method for estimating primary production, respiration, and reaeration in streams: Journal of Environmental Engineering, v. 117, no. 5, p. 640–655.

Coloso, J.J., Cole, J.J., and Pace, M.L., 2011, Difficulty in discerning drivers of lake ecosystem metabolism with high-frequency data, Ecosystems, v. 14, p. 935–948, doi:10.1007/s10021-011-9455-5.

Devine, J.A., and Vanni, M.J., 2002, Spatial and seasonal variation in nutrient excretion by benthic invertebrates in a utrophic reservoir: Freshwater Biology, v. 47, p. 1,107–1,121.

Eilers, J.M., Kann, J., Cornett, J., Moser, K., and St. Amand, A., 2004, Paleolimnological evidence of change in a shallow, hypereutrophic lake—Upper Klamath Lake, Oregon, USA: Hydrobiologia, v. 520, no. 1, p. 7, http://dx.doi.org/10.1023/B:HYDR.0000027718.95901.ae.

Eilers, J.M., Kann, J., Cornett, J., Moser, K., St. Amand, A., and Gubala, C.P., 2001, Recent paleolimnology of Upper Klamath Lake: Bureau of Reclamation, 44 p.

Eldridge, S.L.C., Wherry, S.A., and Wood, T.M., 2014, Statistical analysis of the water-quality monitoring program, Upper Klamath Lake, Oregon, and optimization of the program for 2013 and beyond: U.S. Geological Survey Open-File Report 2014-1009, 82 p., http://dx.doi.org/10.3133/ofr20141009.

Eldridge, S.L.C., Wood, T.M., and Echols, K.R., 2012, Spatial and temporal dynamics of cyanotoxins and their relation to other water quality variables in Upper Klamath Lake, Oregon, 2007–09: U.S. Geological Survey Scientific Investigations Report 2012-5069, 32 p. plus appendixes, http://pubs.usgs.gov/sir/2012/5069/.

Environmental and Water Resources Institute, 2005, The ASCE Standardized Reference Evapotranspiration Equation: ASCE-EWRI Task Committee Report, 59 p.

Fukuhara, H., and Sakamoto, M., 1987, Enhancement of inorganic nitrogen and phosphate release from lake sediment by tubificid worms and chironomid larvae: Oikos, v. 38, p. 312–320.

Fukuhara, H., and Yasuda, K., 1985, Phosphorus excretion by some zoobenthos in a eutrophic freshwater lake and its temperature dependency: Japanese Journal of Limnology, v. 46, p. 287–296.

Gardner, W.S., Nalepa, T.F., Quigley, M.A., and Malczyk, J.M., 1981, Release of phosphorus by certain benthic invertebrates: Canadian Journal of Fisheries and Aquatic Science, v. 38, p. 978–981.

Gelda, R.K., and Effler, S.W., 2002, Metabolic rate estimates for a eutrophic lake from diel dissolved oxygen signals: Hydrobiologia, v. 485, nos. 1–3, p. 51–66, http://dx.doi.org/10.1023/A%3A1021327610570.

Hansen, K., Mouridsen, S., and Kristensen, E., 1998, The impact of *Chironomus plumosus* larvae on organic matter decay and nutrient (N, P) exchange in a shallow eutrophic lake sediment following a phytoplankton sedimentation: Hydrobiologia, v. 364, p. 65–74.

Kann, J., and Walker, W.W., 1999, Nutrient and hydrological loading to Upper Klamath Lake, Oregon, 1991–1998: Klamath Tribes, 48 p. plus appendixes.

Kann, J., and Welch, J.B., 2005, Wind control on water quality in shallow, hypereutrophic Upper Klamath Lake, Oregon: Lake and Reservoir Management, v. 21, no. 2, p. 149–158.

Kann, J., 2011, Upper Klamath Lake 2010 data summary report: Klamath Tribes, 43 p. plus appendixes.

Kannarr, K.E., Tanner, D.Q., Lindenberg, M.K., and Wood, T.M., 2010, Water-quality data from Upper Klamath and Agency Lakes, Oregon, 2007–08: U.S. Geological Survey Open-File Report 2010-1073, 28 p., http://pubs.usgs.gov/of/2010/1073/.

Konopka, A., Kromkamp, J.C., and Mur, L.R., 1987, Regulation of gas vesicle content and buoyancy in light- or phosphate-limited cultures of *Aphanizomenon flos-aquae* (Cyanophyta): Journal of Phycology, v. 23, no. 1, p. 70–78.

Lindenberg, M.K., Hoilman, G., and Wood, T.M., 2009, Water quality conditions in Upper Klamath and Agency Lakes, Oregon, 2006: U.S. Geological Survey Open-File Report 2008-5201, 54 p.

Martin, J.L., and McCutcheon, S.C., 1999, Hydrodynamics and transport for water quality modeling: Boca Raton, Fla., Lewis Publishers.

Mermillod-Blondin, F., 2011, The functional significance of bioturbation and biodeposition on biogeochemical processes at the water-sediment interface in freshwater and marine ecosystems: Journal of the North American Benthological Society, v. 30, no. 3, p. 770–778.

Mermillod-Blondin, F., and Rosenberg, R., 2006, Ecosystem engineering—The impact of bioturbation on biogeochemical processes in marine and freshwater benthic habitats: Aquatic Science, v. 68, p. 434–442.

Michaud, E., Desrosiers, G., Mermillod-Blondin, F., Sundby, B., and Stora, G., 2005, The functional group approach to bioturbation—The effects of biodiffusers and gallery-diffusers of the *Macoma balthica* community on sediment oxygen uptake: Journal of Experimental Marine Biology and Ecology, v. 326, p. 77–88.

Michaud, E., Desrosiers, G., Mermillod-Blondin, F., Sundby, B., and Stora, G., 2006, The functional group approach to bioturbation—II—The effects of the *Macoma balthica* community on fluxes of nutrients and dissolved organic carbon across the sediment-water interface: Journal of Experimental Marine Biology and Ecology, v. 337, p. 178–189.

Morace, J.L., 2007, Relation between selected water-quality variables, climatic factors, and lake levels in Upper Klamath and Agency Lakes, Oregon, 1990–2006: U.S. Geological Survey Scientific Investigations Report 2007-5117, 54 p. [Also available at http://pubs.usgs.gov/sir/2007/5117/.]

Moreno-Ostos, E., Cruz-Pizarro, L., Basanta, A., and George, D.G., 2009, The influence of wind-induced mixing on the vertical distribution of buoyant and sinking phytoplankton species: Aquatic Ecology, v. 43, p. 271–284.

Porat, R., Teltsch, B., Perelman, A., and Dubinsky, Z., 2001, Diel buoyancy changes by the cyanobacterium *Aphanizomenon ovalisporum* from a shallow reservoir: Journal of Plankton Research, v. 23, no. 7, p. 753–763, doi:10.1093/plankt/23.7.753, accessed November 23, 2010, at http://plankt.oxfordjournals.org/content/23/7/753.full.

Odum, H.T., 1956, Primary production in lowing waters: Limnology and Oceanography, v. 1, no. 2, p. 102–117.

Oregon Department of Environmental Quality, 2002, Upper Klamath Lake drainage Total Maximum Daily Load (TMDL) and Water Quality Management Plan (WQMP): Oregon Department of Environmental Quality, 188 p., http://www.deq.state.or.us/WQ/TMDLs/klamath.htm.

R Core Team, 2014, R—A language and environment for statistical computing: Vienna, Austria, R Foundation for Statistical Computing, http://www.R-project.org/.

Raymond, P.A., Zappa, C.J., Butman, D., Bott, T.L., Potter, J., Mulholland, P., Laursen, A.E., McDowell, W.H., and Newbold, D., 2012, Scaling the gas transfer velocity and hydraulic geometry in streams and small rivers: Limnology and Oceanography—Fluids and Environments, v. 2, p. 41–53.

Simon, N., and Ingle, S., 2011, Physical and chemical characteristics including total and geochemical forms of phosphorus in sediment from the top 30 centimeters of cores collected in October 2006 at 26 Sites in Upper Klamath Lake, Oregon: U.S. Geological Survey Open-File Report 2011-1168, 46 p., http://pubs.usgs.gov/of/2011/1168/.

Simon, N., Lynch, D., and Gallaher, T., 2009, Phosphorus fractionation in sediment cores collected In 2005 before and after onset of an *Aphanizomenon flos-aquae* bloom in Upper Klamath Lake, OR, USA: Water, Air, and Soil Pollution, v. 204, no. 1, p. 139–153, http://dx.doi.org/10.1007/s11270-009-0033-9.

Staehr, P.A., Bade, D., Van de Bogert, M.C., Koch, G.R., Williamson, C., Hanson, P. Cole, J.J., and Kratz, T., 2010, Lake metabolism and the diel oxygen technique—State of the science: Limnology and Oceanography—Methods, v. 8, p. 628–644.

Sullivan, A.B., Rounds, S.A., Deas, M.L., Asbill, J.R., Wellman, R.E., Stewart, M.A., Johnston, M.W., and Sogutlugil, I.E., 2011, Modeling hydrodynamics, water temperature, and water quality in the Klamath River upstream of Keno Dam, Oregon, 2006–09: U.S. Geological Survey Scientific Investigations Report 2011-5105, 70 p., http://pubs.usgs.gov/sir/2011/5105/.

University of California, 2014, California weather data, Description of TULELK2.A: University of California Agriculture and Natural Resources—Statewide Integrated Pest Management Program Web site, accessed June 9, 2014, at http://169.237.140.1/calludt.cgi/WXDESCRIPTION?MAP=&STN=TULELK2.A.

U.S. Geological Survey, 2011, Change to solubility equations for oxygen in water: U.S. Geological Survey Office of Water Quality Technical Memorandum 2011.03, 13 p.

Van de Bogert, M.C., Carpenter, S.R., Cole, J.J., and Pace, M.L., 2007, Assessing pelagic and benthic metabolism using free water measurements: Limnology and Oceanography—Methods, v. 5, p. 145–155.

VanderKooi, S.P., Burdick, S.M., Echols, K.R., Ottinger, C.A., Rosen, B.H., and Wood, T.M., 2010, Algal toxins in Upper Klamath Lake, Oregon—Linking water quality to juvenile sucker health: U.S. Geological Survey Fact Sheet 2009-3111, 2 p., http://pubs.usgs.gov/fs/2009/3111/.

Walker, W.W., Jr., 2001, Development of a phosphorus TMDL for Upper Klamath Lake, Oregon: prepared for Oregon Department of Environmental Quality, Bend, Oregon, 80 p., accessed August 26, 2013, at http://www.deq.state.or.us/wq/tmdls/docs/klamathbasin/ukldrainage/devphostmdl.pdf.

Walker, W.W., Walker, J.D., and Kann, J., 2012, Evaluation oof water and nutrient balances for the Upper Klamath Lake Basin in water years 1992–2010: Technical Report to the Klamath Tribes Natural Resources Department, 50 p. plus appendixes.

Whitton, B.A., and Potts, M., eds., 2000, The ecology of cyanobacteria—Their diversity in time and space: Dordrecht, The Netherlands, Kluwer Academic Publishers, 669 p.

Wood, T.M., Fuhrer, G.J., and Morace, J.L., 1996, Relation between selected water-quality variables and lake level in Upper Klamath and Agency Lakes, Oregon: U.S. Geological Survey Water-Resources Investigations Report 96-4079, 57 p., http://pubs.usgs.gov/wri/1996/4079/report.pdf.

Wood, T.M., and Gartner, J.W., 2010, Use of acoustic backscatter and vertical velocity to estimate concentration and dynamics of suspended solids in Upper Klamath Lake, south-central Oregon—Implications for *Aphanizomenon flos-aquae*: U.S. Geological Survey Scientific Investigations Report 2010-5203, 20 p.

Wood, T.M., Hoilman, G.R., and Lindenberg, M.K., 2006, Water-quality conditions in Upper Klamath Lake, Oregon, 2002–04: U. S. Geological Survey Scientific Investigations Report 2006-5209, 52 p., http://pubs.usgs.gov/sir/2006/5209/.

Wood, T.M., Wherry, S.A., Carter, J.L., Kuwabara, J.S., Simon, N.S., and Rounds, S.A., 2013, Technical evaluation of a total maximum daily load model for Upper Klamath and Agency Lakes, Oregon: U.S. Geological Survey Open-File Report 2013-1262, 69 p. plus appendix, http://pubs.usgs.gov/of/2013/1262/.

Appendix A. Derivation of Net Settling Velocity

Cyanobacterial colonies in Upper Klamath Lake, Oregon, probably lie along a continuum between the heaviest colonies that fall with a maximum velocity and the lightest colonies that rise with a maximum velocity, including colonies of neutral buoyancy. To model these dynamics, we assume that the cyanobacterial colonies in the lake can be divided into two groups—rising colonies and falling colonies. We also assume that rising colonies are characterized by a single, constant rising velocity u_r and falling colonies are characterized by a single, constant falling velocity u_f (both with a positive sign). At any given location in the lake and point in time, the chlorophyll *a* associated with rising colonies is given by $r_{rise}(s,z,t)*\hat{B}(s,z,t)$, and the chlorophyll *a* associated with falling colonies is given by $r_{fall}(s,z,t)*\hat{B}(s,z,t)$, where r_{rise} is the fraction of colonies that are rising (buoyant), r_{fall} is the fraction of colonies that are falling (negatively buoyant), and $r_{rise} + r_{fall} = 1$. With these assumptions, the equation for the mass balance of $\hat{B}$ contains a settling term *SET* of the form:

$$SET(s,z,t) = u_r \frac{\partial r_{rise}\hat{B}}{\partial z} - u_f \frac{\partial r_{fall}\hat{B}}{\partial z} \qquad \text{(A1)}$$

When this term is averaged to scale up, the result is:

$$SETTLE = \frac{1}{D}\left\{u_r \overline{\overline{r_{rise}}} + u_f \overline{\overline{r_{fall}}}\right\}_{z=bottom} \qquad \text{(A2)}$$

where the double overbar indicates averaging over area and time. Note that we have allowed for rising colonies at the bottom; in other words, for colonies that previously settled to re-enter the water column. In the current version of the CSTR model, this is approximated as:

$$SETTLE \sim \frac{1}{D}\left(u_r \overline{\overline{r_{rise}}} + u_f \overline{\overline{r_{fall}}}\right)_{z=bottom} = \frac{1}{D}u_{alg} \qquad \text{(A3)}$$

and u_{alg} is the weighted average near-bottom velocity of the buoyant and non-buoyant colonies together, which effectively is a net settling velocity. To make the modeling of net settling velocity more manageable, the term was further simplified by making u_{alg} a calibration parameter.

Publishing support provided by the U.S. Geological Survey
Science Publishing Network, Tacoma Publishing Service Center

For more information concerning the research in this report, contact the
Director, Oregon Water Science Center
U.S. Geological Survey
2130 SW 5th Avenue
Portland, Oregon 97201
http://or.water.usgs.gov

ISSN 2328-0328 (online)
http://dx.doi.org/10.3133/sir20155041